Regulation of deleted mtDNA heteroplasmy in *Saccharomyces cerevisiae*

(出芽酵母において欠失変異ミトコンドリア DNA のヘテロプラスミー状態を制御する機構に関する研究)

Elliot Bradshaw

Science and Technology Major, Life Science Course

Saitama University Graduate School of Science and Engineering

Supervised by Professor Minoru Yoshida

A dissertation for consideration of Doctor of Philosophy degree conferment

September 2018

Abstract

The mitochondrial genome is a small unit residing within the mitochondrial matrix that encodes respiratory chain subunits, tRNAs and rRNAs essential for the majority of ATP production within most eukaryotic cells. Loss of mitochondrial genomic integrity by either point- or deletion-mutagenesis can lead to respiratory defects and several diseases. Mitochondrial DNA (mtDNA) exists as multiple copies within each cell, allowing for complementation of mutant mtDNA with wild-type copies. A mixture of wild-type and mutant molecules, termed heteroplasmy, can lead to mitochondrial dysfunction and disease if the proportion of mutant mtDNA molecules becomes sufficiently high. Deleted mtDNA molecules, which can be several kilobases shorter than wild-type, are particularly hazardous due to the replicative advantage of relatively small molecules. Indeed, the clonal expansion of deleted mtDNA has been observed in several organisms and, in human tissues its proportion can increase with age. Therefore, understanding the mechanisms that govern the generation and clonal expansion of deleted mtDNA may shed light on the aging process and give insights into treatments for mitochondrial diseases.

In this study, we report that ribonucleotide reductase (RNR), which catalyzes the rate-limiting step of deoxyribonucleotide triphosphate (dNTP) synthesis, regulates the replicative advantage of small mtDNA in heteroplasmic yeast cells. Crosses of parental yeast cells containing wild-type (ρ^+) mtDNA with respiratory-deficient (ρ^-) cells containing small mtDNA, results in production of diploid cells containing a heteroplasmic mixture of both parental mtDNA alleles. Due to the replicative advantage of small mtDNA, the majority of colonies formed from these crosses lack mitochondrial function, as demonstrated by an inability to grow in non-fermentable media. *SML1* encodes a protein inhibitor of RNR, and *RNR1* encodes the large subunit of RNR. Deletion of *SML1* or overexpression of *RNR1* significantly increases the proportion of ρ^+ colonies during heteroplasmy with small mtDNA. Reducing RNR activity by overexpressing *SML1* produces the opposite effect. In addition, using Ex Taq and KOD Dash polymerases, we observe a replicative

advantage for small template DNA over large *in vitro*, but only at low dNTP concentrations. These results indicate that dNTP insufficiency contributes to the replicative advantage of small mtDNA over wild-type in yeast and cytosolic dNTP synthesis by RNR is an important regulator of heteroplasmy involving small mtDNA molecules.

Over 100 genes contribute to mtDNA stability in *S. cerevisiae* and genetic requirements for stable mtDNA maintenance depend on growth conditions. In order to study deletion mutagenesis, we constructed a double-mutant strain that undergoes rapid loss of respiratory function. *ABF2* encodes a histone-like mtDNA binding protein that is required for mtDNA stability in fermentable media. *MHR1* encodes an mtDNA recombinase that promotes homologous pairing, a key step in recombination-mediated repair and in the initiation of rolling-circle mtDNA replication. Deletion of *MHR1* causes loss of mtDNA regardless of carbon source, however the *mhr1-1* mutation allows for mtDNA maintenance at a permissive temperature but displays significantly impaired recombination function. We show that *Δabf2 mhr1-1* double-mutant cells selectively grown in non-fermentable media are ρ^+, but rapidly lose respiratory function when shifted to fermentable media due to mtDNA deletion mutagenesis. Importantly, exogenous *MHR1* overexpression significantly rescues this mtDNA-loss phenotype, suggesting that Mhr1-driven mtDNA replication and homologous recombination are crucial for prevention of mtDNA deletion mutagenesis.

Glucose is the preferred carbon source for yeast cells, and its depletion or substitution with nonfermentable carbon sources results in a vastly different transcriptional landscape. One major consequence of glucose depletion is an immediate drop in cytosolic pH, which acts as a second messenger for glucose. We explored whether depletion of glucose during the vegetative growth of diploid cells leads to changes in heteroplasmy of wild-type and small mtDNA. We found that acidification of the cytosol promotes formation of ρ^+ colonies and increases wild-type mtDNA content over several generations, while high glucose media or alkaline cytosolic pH suppress this effect. We confirmed that this mitochondrial genetic response to cytosolic acidification occurs independently of the general stress response by *MSN2*/*4*, through an as of yet undetermined mechanism.

Together, this study introduces two regulatory mechanisms that influence the proportional amount of deleted mtDNA over wild-type in yeast and demonstrates that cytosolic pH influences the rate of ρ^+ colony formation from heteroplasmic cells containing ρ^+ and ρ^- mtDNA. Further exploration of these topics may lead to novel interventions against mtDNA deletion-attributed mitochondrial dysfunction.

Acknowledgements

I am grateful to my supervisor Professor Minoru Yoshida and to Dr. Feng Ling of the Chemical Genomics Research Group at RIKEN for their continuous support, mentorship and guidance and without whom my entry into research would not have been possible. I would also like to thank the members of the Chemical Genomics Research Group for their friendship and helpful discussions, especially Dr. Ken Matsumoto, Dr. Tilman Schneider Poetsch, Dr. Hiroki Kobayashi, Dr. Sheena Li, Dr. Jeff Piotrowski, Dr. Muhammad Ishfaq, Dr. Muhammad Tariq, Dr. Rong Niu, and Jagat Chipishrestha. Finally I would like to thank my wife, parents-in-law and parents for their support and encouragement.

Abbreviations

CFU	colony-forming unit
dNTP	deoxynucleotide triphosphate
ETC	electron transport chain
FAD	flavin adenine dinucleotide
HS	hypersuppressive
Kbp	kilobase pairs
mtDNA	mitochondrial DNA
NAD^+	nicotinamide adenine dinucleotide
nDNA	nuclear DNA
NHEJ	non-homologous end joining
ori	origin of replication
OXPHOS	oxidative phosphorylation
Polg	(DNA) Polymerase γ
PPP	pentose phosphate pathway
RDR	recombination-driven (mtDNA) replication
ρ^+	rho^+, phenotype of cells that contain wild-type mtDNA and have respiratory function
ρ^-	rho^-, phenotype of cells that contain mutant mtDNA and lack respiratory function
ρ^0	rho^0, phenotype of cells lacking mtDNA and respiratory function
RNR	ribonucleotide reductase
ROS	reactive oxygen species
TCA	tricarboxylic acid

Table of Contents

References

Chapter 1: Introduction

1.1 The diverse metabolic functions of mitochondria

Mitochondria are best known as specialized organelles that utilize a proton-motive force to drive the synthesis of adenosine 5'-triphosphate (ATP), the energy currency of the cell. A double-membrane system, consisting of a highly permeable outer membrane and a highly impermeable inner membrane allows for the accumulation of protons within the innermembrane space. Mitochondrial membrane potential ($\Delta\Psi m$) is generated through the oxidation of NADH or $FADH_2$, yielding electrons that proceed through oxidation and reduction reactions and cytochromes before finally reducing molecular oxygen to water. Energy from this process is used to pump protons from the matrix to the innermembrane space by electron transport chain (ETC) complexes I, III and IV. The resulting $\Delta\Psi m$ pushes protons through the F_0 subunit of ATP synthase and physically drives the rotation of the F_1 subunit to produce ATP (*1*). From a biochemical perspective, mitochondrial ATP synthesis is highly efficient, with a net yield of approximately 31 molecules of ATP per molecule of glucose, compared with just two net molecules of ATP produced by glycolysis (*2*).

Mitochondria perform various indispensible roles aside from ATP synthesis. Mitochondrial *β*-oxidation, the process of fatty acid catabolism to yield acetyl-CoA, is a major source of energy for the heart and skeletal muscle of mammals. In the liver, *β*-oxidation of long-chain fatty acids generates ketone bodies, an important energy source for organs when blood glucose is low, such as during starvation or endurance exercise (*3*). Ketone bodies are converted to acetyl-CoA in mitochondria and then oxidized by the tricarboxylic acid (TCA) cycle to eventually yield ATP (*2*). Mitochondria are also essential for the assembly of iron-sulfur (Fe/S) clusters, small inorganic cofactors that function as electron carriers in redox reactions and are involved in many cellular processes such as ribosome biogenesis, regulation of gene expression, respiration, DNA-RNA metabolism and others. Mitochondria are required for Fe/S cluster assembly in eukaryotes (*4*) and defects in Fe/S cluster

assembly can lead to increased spontaneous nuclear DNA mutations, hyper-recombination, and the presence of persistent DNA lesions (*5*). Another crucial aspect of mitochondrial function involves apoptotic signaling. Apoptosis is a mode of programmed cell death that plays an important part in the development of multicellular organisms. During apoptosis, the Bcl-2 family proteins Bax and Bak translocate to the mitochondrial outer membrane and oligomerize to facilitate outer membrane permeabilization, thereby releasing cytochrome c from the innermembrane space (*6*, *7*). Mitochondrial activity also produces reactive oxygen species (ROS) as byproducts of ETC subunits I and III, and α-ketoglutarate dehydrogenase of the TCA cycle. Mitochondrial ROS are notorious for their ability to cause oxidative damage to DNA, proteins and lipids, and are also important signaling molecules involved in numerous biological processes including oncogenic transformation, TNFα-mediated cell death (*8*), stimulation of tissue regeneration (*9*), mtDNA replication (*10*) and mitochondrial allele segregation (*11*).

1.2 Mitochondrial quality control

Evolution has produced several levels of mitochondrial quality control that play crucial roles in maintaining the health of eukaryotic cells. Mitophagy is a selective mode of autophagy that degrades dysfunctional mitochondria with characteristically low $\Delta\Psi_m$ or ATP levels (*12*). In yeast, mitophagy requires the mitochondrial outer-membrane receptor Atg32 (*13*), which interacts with Atg11 and Atg8 to recruit mitochondria into autophagosomes for subsequent transport to the vacuole (*14*). In metazoan cells, loss of $\Delta\Psi_m$ halts the import of the ubiquitin kinase Pink1 and its degradation by the innermembrane protease PARL (*15*), resulting in Pink1 accumulation on the outer membrane (*14*). Stabilized Pink1 then phosphorylates ubiquitin to activate the E3 ubiquitin ligase Parkin (*16*). Parkin ubiquitylates mitochondrial outer membrane proteins, triggering the recruitment of isolation membranes for the eventual transport to lysosomes (*14*). Importantly, mitophagy has been linked to disease and longevity. Hereditary defects in parkin have been associated with the familial early-onset of Parkinson's disease in humans (*17*). In the nematode *Caenorhabditis elegans*, animals defective for mitophagy receptors accumulate defective mitochondria that display lower ATP levels, higher

ROS production during aging and the animals have shortened lifespans in ordinarily long-lived genetic backgrounds (*18*).

Mitochondria form interconnected networks that continuously undergo fission and fusion events, collectively known as mitochondrial dynamics. Fission is a common response to nutrient starvation as a step toward reducing mitochondrial mass during periods of low energy demand (*14*). In yeast, the core fission machinery consists of Fis1, Dnm1, Mdv1 and Caf4. Fis1, a receptor on the outer mitochondrial membrane, interacts with Mdv1 or Caf4 to recruit the dynamin-related GTPase Dnm1. Dnm1 then nucleates into spiral-like structures that physically constrict mitochondria upon GTP hydrolysis (*19*). Orthologs of several of the fusion and fission proteins are present in human cells (*20*). Whether mitochondrial fission is required for mitophagy in yeast is unclear, as it was found that the absence of fission proteins does not limit rapamycin-induced mitophagy and instead the process is dependent on the general stress response and the Ras-protein kinase A (PKA) pathway (*21*). However, a screen for mutants defective for autophagy clearly indicated that *DNM1* is required for mitophagy during starvation (*22*). Additionally, fission is linked to apoptosis, as shown by experiments blocking Drp1 by RNAi or mutation in the fly *Drosophila melanogaster.* In fly hemocytes lacking Drp1 function, mitochondrial fragmentation decreased and caspase activation was absent (*23*). In HeLa cells, downregulation of Fis1 by RNAi inhibits apoptosis by blocking Bax translocation to mitochondria, while RNAi against Drp1 inhibits apoptosis in the step between Bax translocation to mitochondria and cytochrome c release (*24*). Together, several lines of evidence indicate that mitochondrial fission has a key role in the induction of apoptosis (*6*).

Mitochondrial fusion facilitates the mixing of mitochondrial contents and is required for mtDNA maintenance and inheritance (*20, 25, 26*). In yeast, fusion prevents the production of mitochondria lacking mtDNA and stimulates mtDNA replication through the activity of the *i*-AAA protease Yme1, which degrades ETC complex IV subunits and causes ROS production (*27*). Fusion involves the coordinated merging of the outer and inner membranes through the actions of the GTPases Fzo1 and Mgm1, respectively. Fusion also protects healthy mitochondria during non-selective autophagy by allowing healthy mitochondria to elongate in

order to be spared from degradation (*6, 28, 29*). Defects in the human orthologs of the fusion or fission machinery are associated with several neurological diseases (*7, 19*), highlighting the importance of mitochondrial dynamics in human health.

Quality control mechanisms exist inside mitochondria as well. A system of mitochondrial chaperones and proteases promotes proper protein folding, protects against heat stress, and degrades damaged or misfolded proteins (*30*). The major components of this system are the *i*-AAA and *m*-AAA proteases, which reside on the inner membrane with their catalytic sites facing the IMS and matrix, respectively, and proteases that reside within the matrix. Mitochondrial proteolytic enzymes are especially important to the human nervous system, as defects are associated with several neuropathies, including spastic paraplegia, spinocerebellar ataxia, spastic ataxia neuropathy syndrome, Alzheimer's and Parkinson's diseases (*30*). The mitochondrial protease machinery also affects mtDNA metabolism. Lon is the major protease of the matrix and has a regulatory effect on mtDNA content and transcription through degradation of the mtDNA-binding protein TFAM (*31*, 32). In mice, homozygous deletion of *Lonp1* causes loss of mtDNA and embryonic lethality, while Lon also contributes to metabolic reprogramming and its expression level correlates with cancer proliferation (*33*). Interactions between the mitochondrial genome and the quality control machinery therefore have important implications for development and health.

Transmission of healthy mitochondria is another crucial mechanism required for the fitness of eukaryotic cells. Cytoskeletal transport of mitochondria occurs by different means depending on the organism, with microtubule-associated transport as a major pathway in metazoans (*34*). In yeast, mitochondria are transported along actin cables and sorted according to fitness. During S and G2 phases, mitochondria with higher redox potential and lower ROS are preferentially transmitted to buds while those with lower redox potential and higher ROS are retained in mother cells (*35*). Transport of mitochondria to buds requires Mmr1 or Ypt11, and Myo2. Mmr1 is an anchoring protein connecting mitochondria to the cortical ER in the bud tip (*36*) and coordinates with the myosin V motor protein Myo2 and the Rab GTPase Ypt11 (*37*). Deletion of *MMR1* disrupts mother-daughter age asymmetry and cells defective in mitochondrial inheritance produce dead buds, indicating that this process is

essential (*38*). Surprisingly, overexpressing *MMR1* increases mitochondrial transmission to the extent that those of lower fitness are also sent, thereby disrupting asymmetric mitochondrial inheritance (*39*). In mother cells, Num1 is found in abundance (*40*) and interacts with the plasma membrane and Mdm36 (*41*) in order to form the mitochondria-ER-cortex-anchor (MECA). MECA tethers mitochondria to the mother cell, allowing a portion of the organelles to be retained during cell division. The opposing physical forces produced by the mother and bud anchors contribute to mitochondrial fission by Dnm1 (*37*).

In summary, mitochondrial quality control is a complex system comprised of several activities that functionally overlap and have crucial roles in development, health and longevity. Importantly, these quality control functions directly affect mtDNA replication and stability, which has a central role in mitochondrial function.

1.3 Mitochondrial DNA metabolism

Mitochondrial DNA is a small genomic unit that resides within the mitochondrial matrix and encodes ETC subunits, tRNAs and rRNAs essential for mitochondrial ATP production; therefore mtDNA stability is essential for the fitness of eukaryotic organisms* [1]. Unlike nuclear DNA, mtDNA replication occurs independently of the cell cycle and its copy number varies in response to metabolic demand. For vertebrates, mtDNA copy number generally falls within a range of 10^3 ~ 10^4 copies/cell (*42*) while in *S. cerevisiae* copy number is approximately 30 ~ 100 copies/cell (*43*). The unit size of the mitochondrial genome also varies substantially between species; *H. sapiens* mtDNA is 16.5 kbp, compared to 85.7 kbp in *S. cerevisiae*. Despite several decades of study, the various mechanisms surrounding mtDNA replication, including initiation and termination are still not fully understood or agreed upon. What follows is a brief overview of the current models of mtDNA replication in mammalian cells, followed by those of the yeast *S. cerevisiae*.

1.3.1 Replication of mammalian mtDNA

MtDNA is a circular genome consisting of a heavy and light strand owing to differences in base composition (*44*). Mammalian mtDNA contains one prominent

[1] * With the exception of *Monocercomonoides* sp., a recently discovered amitochondriate eukaryote (*45*).

noncoding region known as the displacement loop (D-loop) that houses the heavy- and light-strand promoters, HSP and LSP (*46*). According to the strand displacement (SD) model, replication begins with transcription at the LSP and subsequent processing that generates a primer for the initiation of replication of a nascent heavy strand beginning at the heavy-strand origin (O_H) downstream of the LSP (*42*). Replication then proceeds by continuous SD, whereby the heavy strand is gradually displaced as exposed single-stranded DNA. When replication of the heavy strand is approximately two-thirds complete, the light-strand origin (O_L) becomes exposed, prompting replication initiation on the light strand (*47*). Priming and replication of the light-strand proceeds and the entire process yields two daughter molecules. Subsequently, the two molecules are separated, the RNA primers are removed and processed, and two closed circular mtDNA molecules are produced (Figure 1.1A).

Asymmetric SD was the dominant model of mammalian mtDNA replication until two-dimensional agarose gel electrophoresis (2D-AGE) revealed long, double-stranded replication intermediates that were inconsistent with the SD model (*48*). In fact, these double-stranded replication intermediates were long stretches of DNA-RNA hybrid, as confirmed by RNase H digestion, which acts on RNA only that is hybridized to DNA (*49*). The confirmation that long stretches of RNA were complementary to the sequence of the light strand (*50*) led to a model of synchronous RNA incorporation during mtDNA replication (RITOLS; *51*). In light of these results, it is hypothesized that exposed single-stranded mtDNA is rapidly filled in with RNA, offering protective effects including against oxidative damage by ROS (Figure 1.1B; *51*).

In summary, the RITOLS model of mammalian mtDNA replication currently fits well with observations, however several unknowns remain about human mtDNA replication including its mechanisms of regulation, termination and subsequent processing. Future detailed studies will be essential to answering these questions and perhaps for devising novel treatments for mtDNA-associated diseases.

1.3.2 RNA-primed mtDNA replication in *Saccharomyces cerevisiae*

S. cerevisiae mtDNA contains eight replication origin (*ori*) sequences, of which three are active (*ori2*, *3* and *5*). Active *ori* are considered functionally equivalent to the O_H and O_L promoter sequences of mammalian mtDNA, as both are sites of RNA

primer synthesis. Active *ori* in yeast consist of three GC-rich clusters, termed boxes A, B and C, which are separated by AT sequences (*52*). *RPO41* is the mitochondrial RNA polymerase and is required for mtDNA transcription and maintenance of ρ^+ mtDNA (*53*). *RPO41* synthesizes primers, detected as short stretches of RNA-DNA hybrid sequences, at the initiation sites of *ori* sequences (*54*). In addition, the yeast C box bears similarity to the conserved sequence block (CSB) II of the O_H promoter of vertebrate mtDNA, which also contains hybrid RNA-DNA (*42*). These observations appeared consistent with a model of yeast RNA-primed mtDNA replication dependent on *RPO41*, where short RNA provides a free 3'-OH end for initiation of replication. However, questions about this model arose when it was shown that maintenance of ρ^- mtDNA can occur independently of *RPO41* (*55*) and crosses of ρ^- × HS ρ^- cells lacking *RPO41* still showed biased inheritance for the HS ρ^- allele (*56*). Together, these observations questioned the contribution of RNA priming and raised the possibility that another mode of mtDNA replication exists.

1.3.3 Recombination-driven mtDNA replication

Elucidation of the recombination-driven mtDNA replication (RDR) pathway began with the isolation of *mhr1-1*, a nuclear mutation defective for homologous mitochondrial gene conversion. Yeast cells containing the *mhr1-1* mutation show a significantly lower production rate of recombinant mtDNA molecules compared to wild-type cells and rapidly lose mtDNA during cultivation at 37°C, indicating important roles for *MHR1* in mtDNA recombination and stability (*57*). Mhr1 promotes homologous pairing of single- to double-stranded DNA *in vitro* and functions in coordination with the mitochondrial cruciform cutting endonuclease Cce1p, which resolves Holliday-junction intermediates. Double-mutant *mhr1-1 Δcce1* cells display a total loss-of-mtDNA phenotype (ρ^0), highlighting the fact that mtDNA recombination is essential for stable mtDNA maintenance (*58*).

Concatemers are linear multiple-unit-length strands of nascent mtDNA produced by a continuous, rolling-circle replication mode (*59*). Importantly, concatemers allow for the transmission of multiple mtDNA copies as a single segregation unit to buds. In contrast to random mtDNA template replication and transmission that is highly unlikely to result in homoplasmy formation (Figure 1.2A), production and transmission of concatemeric mtDNA can explain the observed rapid

restoration of homoplasmy from heteroplasmy that typically occurs within ten generations in yeast (Figure 1.2B; *43*). Notably, mtDNA concatemer synthesis is suppressed by the *mhr1-1* mutation and enhanced by Mhr1 overproduction. In addition, *mhr1-1* mutants display a slower rate of homoplasmy restoration, indicating that mitochondrial allele segregation correlates with concatemeric mtDNA production through Mhr1 (*43*).

Initiation of Mhr1-dependent mtDNA replication is dependent on DNA double-stranded breaks (DSBs). *NTG1* encodes a DNA N-glycosylase and apurinic/apyrimidinic (AP) lyase that excises damaged bases from DNA and creates DSBs at the *ori5* locus in yeast mitochondria (*59*). In mitochondria, DNA damage can be caused by production of reactive oxygen species (ROS), byproducts of the nearby ETC complexes I and III or α-ketoglutarate dehydrogenase complex of the TCA cycle (*60*). The *ori5* region of yeast mtDNA contains exposed single-stranded DNA and accumulates a relatively high number of oxidized bases, leading to DSB formation in the presence of Ntg1. Exposure of isolated mitochondria to hydrogen peroxide (H_2O_2) *in vitro* leads to increased mtDNA copy number in a manner dependent on Ntg1 and Mhr1 (*10*). Similarly, chronic H_2O_2 exposure can also increase mtDNA copy number *in vivo* (*10*).

Following the generation of DSBs, Mhr1 requires a free 3' single-stranded (ss) DNA tail to initiate strand invasion of a circular double-stranded mtDNA template for heteroduplex formation. *DIN7* encodes a DNA damage-inducible mitochondrial 5'-3' exodeoxyribonuclease that produces 3'-ssDNA tails and is required for mtDNA copy number increase upon H_2O_2 exposure *in vivo* (*61*). Furthermore, blocking mtDNA DSBs with the mitochondrially-targeted DSB-binding protein MmKu causes petite formation and induces mtDNA depletion (*62*), indicating that the DSB-triggered RDR pathway is the predominant form of mtDNA replication in *S. cerevisiae*.

The existence of a recombination-directed mtDNA replication mode in higher organisms remains an open question. MtDNA replication via a rolling-circle mode that produces multimeric tails from a single circular template has been reported in the nematode *C. elegans* and the higher plant *Chenopodium album* (*63*, *64*). In human MELAS cells heteroplasmic for the m.3243A>G mutation, H_2O_2 treatment stimulates mitochondrial allele segregation towards homoplasmy and correlates

with concatemeric mtDNA production (*11*). In addition, evidence suggesting that recombination occurs within human mitochondria has been reported (*65*, *66*). On the other hand, recent studies have suggested that mtDNA DSBs in human cells are rapidly degraded (*67, 68*) and blocking mtDNA DSBs in a human cell line did not cause observable changes to mtDNA level (*62*). Further study will be needed to determine the existence of RDR in human mitochondria.

1.4 MtDNA deletion mutations

MtDNA resides in close proximity to the ROS-producing machinery of the ETC and is therefore subjected to a higher rate of mutagenesis than nuclear DNA. The relative amount of mutant to wild-type mtDNA is a crucial factor in pathology; when the proportion of mutant mtDNA exceeds a threshold level, mitochondrial dysfunction or disease may occur (*69*). MtDNA mutations are categorized as point mutations or deletions. Point mutations are typically single nucleotide substitutions and are generally well tolerated due to complementation by multiple copies of mtDNA. On the other hand, deleted mtDNA are molecules shorter than wild-type and can lack up to several kilobases, raising the possibility that they can replicate more quickly and frequently than wild-type (*51, 70*). Over time, this replicative advantage can lead to large changes in the heteroplasmy level and threaten the respiratory function of the cell. The clonal expansion of deleted mtDNA has been observed in several organisms including yeast, nematodes, mice and humans (*70-74*).

Deleted mtDNA molecules are commonly formed by the joining of two direct repeats (*75*) due to replication slippage, or perhaps less commonly, by non-homologous end joining (NHEJ) of mtDNA DSBs (*68*). Multiple studies indicate that mtDNA polymerase γ has an important role in mtDNA deletion mutagenesis, and its proofreading function is especially important for preventing deletion formation. Notable examples of this were shown in *Polg* mutator mice expressing proofreading-deficient mtDNA polymerase γ. These mtDNA-mutator mice showed severe respiratory chain defects across several tissues, the rapid onset of aging phenotypes, shortened lifespans and increased amounts of deleted mtDNA (*76*, *77*). The

distribution of deleted mtDNA in mammalian tissue is irregular (*78*), and often observed as a mosaic pattern of respiratory defects (*65, 76, 79*).

In humans, clonal expansion of deleted mtDNA notably occurs in the substantia nigra, a region of the brain associated with Parkinson's disease (*65, 79*). Also, in iPS cells derived from patient fibroblasts harboring a ~6-kb mtDNA deletion, small mtDNA undergoes clonal expansion that increases in proportion to wild-type with each passage, while levels of point-mutant mtDNA remain relatively stable under the same conditions (*80*). Importantly, a common feature of deleted mtDNA molecules is the requirement for a replication origin. In yeast, an active *ori* sequence is required for the suppressive phenotype of small mtDNA (*71*), while human deleted mtDNA molecules are found to retain a portion of the noncoding region including the D-loop (*75*). Further research will be needed to identify other factors contributing to mtDNA deletion mutagenesis and a more complete understanding of these issues may provide methods for eliminating these hazardous molecules.

1.5 Aims of this study

Our group at the Chemical Genomics Research Group at RIKEN previously identified the Mhr1-mediated recombination-driven replication pathway for mtDNA replication and inheritance in *S. cerevisiae.* We revealed that ROS regulate mtDNA copy number in yeast by triggering mtDNA replication (*10*) through formation of DSBs (*61*) and that ROS can contribute to human mitochondrial allele segregation (*11*). As explained in the introduction, mtDNA replication is closely associated with the formation of mtDNA deletions. Therefore, this study aims to explore possible relationships between the recombination-mediated mtDNA replication pathway and mtDNA deletion mutagenesis or its replicative advantage during heteroplasmy with wild-type mtDNA.

In Chapter 2 of this study, I report that dNTP synthesis by ribonucleotide reductase affects the replication of wild-type mtDNA in heteroplasmy with small, hypersuppressive mtDNA. Using yeast genetics, I show that modifications that increase or decrease the activity of ribonucleotide reductase affect the relative amounts of small and wild-type mtDNA in heteroplasmic cells. In Chapter 3, we use *Δabf2 mhr1-1* double-mutant cells, which rapidly lose mtDNA integrity in

fermentable media due to mtDNA deletion mutagenesis, to show that mtDNA recombination function is crucial for prevention of mtDNA deletions in yeast. Finally, in Chapter 4, I show that cytosolic pH influences the segregation of small and wild-type mtDNA in heteroplasmic yeast cells during several generations of vegetative growth.

1.6 Figures

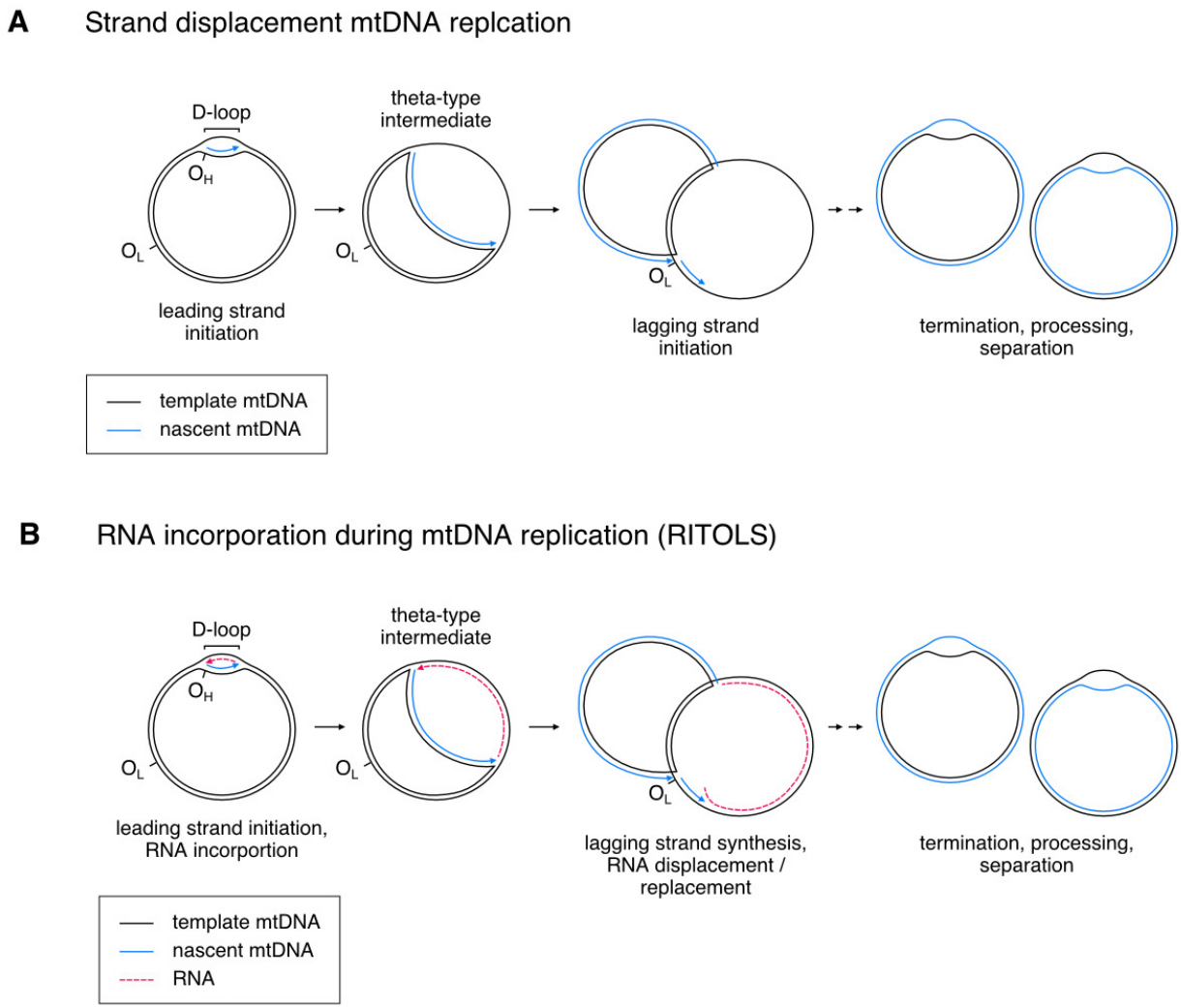

Figure 1.1 | Models of mammalian mtDNA replication. (A) Major steps of the strand-displacement model of mtDNA replication. Nascent mtDNA synthesis begins at the heavy-strand replication origin (O_H) within the displacement loop (D-loop) and proceeds continuously while displacing the light strand. Exposure of the light-strand

replication origin (O_L) prompts synthesis of the complementary light strand. Finally, termination and processing steps yield two identical circular molecules. (B) Model of RNA incorporation during mtDNA replication (RITOLS). MtDNA replication initiates and proceeds similarly to SD, however complementary RNA is immediately incorporated into exposed single-stranded mtDNA.

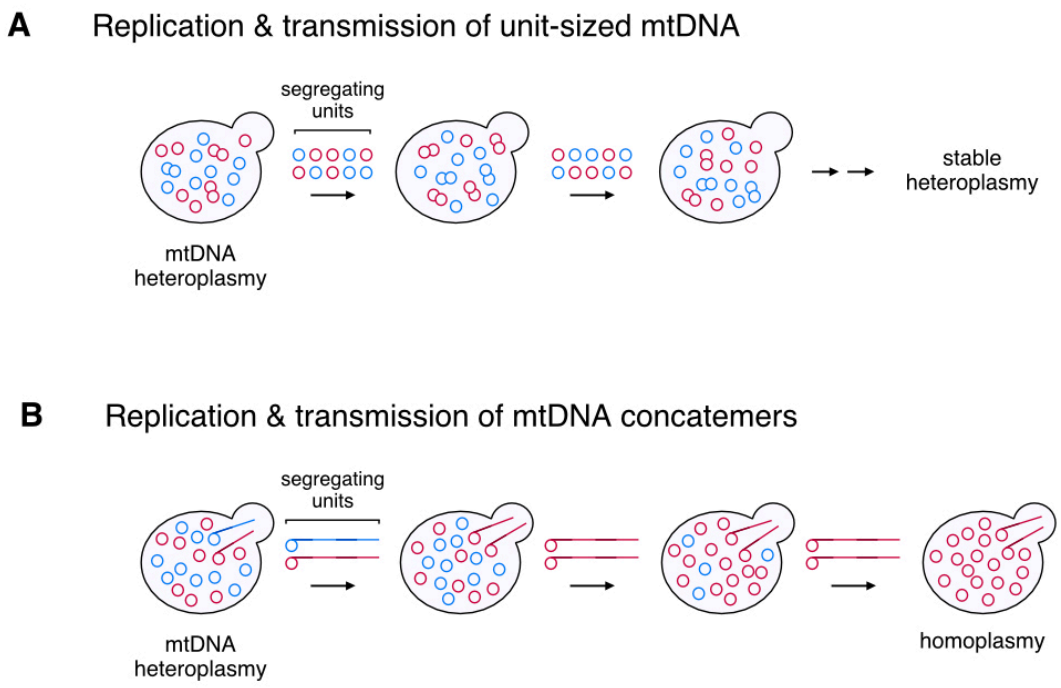

Figure 1.2 | Model of rapid mtDNA segregation from heteroplasmy to homoplasmy in *S. cerevisiae*. (A) Replication and transmission of unit-sized mtDNA molecules from a heteroplasmic pool maintains a heteroplasmic state over several generations. (B) Production and transmission of multiple-unit-sized concatemeric mtDNA results in rapid mt-allele segregation and formation of homoplasmy.

Chapter 2: Regulation of small mitochondrial DNA replicative advantage by ribonucleotide reductase in *Saccharomyces cerevisiae*

2.1 Introduction

2.1.1 Ribonucleotide reductase

Ribonucleotide reductase (RNR) catalyzes the irreversible, rate-limiting step of deoxynucleotide triphosphate (dNTP) synthesis through the reduction of ribonucleoside diphosphates (NDPs) to deoxyribonucleoside diphosphates (dNDPs), providing the DNA building blocks essential to life. RNR has an $\alpha_2\beta_2$ structure that consists of a large and small subunit, termed R1 and R2, respectively (*81*). In *S. cerevisiae*, R1 consists of a large Rnr1-Rnr1 homodimer containing the allosteric feedback and catalytic sites, and R2 is a small Rnr2-Rnr4 heterodimer housing the diferric-tyrosyl radical cofactor required for the reduction reaction (*82*). Control of RNR activity in *S. cerevisiae* occurs at four levels: regulation by the transcriptional repressor Crt1 (*83*), prevention of Rnr1p homodimerization by binding of the inhibitor Sml1 (*84*), sequestration of the Rnr2-Rnr4 heterodimer in the nucleus (*82*) and allosteric inhibition on the Rnr1 subunit (*85*).

2.1.2 The Mec1/Rad53 DNA damage checkpoint pathway

The Mec1/Rad53 DNA damage checkpoint was the first conserved signaling pathway in *S. cerevisiae* found to regulate mtDNA copy number (*86*). Eukaryotic cells halt the cell cycle in response to blocked DNA replication or DNA damage, allowing time for DNA repair. In order to accomplish this, a specific signal transduction cascade must occur. Mec1, the yeast homolog of human *ATM1*, is a phosphoinositide (PI)-3-kinase-related protein kinase which activates Rad9p, which then in turn activates the protein kinases Rad53p and Chk1p. Mec1 is required for cell cycle arrest, as DNA lesions themselves are insufficient to slow the cell cycle. For example, *mec1* and *rad53* mutants were shown to progress rapidly through S phase in response to the DNA alkylating agent methyl methanesulfonate (MMS), while wild-type cells display a large-budded morphology and take a significantly longer time to perform DNA replication (*87*). Aside from subjecting yeast to mutagenic

reagents, the *Δrrm3* mutation has been used to recapitulate the Mec1/Rad53 checkpoint. *RRM3* encodes a 5' to 3' DNA helicase required for DNA replication-fork progression through ribosomal DNA genes, subtelomeric and telomeric regions, all of which contain repetitive sequences. *RRM3* deletion causes replication fork stalling, strand breakage, recombination at tandem repeats (*88*) and triggers the phosphorylation of Rad53p, leading to induction of the S-phase checkpoint (*86*).

One major consequence of checkpoint activation is the induction of dNTP synthesis by ribonucleotide reductase. Upon DNA damage, Rad53p activates Dun1p, a protein serine/threonine kinase that phosphorylates Sml1p, a protein inhibitor of Rnr1 (*89*). Sml1p phosphorylation by Dun1p leads to its degradation (*90*), while *dun1* mutants show neither phosphorylation nor removal of Sml1p at S-phase (*91*). Checkpoint activation also increases dNTP synthesis by increasing transcription of the RNR genes through removal of the transcriptional repressor Crt1 (*83*). In summary, several lines of evidence show that increased dNTP synthesis by RNR is a major endpoint of Mec1/Rad53-mediated checkpoint activation.

2.1.3 Suppressive mtDNA

S. cerevisiae has served as an important tool for study of the biased inheritance displayed by small mtDNA, termed suppressiveness (*92*). Crosses of strains possessing wild-type (ρ^+) genomes results in bi-parental inheritance and produces a transient heteroplasmic state that persists for fewer than 20 generations (*43, 93*). In contrast, suppressiveness is observed in crosses between parental ρ^+ and ρ^- strains due to biased inheritance of the ρ^- allele, which yields a portion of diploid offspring lacking respiratory function. Hypersuppressive (HS) petites are the most extreme case, wherein crossing produces a high frequency of diploid colonies (>95%) lacking respiratory function (*71*). HS ρ^- strains contain small mtDNA fragments bearing an active origin of replication (*ori*) sequence, which includes a promoter (*52*) and is required for hypersuppressiveness. In contrast to HS ρ^- mtDNA, *ori* are not required for maintenance of normal suppressive mtDNA, highlighting the complexity of mtDNA inheritance.

How the replicative advantage of short mtDNA over wild-type is affected by alterations in RNR activity remains unexplored. In this chapter, we present evidence to demonstrate a negative correlation between dNTP synthesis by RNR and the

replicative advantage for small, moderately suppressive or hypersuppressive mtDNA molecules during heteroplasmy with wild-type mtDNA.

2.2 Materials and methods

2.2.1 Yeast strains and transformation

Yeast strains used in this chapter are listed in Table 1. Yeast transformation was performed using the lithium-acetate method (*94*) using a High-Efficiency Yeast Transformation Kit (MoBiTec GMBH). Cloning and overexpression of *RNR1* and *SML1* were performed through modification of the plasmid pVT100U (*95*), which contains the 397-bp constitutive ADH promoter. Selection for cells harboring pVT100U was conducted on synthetic dropout minus uracil (SD-U) plates.

2.2.2 Yeast crossing experiments

Crossing experiments were conducted using overnight pre-cultures of two parental haploid strains in rich media. YPGlycerol (yeast extract, peptone, 50mM KH_2PO_4, 3% glycerol v/v, pH 6.4) was used for cultivation of parental ρ^+ strains, while YPD (yeast extract, peptone, dextrose) was used for parental ρ^- strains. Cell concentrations were counted by haemocytometer and 10^7 cells per haploid strain were added to 1 ml of fresh YPD and crossed for 6 h at 30°C. Mated cells were then diluted and spread onto synthetic defined minimal media plus leucine and/or uracil (SD+LU or SD+L) plates to select for diploid cells. Diploid selection plates were then cultivated for 2 d at 30°C and photographed with a LAS-4000 imaging system (GE Healthcare). Diploid selection plates were then replica-plated to YPGlycerol plates, which were incubated for another 2 d at 30°C and then photographed. Images of each SD master plate and corresponding YPGlycerol plate were overlaid with Photoshop Elements software (Adobe) and colonies were counted to determine the percentage of ρ^+ colony-forming units (CFUs) formed.

2.2.3 Quantification of mtDNA levels in heteroplasmic cells

Diploid colonies from crossing experiments were eluted from diploid selection plates with 1x PBS buffer, pelleted by centrifugation, and frozen at -80°. Total DNA including mtDNA was prepared and DNA concentrations were measured with a NanoVue spectrophotometer (GE Healthcare). 95 ng of total DNA was used as the standard template concentration for PCR analyses. Primers used to specifically

detect nuclear DNA, ρ^+ mtDNA and HS ρ^- mtDNA were: *NUC1*-Fwd, 5'-GATACTCTTGTCCGGTTTAGTCG-3'; *NUC1*-Rev, 5'- ATCTTTCGACTGTTTGATCGCC-3'; *COX3*-Fwd, 5'-ATGCCTTCACCATGACCTATTG-3'; *COX3*-Rev, 5'-CCAACATGATGTCCAGCTGTTA-3'; HSC1-Fwd, 5'-GAAGATATCCGGGTCCCAATAATAA-3'; HSC1-Rev, 5'-AATATAATAGTCCCCACTCCGCG-3'. Gels were photographed using a FAS-IV imaging system (Nippon Genetics) and band intensities were measured with ImageJ software (*96*). MtDNA level was calculated relative to nuclear DNA using the $2^{-\Delta CT}$ method (*97*).

2.2.4 Western blotting

Parental ρ^+ and HS ρ^- haploid yeast cells expressing the plasmids pVT100U-Empty, pVT100U-*RNR1*-FLAG or pVT100U-*SML1*-FLAG were grown on SD-U selection plates. Diploid cells were obtained under conditions identical to crossing experiments, and then selectively grown to mid log-phase by transferring 20 µl of mated cells to SD+L media and cultivating overnight at 30°C. Protein extraction was performed using the LiAc/NaOH method on ice (*98*). 10 µl of protein extracts were run on 10 or 15% PAGE gels and semidry transferred onto Immobilon-P transfer membranes (Millipore). Primary antibodies used for protein detection were anti-FLAG M2 (Sigma-Aldrich) and yeast anti-Phosphoglycerate Kinase (Invitrogen).

2.2.5 PCR assay for competitive template amplification under varying dNTP concentrations

Templates used in the PCR assay were created by inserting tdTomato (Clontech) between the *Kpn*I and *Xba*I cutting sites, or *RNR1* between the *Kpn*I and *Xho*I cutting sites of the plasmid pUC119. Template DNA concentrations were adjusted to give control signals of nearly equivalent apparent strength following ethidium bromide (EtBr) staining. All PCR reactions were performed with *Sca*I-linearized pUC119 templates for 12 PCR cycles. The set of primers flanking the multi-cloning site of pUC119 and used for all reactions was: pUC119-MCS-Fwd, 5'-TTGTGTGGAATTGTGAGCGG-3'; pUC119-MCS-Rev, 5'-TGCAAGGCGATTAAGTTGGG-3'. KOD Dash (TOYOBO) or Ex Taq (Takara Bio.) polymerases were used for PCR. Gels were photographed with a FAS-IV imaging system (Nippon Genetics) and band intensities were measured with ImageJ software (*96*). All band intensities were normalized against the control band with the weakest EtBr signal (left side of gel;

amplified with 200 µM dNTPs). Relative DNA levels (EtBr signal %) at each dNTP concentration were calculated as A_{norm} / A_{norm} + B_{norm}.

2.2.6 Microscopy

Parental haploid cells were cultivated in SD-U liquid medium overnight and then transferred to rich media and grown to mid log-phase at 30°C on a shaker at 120 rpm for 2—6 hrs, using YPGlycerol (pH 6.9) for ρ^+, or YPD medium for ρ^- cells. Cells were then treated with 1 µg/ml DAPI and incubated at 30° for 15 min. DAPI-stained cells were then mounted on glass slides and observed with a DeltaVision fluorescence microscopy system (Applied Precision) equipped with an IX71 microscope (Olympus).

2.3 Results

2.3.1 Sml1 is required for the hypersuppressive phenotype

To investigate the possible effects of checkpoint signaling on heteroplasmy with HS ρ^- mtDNA and the involvement of the Mhr1 pathway, we began by examining cells lacking *DIN7*, *RRM3* or *SML1*. *DIN7* encodes a mitochondrial 5' to 3' exodeoxyribonuclease that generates 3' single-stranded DNA tails that contribute to mtDNA replication initiation by Mhr1. *RRM3* encodes a nuclear DNA helicase and its disruption leads to nuclear replication fork stalling and activation of the Mec1/Rad53 checkpoint pathway. *SML1* encodes an inhibitor of Rnr1 homodimer formation. We crossed parental strains with the mutations: *Δdin7*, *Δrrm3*, *Δsml1*, *Δdin7 Δrrm3* and *Δdin7 Δsml1*. Heteroplasmic diploids containing 85.7-kbp wild-type (ρ^+) and 1.1-kbp hypersuppressive (HS ρ^-) mitochondrial genomes were produced after mating (Figure 2.1A) as previously described (*59*). The *Δsml1* diploids displayed a marked increase in the proportion of heteroplasmic ρ^+ colony-forming units (CFUs), from 3.5 ± 1.7% in WT cells to 19.2 ± 2.6% and 25.3 ± 4.5% in *Δsml1* and *Δdin7 Δsml1* mutants, respectively (Figure 2.1B and C). *Δdin7* cells showed a small increase to 8.5 ± 1.6%, while *Δrrm3* cells gave a slight decrease in ρ^+ CFU formation to 2.3 ± 1.1%, suggesting that neither lack of mitochondrial 5' to 3' exonuclease activity nor checkpoint activation induced by nuclear replication-fork stalling, respectively, strongly affected the replicative advantage of HS ρ^- mtDNA.

To rule out effects from altered mitochondrial morphology or mtDNA nucleoid size in *Δsml1* cells, which could potentially affect mtDNA transmission (*19, 99*), we tagged mitochondria in ρ^+ parental cells with tdTomato and in HS ρ^- cells with GFP, and stained mtDNA nucleoids with DAPI. We did not observe any apparent differences in mitochondrial morphology or nucleoid size among WT and *Δsml1* cells of the same parental background (Figure 2.1F), indicating that the phenotype of *Δsml1* cells is not likely due to irregular transmission of mitochondria or nucleoids.

We detected the proportional amounts of ρ^+ and HS ρ^- mtDNA in heteroplasmic cells using PCR primers specific for a nuclear gene, ρ^+ mtDNA and HS ρ^- mtDNA. Analysis of total genomic DNA including mtDNA, obtained by washing all colonies from diploid selection plates, revealed that relative to nuclear DNA (nDNA), levels of ρ^+ mtDNA were 0.38 ± 0.26-fold in WT cells compared with 1.64 ± 0.12-fold in *Δsml1* cells (Figure 2.1D and E), indicating that the *Δsml1* mutation significantly increased the proportional level of ρ^+ mtDNA in heteroplasmic cells containing HS ρ^- mtDNA. On the other hand, we observed no significant difference in HS ρ^- mtDNA levels among the WT and *Δsml1* backgrounds, indicating that replication of wild-type mtDNA is increased to a greater extent than HS ρ^- mtDNA in *Δsml1* cells.

In order to rule out the possibility that changes to the hypersuppressive phenotype seen in *Δsml1* crosses were specific to our hypersuppressive ρ^- strain YKN1423-C1, we conducted additional crossing experiments with two other parental ρ^- strains, YKN1423-A1 and YKN1423-A2, which are hypersuppressive and normal suppressive, respectively. Following A1 wild-type crosses, 4.4 ± 0.9% of CFUs were ρ^+, while A1*Δsml1* crosses gave rise to 75.8 ± 7.8% ρ^+ CFUs. Wild-type A2 crosses resulted in 66.4 ± 4.0% ρ^+ CFUs, while A2*Δsml1* crosses gave 79.6 ± 8.1% ρ^+ CFUs (Figure 2.2A and B). Despite multiple attempts, efforts to find unique restriction sites in A1 and A2 ρ^- mtDNA as a prerequisite step for cloning, sequencing and then designing specific PCR primers for measurements of ρ^- mtDNA content in these crosses were unsuccessful. However, we did observe significant increases in ρ^+ mtDNA content in the *Δsml1* backgrounds of diploids from both crosses (Figure 2.2C and D). Taken together, the *Δsml1* mutation increased wild-type mtDNA levels in heteroplasmic cells containing either moderately suppressive or hypersuppressive mtDNA.

2.3.2 *RNR1* overexpression enhances ρ^+ mtDNA replication in hypersuppressive crosses

RNR1 overexpression is sufficient to rescue the temperature-sensitive mtDNA loss phenotype of mitochondrial DNA polymerase *mip1-1* mutants, demonstrating a close relationship between RNR activity and mtDNA maintenance (*100*). Both *RNR1* overexpression and the *Δsml1* mutation increase cellular dNTP concentration (*89, 101*) and mtDNA copy number (*86, 102*). Furthermore, the *Δsml1* mutation was shown to reduce rates of spontaneous petite colony formation (*89*). Sml1 inhibits RNR by binding and preventing Rnr1 homodimerization (*84, 101*), therefore we hypothesized that increased dNTP synthesis by RNR was responsible for the observed increases in ρ^+ CFU formation.

To confirm the role of elevated dNTP synthesis, we overexpressed *RNR1* via plasmid and confirmed by immunoblot analysis (Figure 2.3A). In agreement with the behavior of *Δsml1* crosses, we observed that 20.6 ± 5.9% of heteroplasmic diploid cells overexpressing RNR1 were ρ^+, compared with 7.2 ± 3.7% of diploid CFUs containing the empty vector (Figure 2.3B and C). In diploid cells containing the empty vector, the level of ρ^+ mtDNA was 0.53 ± 0.29-fold relative to the *NUC1* signal, compared to 1.97 ± 0.64-fold in the *RNR1*-overexpressing cells (Figure 2.3D and E). There was no significant change in levels of HS ρ^- mtDNA in diploid cells containing the empty vector or *RNR1* plasmid. In addition, we expressed a mutant isoform, *rnr1*-Y629C, and observed that 15.9 ± 1.7% and 23.2 ± 3.7% of wild-type and *Δsml1* diploid CFUs, respectively, were ρ^+ in *rnr1*-Y629C expressing cells. The lower CFU formation rate suggests a lower catalytic activity of the *rnr1*-Y629C mutant gene product and supports the notion that elevated RNR activity contributes to the replication of ρ^+ genomes in the presence of HS ρ^- mtDNA, consistent with the observation of cells lacking Sml1.

2.3.3 Overproducing Sml1 in *Δsml1* cells restores the hypersuppressive phenotype

Sml1 inhibits RNR outside of S phase when demand for dNTP synthesis is low and is removed during S phase or in response to DNA damage (*85, 90*). *SML1* overexpression increases the frequency of spontaneous petite colony formation compared to wild-type cells, indicating that mitochondrial genome maintenance is

impaired by the inhibition of cytosolic dNTP synthesis (*89*). To further demonstrate the relationship between the RNR pathway and selfish mtDNA dynamics, we examined whether artificially lowering RNR activity by increasing its inhibition can restore the replicative advantage of small hypersuppressive mtDNA. We cloned *SML1* and confirmed overproduction by immunoblot (Figure 2.4A) and found a significant decrease in the proportion of ρ^+ CFUs from 24.9 ± 5.6% in *Δsml1* cells containing the empty vector, to 5.9 ± 0.7%, 10.3 ±1.6% and 7.2 ± 1.1% in *Δsml1* cells overexpressing *SML1*, *SML1*-FLAG, or *sml1*-FLAG-*Q18del*, respectively (Figure 2.4B and C). Since the Sml1 protein consists of only 111 amino acids, the relative size of the FLAG tag may have lowered its binding and inhibitory effect on Rnr1p, while the Q18 deletion appears to have slightly improved inhibitory function. Consistent with the drop in ρ^+ CFU formation rate, ρ^+ mtDNA level declined approximately five-fold, from 2.23 ± 0.61-fold relative to NUC1 in *Δsml1* cells expressing the empty plasmid to 0.43 ± 0.34-fold upon SML1 expression (Figure 2.4D and E). On the other hand, we observed a small but not statistically significant decrease in the level of HS ρ^- mtDNA upon *SML1* expression. Together, these results indicate that artificially lowering RNR activity enhances the replicative advantage of hypersuppressive over wild-type mtDNA.

2.3.4 *GND1* overexpression increases ρ^+ colony formation in hypersuppressive crosses

The active site of the ribonucleotide reductase large subunit contains redox-active dithiols, which reduce substrate NDPs to dNDPs (*84*). After each reaction, the active site cysteine residues form disulfide bonds. In order to regenerate these residues, electrons are donated by thioredoxin or glutaredoxin, which themselves are reduced by thioredoxin reductase or glutathione reductase, respectively. In both cases, the ultimate electron donor for RNR activity is NADPH (*103*). The oxidative branch of the pentose phosphate pathway (PPP) converts glucose 6-phosphate to ribulose 5-phosphate in three steps, and in the process reduces two molecules of $NADP^+$ to NADPH. If NADPH is limiting for RNR activity in heteroplasmic cells, genetic alterations that increase NADPH production may increase dNTP synthesis and therefore the proportional amount of ρ^+ mtDNA in heteroplasmic cells. To investigate, we cloned three genes that encode two NADPH producing enzymes of

the PPP. *ZWF1* encodes glucose-6-phosphate dehydrogenase (G6PD), which catalyzes the first, rate-limiting step of the PPP. *GND1* encodes the major isoform of 6-phosphogluconate dehydrogenase (6PGD) and is responsible for ~80% of 6PGD activity in yeast (*104*), while *GND2* encodes a minor 6PGD isoform.

We found that *GND1* overexpression increased ρ^+ CFU formation in hypersuppressive crosses from 7.0 ± 2.5% in diploids containing the empty vector, to 13.6 ± 4.5% in diploids containing the *GND1* plasmid. On the other hand, *ZWF1* and *GND2* overexpressing crosses showed no significant differences from controls (Figure 2.5A and B). These results indicate that 6PGD, but not G6PD, can affect mtDNA heteroplasmy.

2.3.5 Low dNTP concentration enhances the replicative advantage of small template DNA over large *in vitro*

Overexpression of *RNR1* or the *Δsml1* mutation are known to positively regulate dNTP concentration and mtDNA copy number in yeast, and our experimental results suggest that relatively low dNTP concentration may contribute to the replicative advantage of small mtDNA. To further illustrate the effect of low dNTP concentration, we tested competitive amplification by PCR using Ex Taq or KOD Dash polymerases and templates of different size (Figure 2.6A). We examined a dNTP concentration rage of 0 to 20μM, as these levels reflect physiological dNTP concentrations within mammalian mitochondria (*105*).

Consistent with our observations of suppressive mtDNA in yeast crossing experiments, the small template was amplified much more readily compared to large at dNTP concentrations of <10 μM (Figure 2.6B and C; F and G). The strength of this effect varied between the two polymerases tested; however, the replicative advantage of the smallest template decreased with increasing dNTP concentration and signals from either large PCR product (2,866 or 1,630-bp) did not significantly exceed those of the small (187-bp) PCR product at any dNTP concentration. On the other hand, during PCR amplification of two templates of closer size, the small template only displayed a replicative advantage at 2.5 μM with one of the two polymerases under our experimental conditions (Figure 2.6D and E). Additionally, PCR reactions using a mixture of all three templates showed that the smallest template was amplified almost exclusively at dNTP concentrations of <7.5 μM

(Figure 2.6H and I). These data show that dNTP concentration and the relative sizes of templates are important factors in replicative advantage during PCR.

2.4 Discussion

Disruption of dNTP balance or availability within mitochondria has been previously linked to mtDNA depletion and disease (*106-108*) and promotes mtDNA deletion mutagenesis in cultured cells (*105*). In this chapter, we demonstrated that the replicative advantage of moderately suppressive or hypersuppressive mtDNA molecules is partially due to insufficient dNTP synthesis by RNR. Competition between small and full-length mtDNA in heteroplasmic cells is naturally weighted against a larger allele; however, reducing RNR activity appears to enhance the replicative advantage of small mtDNA. Indeed, competitive amplification of a mixture of small and large templates via PCR showed that the replicative advantage of small DNA is affected by relative template size and dNTP concentration *in vitro*. Though mtDNA replication *in vivo* by mtDNA polymerase γ occurs under physiological conditions and in conjunction with the mitochondrial replisome, both mtDNA polymerase γ and Taq polymerases are derived from family A DNA polymerases (*109*), while KOD enzymes belong to family B (*110*), which possess a catalytic "palm" domain homologous to family A polymerases. Both PCR enzymes showed a general trend of increasing replicative advantage for smaller templates as dNTP concentrations decrease. Taken together, these results support a model wherein dNTP synthesis by RNR influences the extent of the replicative advantage of small mtDNA in yeast, and therefore affects mtDNA heteroplasmy level and respiratory function (Figure 2.7).

Nuclear DNA damage in yeast activates the Mec1/Rad53 nuclear checkpoint pathway, halts the cell cycle (*87*), and increases dNTP production through the removal of Sml1 (*85, 90*) and increases transcription of the RNR genes (*83*). Importantly, checkpoint activation was shown to increase mtDNA copy number by as much as twofold in *Δrrm3* and *Δsml1* deletion mutants (*86*). However, as shown in Figure 2.1, the *Δrrm3* mutation did not increase the proportion of ρ^+ CFUs formed during heteroplasmy with HS ρ^- mtDNA, suggesting that the increased mtDNA point-

mutagenesis of the *Δrrm3* background (*111*) may have suppressed any beneficial effect of increased RNR activity.

We previously showed that the Mhr1 pathway regulates DSB-induced RDR in response to oxidative stress. The *ori5* region is particularly sensitive to oxidative modification, and following exposure to H_2O_2, Ntg1 was shown to increase DSB formation in this locus (*10, 59*). Supporting this notion, the mitochodrially-targeted DSB-binding protein MmKu binds preferentially to the *ori5* region, though *Δntg1* cells showed only a slight decrease in MmKu binding, indicating that additional factors likely contribute to DSB formation at *ori5* (*62*). DSBs are substrates of Din7, which catalyzes 5' end resection to yield 3'-ssDNA tails, which can then be used for homologous pairing by Mhr1 to initiate RDR (*61*). Compared to 85.7-kbp wild-type mtDNA, the 1.1-kbp genome of HS [*ori5*] ρ^- mtDNA has a much higher density of active *ori* sequences. Therefore, reduced Mhr1 pathway activity in the *Δdin7* background could be expected to disproportionately inhibit the replication of HS [*ori5*] ρ^- mtDNA compared to wild-type. In our experiments, crosses of *Δdin7* mutants did show a small but statistically significant increase (P = 0.002) in the ρ^+ CFU formation rate compared to wild-type crosses. However, due to the presence of a functional SML1 gene, any benefit for wild-type mtDNA synthesis in the *Δdin7* background was likely reduced due to the suppression of dNTP synthesis. Indeed, the *Δdin7Δsml1* background showed an additive effect compared with *Δdin7* (P = 0.003) or *Δsml1* (P = 0.032) single-mutants, indicating that dNTP availability plays an important regulatory role in the replicative advantage of HS ρ^- mtDNA.

RNR is considered an attractive target for inhibiting cell proliferation in cancer therapy and other diseases. Our study in yeast suggests that inhibiting dNTP synthesis may produce the undesirable side effect of increasing the replicative advantage of small mtDNAs, which are associated with aging and several diseases in humans (see *112* for review). Precisely how RNR may contribute to human aging and disease in this context remains for future study.

2.5 Figures and Table

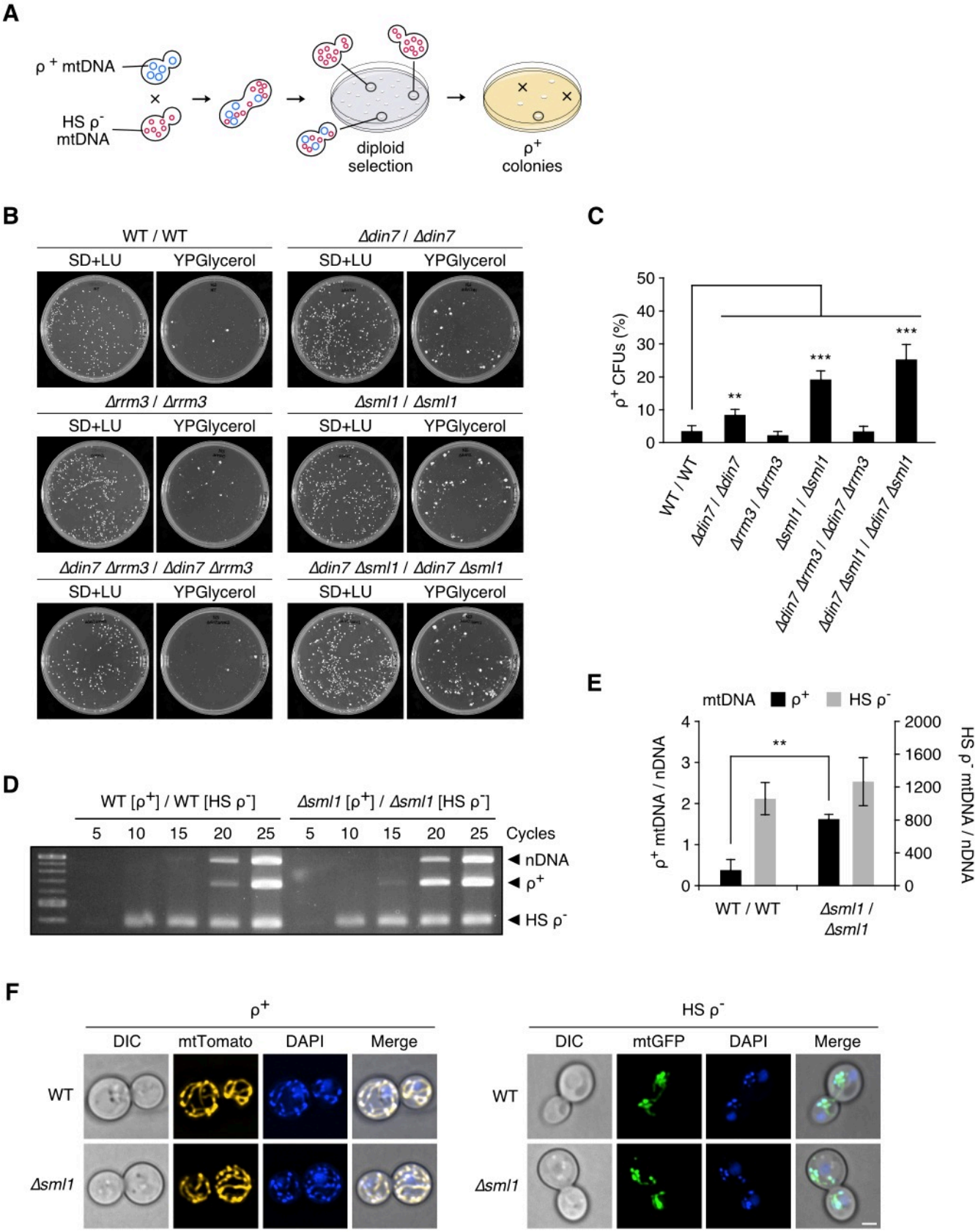

Figure 2.1 | *SML1* deletion increases the proportional amounts of ρ^+ colonies and full-length mtDNA during heteroplasmy with hypersuppressive mtDNA. (A) Scheme of crossing experiments to monitor the hypersuppressive phenotype. (B) Representative images of diploid selection and glycerol plates from crossing experiments. (C) Quantified results from crossing experiments with the diploid genotypes: WT/WT (*n* = 7); *Δdin7*/*Δdin7* (*n* = 3); *Δrrm3*/*Δrrm3* (*n* = 3); *Δsml1*/*Δsml1* (*n* = 6); *Δdin7Δrrm3*/*Δdin7Δrrm3* (*n* = 3); *Δdin7Δsml1*/*Δdin7Δsml1* (*n* = 3). (D) PCR amplification of nuclear and mitochondrial DNA from WT/WT and *Δsml1*/*Δsml1* heteroplasmic cells washed from master plates 2 d after crossing. (E) Quantification of ρ^+ and HS ρ^- mtDNA levels relative to nDNA signals. (F) Microscopic observation of mitochondrial morphology in wild-type or *Δsml1* cells by plasmid expression of mtTomato or mtGFP to visualize the mitochondria of parental ρ^+ and HS ρ^- cells, respectively. DAPI signals indicate mt-nucleoids. Quantified mtDNA levels are from three independent PCR experiments. Error bars indicate ±SD. ** $P < 0.005$, *** $P < 0.0005$. Scale bar = 2 μm.

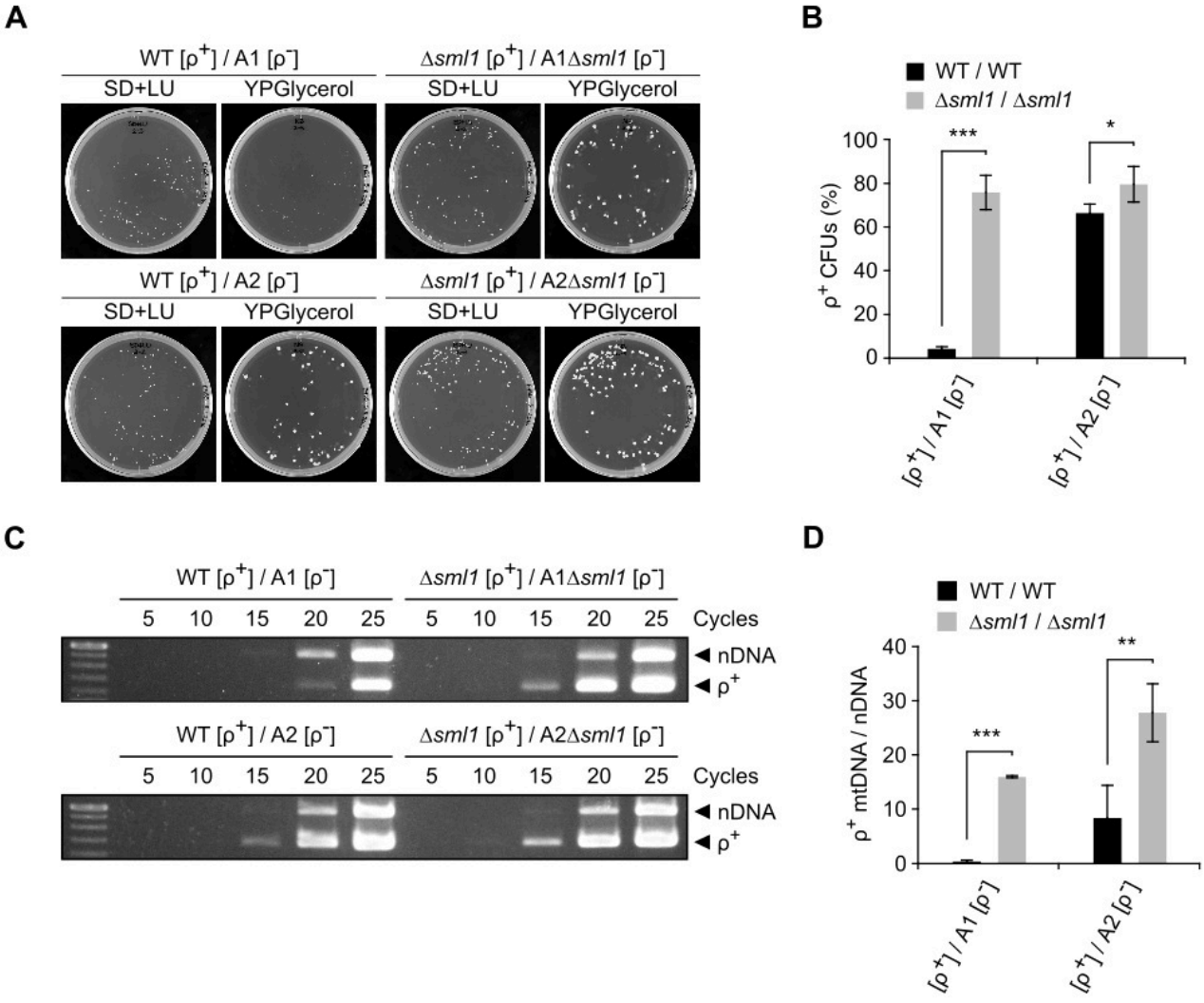

Figure 2.2 | Effect of *SML1* deletion on heteroplasmic cells containing different HS ρ^- and normal suppressive ρ^- alleles. (A) Representative images of diploid selection and glycerol plates from crossing experiments. (B) Quantified crossing results from crossing experiments with the diploid genotypes: WT/A1 (*n* = 3); *Δsml1*/A1*Δsml1* (*n* = 3); WT/A2 (*n* = 4); *Δsml1*/A2*Δsml1* (*n* = 4). (C) PCR amplification of nuclear and mitochondrial DNA from WT/A1, *Δsml1*/A1*Δsml1*, WT/A2 and *Δsml1*/A2*Δsml1* heteroplasmic cells washed from master plates 2 d after crossing. (D) Quantification of ρ^+ and HS ρ^- mtDNA levels relative to nDNA signals. Quantified results were obtained from independent crossing experiments for WT/A1 (*n* = 3); *Δsml1*/A1*Δsml1* (*n* = 3); WT/A2 (*n* = 4); and *Δsml1*/A2*Δsml1* (*n* = 4) cells. Error bars indicate ±SD. * $P < 0.05$, ** $P < 0.005$, *** $P < 0.0005$.

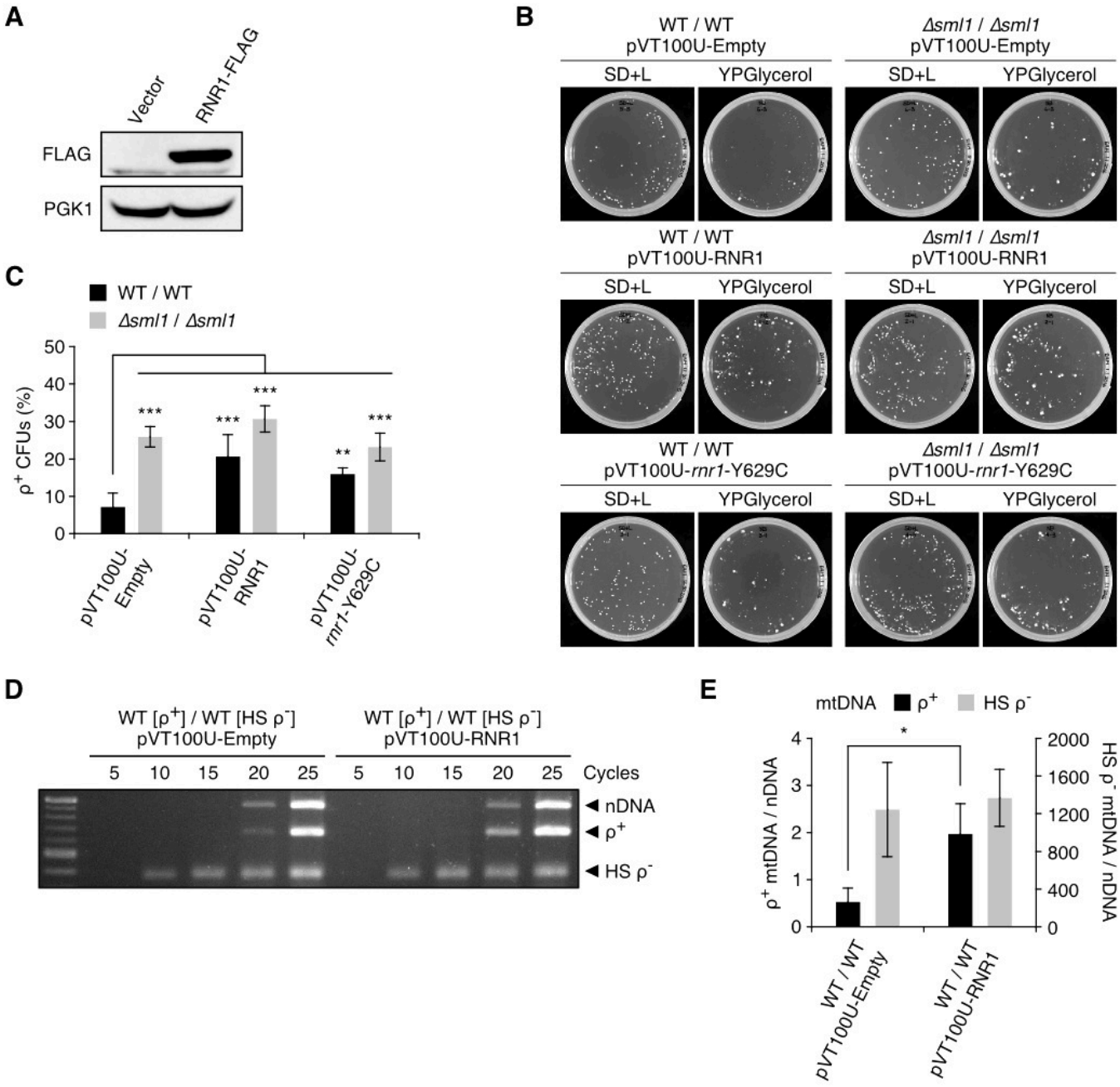

Figure 2.3 | *RNR1* overexpression increases respiratory function and ρ+ mtDNA content in heteroplasmic cells. (A) Immunoblot of *RNR1*-FLAG indicating overexpression in heteroplasmic diploid cells following crossing. (B) Representative images of diploid selection and glycerol plates from crossing experiments of WT/WT or *Δsml1/Δsml1* strains expressing: an empty vector (pVT100U-Empty); overexpressing RNR1 (pVT100U-*RNR1*); or a mutant *rnr1* isoform (pVT100U-*rnr1*-Y629C). (C) Quantified results from crossing experiments with the diploid genotypes:

WT/WT/pVT100U-Empty (*n* = 14); *Δsml1*/*Δsml1*/pVT100U-Empty (*n* = 3); WT/WT/pVT100U-*RNR1* (*n* = 12); *Δsml1*/*Δsml1*/pVT100U-*RNR1* (*n* = 3); WT/WT/pVT100U-*rnr1*-Y629C (*n* = 3); *Δsml1*/*Δsml1*/pVT100U-*rnr1*-Y629C (*n* = 3). (D) PCR amplification of nuclear and mitochondrial DNA from WT/WT heteroplasmic cells expressing pVT100U-Empty or pVT100U-*RNR1* washed from master plates 2 d after crossing. (E) Quantification of ρ^+ and HS ρ^- mtDNA levels relative to nDNA signals. Error bars indicate ±SD. * $P < 0.05$, ** $P < 0.005$, *** $P < 0.0005$.

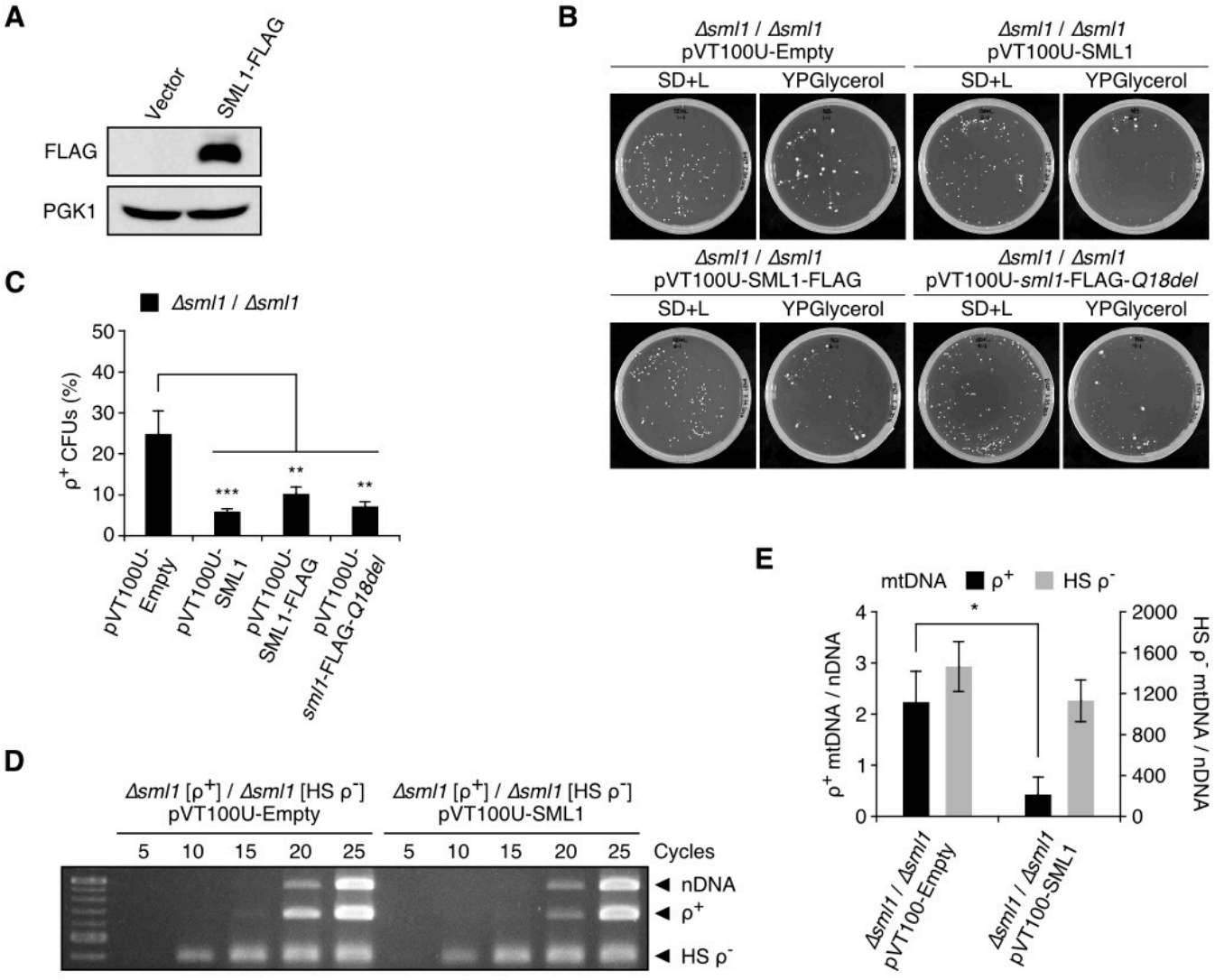

Figure 2.4 | *SML1* overexpression restores the hypersuppressive phenotype in *Δsml1* cells. (A) Immunoblot of *SML1*-FLAG indicating overexpression in heteroplasmic diploid cells following crossing. (B) Representative images of diploid selection and glycerol plates from crossing experiments of *Δsml1*/*Δsml1* strains expressing: an

empty vector (pVT100U-Empty), or overexpressing *SML1* (pVT100U-*SML1*), *SML1*-FLAG (pVT100U-*SML1*-FLAG), or a mutant sml1 isoform (pVT100U-*sml1*-FLAG-Q18del). (C) Quantified results from crossing experiments with the diploid genotypes: *Δsml1*/*Δsml1*/pVT100U-Empty (*n* = 8); *Δsml1*/*Δsml1*/pVT100U-*SML1* (*n* = 8); *Δsml1*/*Δsml1*/pVT100U-*SML1*-FLAG (*n* = 3); *Δsml1*/*Δsml1*/pVT100U-*sml1*-FLAG-Q18del (*n* = 3). (D) PCR amplification of nuclear and mitochondrial DNA from *Δsml1*/*Δsml1* heteroplasmic cells expressing pVT100U-Empty or pVT100U-*SML1* washed from master plates 2 d after crossing. (E) Quantification of ρ^+ and HS ρ^- mtDNA levels relative to nDNA signals. Error bars indicate ±SD. * $P < 0.05$, ** $P < 0.005$, *** $P < 0.0005$.

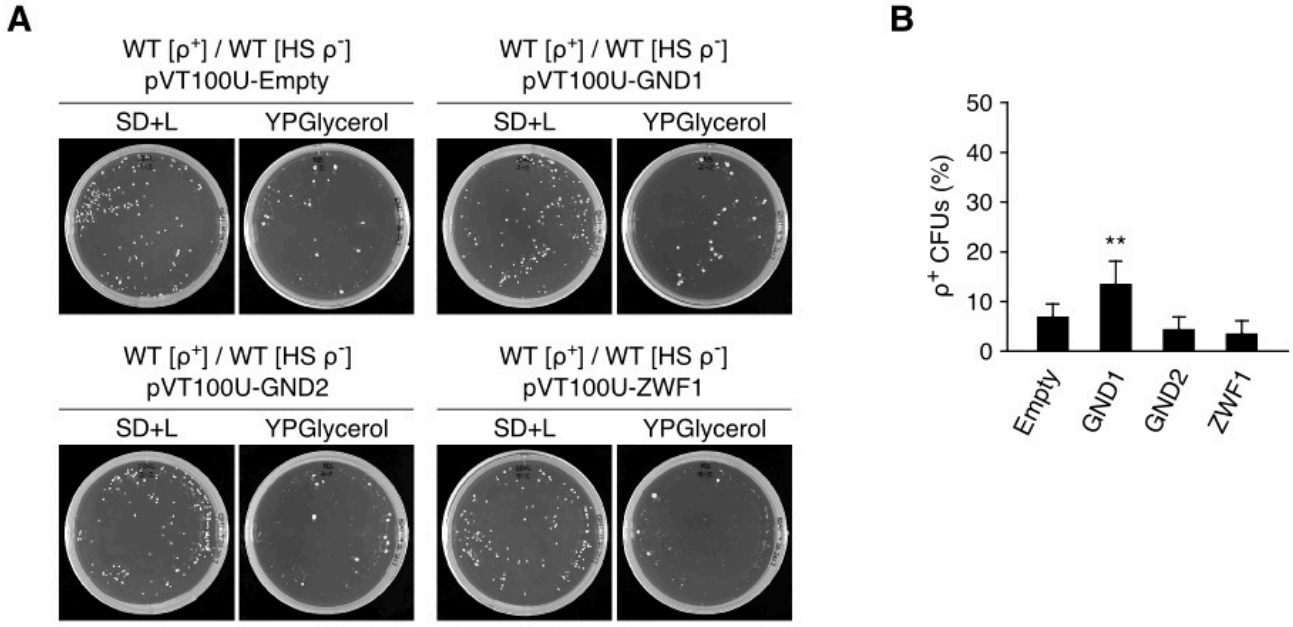

Figure 2.5 | Overexpression of genes encoding the NADPH producing enzymes of the pentose phosphate pathway. (A) Representative images of diploid selection and glycerol plates from crossing experiments of WT ρ^+ / WT HS ρ^- cells expressing an empty vector (pVT100U-Empty); overexpressing GND1 (pVT100U-*GND1*), GND2 (pVT100U-*GND2*), or ZWF1 (pVT100U-*ZWF1*). (B) Quantified results from crossing experiments with the diploid genomes: WT/WT/pVT100U-Empty (*n* = 8); WT/WT/pVT100U-*GND1* (*n* = 8); WT/WT/pVT100U-*GND2* (*n* = 3); WT/WT/pVT100U-*ZWF1* (*n* = 3). Error bars indicate ±SD. ** $P < 0.005$.

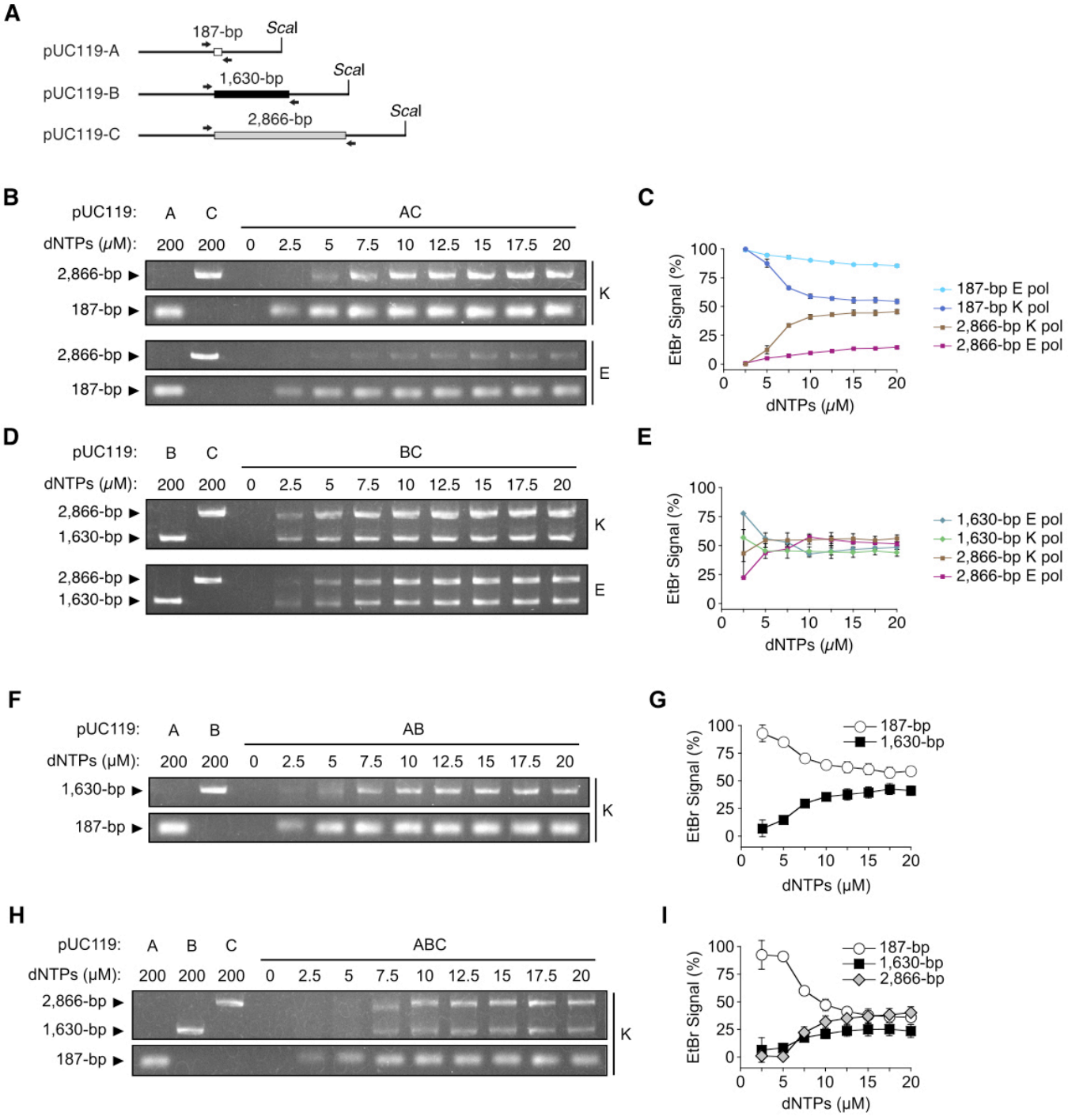

Figure 2.6 | Competitive amplification of DNA templates of different lengths over a range of dNTP concentrations *in vitro*. (A) Schematic of three *Sca*I-linearized pUC119 DNA templates. (B) DNA amplification following 12 PCR cycles with templates pUC119-A and -C in isolation at a dNTP concentration of 200 µM (left), or a mixture of pUC119-A and –C at dNTP concentrations of 0 to 20 µM. (C) Percentage of total

signal representing the relative amounts of 187- or 2,866-bp PCR products at the indicated dNTP concentrations. (D) DNA amplification following 12 PCR cycles with templates pUC119-B and -C in isolation at a dNTP concentration of 200 µM (left), or a mixture of pUC119-B and –C at dNTP concentrations of 0 to 20 µM. (E) Percentage of total signal representing the relative amounts of 1,630- or 2,866-bp PCR products amplified at the indicated dNTP concentrations. (F) DNA amplification following 12 PCR cycles with templates pUC119-A and -B in isolation at a dNTP concentration of 200 µM (left), or a mixture of pUC119-A and –B at dNTP concentrations of 0 to 20 µM. (G) Percentage of total signal representing the relative amounts of 187- or 1,630-bp PCR products at the indicated dNTP concentrations. (H) DNA amplification following 12 PCR cycles with templates pUC119-A, -B and -C in isolation at a dNTP concentration of 200 µM (left), or a mixture of pUC119-A, -B and –C at dNTP concentrations of 0 to 20 µM. (I) Percentage of total signal representing the relative amounts of 187-, 1,630- or 2,866-bp PCR products at the indicated dNTP concentrations. K, KOD Dash polymerase; E, Ex Taq polymerase. Results in C, E, G and I represent three independent PCR experiments using KOD Dash polymerase and results in C and E represent two independent experiments using Ex Taq polymerase. Error bars indicate ±SD.

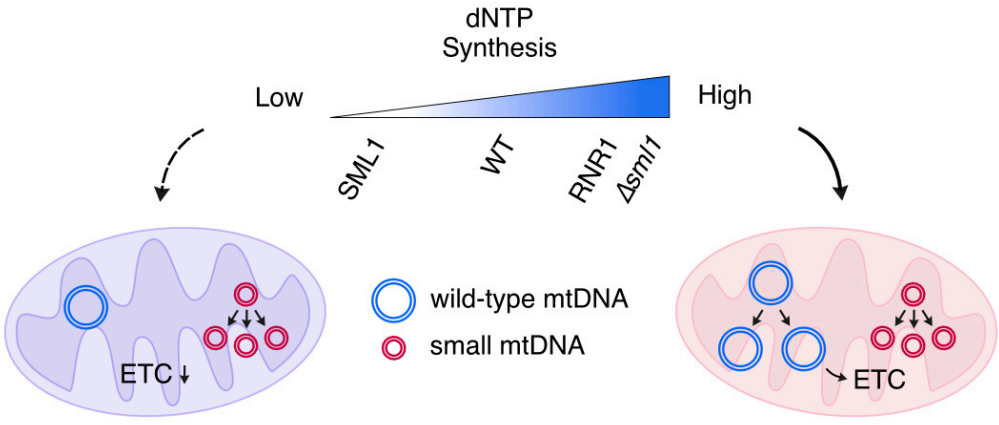

Figure 2.7 | Model for the role of cytosolic dNTP synthesis in regulating the replicative advantage of small mtDNA during heteroplasmy in yeast. Wild-type mtDNA replication and respiratory function in heteroplasmic yeast cells containing a mixture of small and full-length mtDNA is dependent on the level of dNTP synthesis.

Increased dNTP synthesis by SML1 deletion or RNR1 overexpression allows for full-length mtDNA replication, resulting in improved respiratory function due to electron transport chain activity. Reduced dNTP synthesis by SML1 overexpression on the other hand, produces dNTP levels sufficient only for small mtDNA replication.

Table 2.1 | Yeast strains used in this chapter

Strain	Nuclear genotype	Mitochondrial genotype	Source
IL166-5B ρ^0	*MATα his1 trp1 can1*	[ρ^0]	EtBr treatment of IL166-187
OP11c-55R5	*MAT*a *leu2 ura3 trp1*	[ρ^+ ω^- *ens*2 Oli_1^R]	(*57*)
OP11c-55R5/pVT100U	*MAT*a *leu2 ura3 trp1* pVT100U (*URA3*)	[ρ^+ ω^- *ens*2 Oli_1^R]	This study
OP11c-55R5/pVT100U-*GND1*	*MAT*a *leu2 ura3 trp1* pVT100U (*GND1*, *URA3*)	[ρ^+ ω^- *ens*2 Oli_1^R]	This study
OP11c-55R5/pVT100U-*GND2*	*MAT*a *leu2 ura3 trp1* pVT100U (*GND2*, *URA3*)	[ρ^+ ω^- *ens*2 Oli_1^R]	This study
OP11c-55R5/pVT100U-mtTomato	*MAT*a *leu2 ura3 trp1* pVT100U (mtTomato, *URA3*)	[ρ^+ ω^- *ens*2 Oli_1^R]	This study
OP11c-55R5/pVT100U-*RNR1*	*MAT*a *leu2 ura3 trp1* pVT100U (*RNR1*, *URA3*)	[ρ^+ ω^- *ens*2 Oli_1^R]	This study
OP11c-55R5/pVT100U-*rnr1*-Y629C	*MAT*a *leu2 ura3 trp1* pVT100U (*rnr1*, *URA3*)	[ρ^+ ω^- *ens*2 Oli_1^R]	This study
OP11c-55R5/pVT100U-*SML1*	*MAT*a *leu2 ura3 trp1* pVT100U (*SML1*, *URA3*)	[ρ^+ ω^- *ens*2 Oli_1^R]	This study
OP11c-55R5/pVT100U-*ZWF1*	*MAT*a *leu2 ura3 trp1* pVT100U (*ZWF1*, *URA3*)	[ρ^+ ω^- *ens*2 Oli_1^R]	This study
OP11c-55R5 *Δsml1*/pVT100U	*MAT*a *leu2 ura3 trp1 sml1::KAN* pVT100U (*URA3*)	[ρ^+ ω^- *ens*2 Oli_1^R]	This study
OP11c-55R5 *Δsml1*/pVT100U-mtTomato	*MAT*a *leu2 ura3 trp1 sml1::KAN* pVT100U (mtTomato, *URA3*)	[ρ^+ ω^- *ens*2 Oli_1^R]	This study
OP11c-55R5 *Δsml1*/pVT100U-*RNR1*	*MAT*a *leu2 ura3 trp1 sml1::KAN* pVT100U (*RNR1*, *URA3*)	[ρ^+ ω^- *ens*2 Oli_1^R]	This study
OP11c-55R5 *Δsml1*/pVT100U-*rnr1*-Y629C	*MAT*a *leu2 ura3 trp1 sml1::KAN* pVT100U (*rnr*1, *URA3*)	[ρ^+ ω^- *ens*2 Oli_1^R]	This study
OP11c-55R5 *Δdin7*	*MAT*a *leu2 ura3 trp1 din7::URA3*	[ρ^+ ω^- *ens*2 Oli_1^R]	This study
OP11c-55R5 *Δdin7 Δrrm3*	*MAT*a *leu2 ura3 trp1 din7::URA3 rrm3::KAN*	[ρ^+ ω^- *ens*2 Oli_1^R]	This study
OP11c-55R5 *Δdin7 Δsml1*	*MAT*a *leu2 ura3 trp1 din7::URA3 sml1::KAN*	[ρ^+ ω^- *ens*2 Oli_1^R]	This study
OP11c-55R5 *Δrrm3*	*MAT*a *leu2 ura3 trp1 rrm3::KAN*	[ρ^+ ω^- *ens*2 Oli_1^R]	This study
OP11c-55R5 *Δsml1*	*MAT*a *leu2 ura3 trp1 sml1::KAN*	[ρ^+ ω^- *ens*2 Oli_1^R]	This study
W303a-187	*MAT*a *ade2 leu2 his3 ura3 trp1 can1*	[ρ^+ ω^- *ens*2 Chl_{321}^R]	(*58*)
YKN1423A-1	*MATα leu2 ura3 met3*	[HS ρ^-]	(*59*)
YKN1423A-1 *Δsml1*	*MATα leu2 ura3 met3 sml1::KAN*	[HS ρ^-]	This study
YKN1423A-2	*MATα leu2 ura3 met3*	Normal suppressive [ρ^-]	(*59*)
YKN1423A-*2 Δsml1*	*MATα leu2 ura3 met3 sml1::KAN*	Normal suppressive [ρ^-]	This study
YKN1423C-1	*MATα leu2 ura3 met3*	[HS ρ^-]	(*59*)
YKN1423C-1/pVT100U	*MATα leu2 ura3 met3* pVT100U (*URA3*)	[HS ρ^-]	This study
YKN1423C-1/pVT100U-*GND1*	*MATα leu2 ura3 met3* pVT100U (*GND1*, *URA3*)	[HS ρ^-]	This study
YKN1423C-1/pVT100U-*GND2*	*MATα leu2 ura3 met3* pVT100U (*GND2*, *URA3*)	[HS ρ^-]	This study
YKN1423C-1/pVT100U-mtGFP	*MATα leu2 ura3 met3* pVT100U (mtGFP, *URA3*)	[HS ρ^-]	This study
YKN1423C-1/pVT100U-*RNR1*	*MATα leu2 ura3 met3* pVT100U (*RNR1*, *URA3*)	[HS ρ^-]	This study
YKN1423C-1/pVT100U-*rnr1*-Y629C	*MATα leu2 ura3 met3* pVT100U (*rnr1*, *URA3*)	[HS ρ^-]	This study

YKN1423C-1/pVT100U-*ZWF1*	*MATα leu2 ura3 met3* pVT100U (*ZWF1*, *URA3*)	[HS ρ$^-$]	This study
YKN1423C-1 *Δsml1*/pVT100U	*MATα leu2 ura3 met3 sml1::KAN* pVT100U (*URA3*)	[HS ρ$^-$]	This study
YKN1423C-1 *Δsml1*/pVT100U-mtGFP	*MATα leu2 ura3 met3 sml1::KAN* pVT100U (mtGFP, *URA3*)	[HS ρ$^-$]	This study
YKN1423C-1 *Δsml1*/pVT100U-*RNR1*	*MATα leu2 ura3 met3 sml1::KAN* pVT100U (*RNR1*, *URA3*)	[HS ρ$^-$]	This study
YKN1423C-1 *Δsml1*/pVT100U-*rnr1*-Y629C	*MATα leu2 ura3 met3 sml1::KAN* pVT100U (*rnr1*, *URA3*)	[HS ρ$^-$]	This study
YKN1423C-1 *Δdin7*	*MATα leu2 ura3 met3 din7::URA3*	[HS ρ$^-$]	This study
YKN1423C-1 *Δdin7 Δrrm3*	*MATα leu2 ura3 met3 din7::URA3 rrm3::KAN*	[HS ρ$^-$]	This study
YKN1423C-1 *Δdin7 Δsml1*	*MATα leu2 ura3 met3 din7::URA3 sml1::KAN*	[HS ρ$^-$]	This study
YKN1423C-1 *Δrrm3*	*MATα leu2 ura3 met3 rrm3::KAN*	[HS ρ$^-$]	This study
YKN1423C-1 *Δsml1*	*MATα leu2 ura3 met3 sml1::KAN*	[HS ρ$^-$]	This study

Chapter 3: Prevention of mitochondrial genomic instability in *Saccharomyces cerevisiae* by the mitochondrial recombinase Mhr1

3.1 Introduction

3.1.1 The mitochondrial nucleoid protein Abf2

MtDNA is packaged into a nucleoprotein complex termed the mitochondrial nucleoid, which is regarded as the unit of mtDNA inheritance (*113*). Abf2 is a key component of the nucleoid with a histone-like role (*114, 115*), and contains two high mobility group (HMG) domains for the binding and efficient packaging of linear double-stranded DNA without supercoiling (*116*). Abf2 wraps and bends mtDNA, but is not required for activity of promoters at *ori* sequences and has no transcriptional role in yeast (*117-119*). Mutants lacking *ABF2* (*Δabf2*) display a loss-of-mtDNA phenotype when utilizing fermentable carbon sources for growth (*114, 120-122*), but are able to maintain wild-type mtDNA in non-fermentable media, indicating that the requirement for Abf2 in ρ^+ cells is conditional. The *Δabf2* phenotype is considered typical of nuclear gene mutations that affect mtDNA maintenance, since more than 100 nuclear genes that influence mtDNA integrity in yeast have been identified (*123, 124*).

3.1.2 Functional roles of the mtDNA recombinase Mhr1

Mhr1 is a mitochondrial recombinase (*10, 58*) that acts in DSB repair, mediates the predominant form of mtDNA replication in ρ^+ cells (*43, 57, 58, 61, 125*) and increases mtDNA content without additional Abf2 (*10*). DSBs act as substrates for mtDNA replication initiation and can be formed at *ori* sequences by excision repair enzymes such as Ntg1 (*10, 59*). Following procession of DSBs by the 5'-3' exonuclease activity of Din7 (*61*), 3'-single stranded DNA can be used by Mhr1 to form a heteroduplex joint, in which the 3'-single stranded DNA tail serves as a primer to initiate rolling-circle mtDNA replication and produce linear stretches of multiple-unit-sized mtDNA molecules, termed concatemers, which promote segregation of heteroplasmy towards homoplasmy (*43*).

In this chapter, we investigate whether Mhr1-driven mtDNA replication and homologous recombination contribute to the maintenance of mtDNA content and genome integrity in *mhr1-1* cells with a *Δabf2* genetic background, which show a loss-of-mtDNA phenotype in fermentable media due to deletion mutagenesis.

3.2 Materials and methods

3.2.1 Yeast strains and media

Yeast strains used in this chapter are listed in Table 3.1. General genetic techniques used in this chapter are those described by Kaiser *et al*. (*127*). Yeast transformation was carried out using the lithium-acetate method (*94*). The assay for hypersuppressiveness was carried out according to a procedure previously described (*59*). Overexpression of *MHR1* was achieved using a yeast multicopy plasmid with a constitutive promoter (pVT100U; *95*). The ORF (open reading frame) of *MHR1* was amplified by PCR with addition of *Sac*I and *Xba*I restriction sites at the 5' and 3' ends, respectively and inserted into pVT100U to generate pVT100U-*MHR1*. Immunoblot analysis for Mhr1 detection was performed using rabbit antiserum against Mhr1, according to a previously established procedure (*61*).

Media were prepared as previously described (*57-59*). Selective pre-cultivation of cells for respiratory function assays was conducted either in rich glycerol (YPGly), synthetic glycerol (Gly) or synthetic glycerol minus uracil (Gly-U) media. Fermentable media, used to promote loss of respiratory function, was rich glucose (YPD), synthetic glucose (Glu), synthetic glucose minus uracil (Glu-U), synthetic raffinose-galactose (RGal), or synthetic raffinose-galactose minus uracil (RGal-U). Glycerol, glucose, raffinose and galactose concentrations used were 3% v/v, 2%, 2% and 2%, respectively. Selection for diploid cells following crossing with *Δabf2* or *Δabf2 mhr1-1* cells was carried out by cultivating cells in liquid synthetic minimal (SD) or synthetic minimal plus tryptophan (SD+W) medium containing 2% glucose at 30°C overnight and then spreading cells on agar plates containing the same nutrients. For control crosses, diploids were selected by spreading mated cells directly onto synthetic minimal media agar plates containing leucine plus uracil (SD+LU) or tryptophan (SD+W) and 2% glucose.

3.2.2 Mitochondrial nucleoid analysis

WT, *mhr1-1*, *Δabf2* and *Δabf2 mhr1-1* cells were cultivated in YPGly media to early log-phase at 30°C and stained with DAPI. Cells were subsequently transferred to YPD media and cultivated for two consecutive rounds at 30°C or 34°C, stained with DAPI and observed again. DAPI staining was performed by transferring aliquots to fresh media containing 1 μg/ml DAPI and incubating for 15 min. Cells were then washed and resuspended in fresh media and 1% low-melting point agarose at a 1:1 ratio. Cells were then mounted on glass slides and analyzed with a Deltavision fluorescence microscopy system (Applied Precision, Inc.) equipped with an Olympus IX71 microscope. DAPI foci in mother cells were counted using ImageJ software (*96*).

3.2.3 Tetrad analysis

We used an Olympus micromanipulation system for tetrad dissection to separate the four spores encapsulated in an ascus derived from diploid WT/*Δmhr1* cells. Spores were separated and placed on synthetic defined (SD) complete plates supplemented with adenine (A), leucine (L), uracil (U), histidine (H) and tryptophan (W), and cultivated at 30°C for 7 days. Colonies were then replica-plated on SD complete plates lacking L and YPGly plates.

3.2.4 Purification of yeast mtDNA and analysis by restriction digestion

MtDNA was purified from *Δmhr1* spore-derived yeast cells using cesium chloride density-gradient centrifugation (*128*). The purified mtDNA was digested with *Apa*I and run on a 1% agarose gel alongside DNA size markers. The DNA fragments were photographed under ultraviolet irradiation after staining the gel with 0.5 μg/ml ethidium bromide.

3.2.5 Southern blot analysis

Δabf2 and *Δabf2 mhr1-1* cells were cultivated in YPGly media and then transferred to RGal complete media and cultivated at 30°C for two days. Total cellular DNA was then prepared and digested by *Apa*I. Approximately 15 μg of total DNA was separated by electrophoresis on a 1.0% agarose gel, run at 24°C for 80 h at 5 V/cm, and transferred to a nylon membrane (Amersham Hybond N Plus; GE Healthcare). Signals for mtDNA were detected using ^{32}P-labeled full-length mtDNA from budding yeast as a probe. Signals were analyzed using a Typhoon FLA 7000 biomolecular imager (GE Healthcare).

3.2.6 Analysis of mtDNA level by quantitative real-time PCR

Primers used for real-time PCR were as follows: *COX3*-Forward, 5'-TCCATTCAGCTATGAGTCCTGATG-3'; *COX3*-Reverse, 5'-AATTCGGTAGGTTGTACAGCTTCAA-3'; *NUC1*-Forward, 5'-TTTAGGTCGGGCTATGATCGA-3'; *NUC1*-Reverse, 5'-TCCATGGCCTGTTGAGAAAAT-3'. The 20 µl reaction volumes contained 10 µl SYBR Premix Ex Taq^{TM} II (Takara), 0.4 µM of each primer, and 100 ng of template genomic DNA. A LightCycler 480 (Roche) was used for real-time PCR analysis.

3.3 Results

3.3.1 Double-mutant *Δabf2 mhr1-1* cells rapidly lose respiratory function in fermentable media

In order to examine severely compromised mtDNA maintenance, we opted to examine *Δabf2* cells, which display a well-documented loss-of-mtDNA phenotype upon cultivation in fermentable media (*114, 120, 121*). In order to compare the extent of respiratory function loss in these backgrounds, we first selectively pre-cultivated wild-type (WT), single-mutant *Δabf2*, *mhr1-1,* or double-mutant *Δabf2 mhr1-1* cells in glycerol medium, a carbon source requiring mitochondrial respiration for its utilization. We then transferred the cells to synthetic complete fermentable media containing glucose (Glu) or raffinose and galactose (RGal) as carbon sources. While both Glu and RGal media are fermentable, the use of RGal allows for distinction from the transcriptional effects of glucose, which changes the global gene expression pattern (*122*). We cultivated cells for nearly eight generations at 30°C or 34°C (Fig. 3.1A) and then spread equal amounts of dilute culture of each strain onto rich glucose (YPD) and rich glycerol (YPGly) plates (Fig. 3.1B). The proportion of colony-forming units (CFUs) that retained mitochondrial respiratory activity and were thus able to grow on YPGly, compared to the total number of CFUs on YPD, was quantified (Fig. 3.1C).

We observed that WT cells retained almost all respiratory function under each condition, while *Δabf2* cells showed remarkable loss of respiratory activity in Glu media, to 59.1 ± 5.9% ρ^+ at 30°C and 14.0 ± 5.3% ρ^+ at 34°C. On the other hand, cultivation of *Δabf2* cells in RGal medium resulted in a large proportion of cells

retaining respiratory activity, forming ρ^+ CFUs at rates of 103.9 ± 14.3% at 30°C and 83.9 ± 20.7% at 34°C. These observations appear consistent with the previously reported mtDNA instability phenotype of *Δabf2* cells in glucose (*120*). In the *mhr1-1* background, a large proportion of CFUs retained respiratory activity, with ρ^+ CFU formation rates of 103.9 ± 0.7% and 77.6 ± 6.0% ρ^+ in Glu, and 96.5 ± 13.5% and 83.7 ± 10.6% ρ^+ in RGal, at 30°C and 34°C, respectively. The slight decrease in respiratory activity of *mhr1-1* cells grown at 34°C was previously observed as *mhr1-1* temperature sensitivity (*43*, *57*). Furthermore, *Δabf2 mhr1-1* double-mutant cells displayed ρ^+ CFU formation rates of 68.3 ± 10.4% and 15.4 ± 7.3% ρ^+ in Glu, and 64.3 ± 8.8% and 37.2 ± 3.7% ρ^+ in RGal, at 30°C and 34°C, respectively. Severe, temperature-dependent loss of respiratory function occurred in the *Δabf2* single-mutant in Glu but not RGal, while *Δabf2 mhr1-1* double mutant cells displayed an additive increase in temperature sensitivity in RGal. These results indicate that loss of mitochondrial function in this background occurs independently of glucose repression.

We next explored the effect of extended cultivation time on loss of cellular respiratory function. We pre-cultivated the four strains in YPGly medium, then transferred the cells to RGal medium and cultivated for approximately 20 generations (Fig. 3.1D). Finally, we spread the cells on YPD and subsequently replicated the colonies onto YPGly plates (Fig. 3.1E), or simultaneously spread equal amounts of dilute culture onto YPD and YPGly plates (Fig. 3.1F). In contrast to WT and *mhr1-1* single-mutant cells, which remained almost entirely ρ^+, only 27.0 ± 18.4% of the *Δabf2* cells were able to form ρ^+ colonies on glycerol plates following simultaneous spreading. Remarkably, none of the *Δabf2 mhr1-1* double-mutant cells were able to grow on YPGly plates after growth for approximately 20 generations in RGal (Fig. 3.1G). Therefore, extended cultivation of the *Δabf2* single-mutant in fermentable RGal media increases loss of cellular respiratory function, while the additional loss of Mhr1 function causes rapid and complete loss of cellular respiratory function (*120*, *124*, *129*).

3.3.2 Nucleoid numbers are significantly reduced in *Δabf2 mhr1-1* cells

Next, we investigated the relative abundance of mtDNA nucleoids in WT, *Δabf2* or *mhr1-1* single-mutant, or *Δabf2 mhr1-1* double-mutant cells selectively

grown in YPGly media, or grown in YPD media at 30°C or 34°C for more than 20 generations (Fig. 3.2). In *Δabf2* single-mutants, approximately 27% of CFUs remained ρ^+ after cultivation in glucose (Fig. 3.1G), yet all *Δabf2* mother cells we observed displayed mtDNA-derived nucleoid signals after cultivation in YPD at 30°C (Fig. 3.2B), suggesting that loss of respiratory function in *Δabf2* cells may be due to mtDNA deletion mutagenesis. In addition, double-mutant *Δabf2 mhr1-1* cells showed the lowest number of mitochondrial nucleoid signals after cultivation in YPD media (Fig. 3.2A-B), and nucleoid signals were absent from 44.4% of *Δabf2 mhr1-1* mother cells following cultivation at 34°C, compared to 0% of WT and *mhr1-1* cells and only 10.0% of *Δabf2* mother cells. These results indicate that mtDNA maintenance is defective without Abf2 and fully functional Mhr1. Since we observed that respiratory function and nucleoid abundance generally decrease in *Δabf2 mhr1-1* cells relative to *Δabf2* cells, it is likely Mhr1 plays a role in protecting mtDNA genomic integrity.

3.3.3 Loss of *MHR1* causes mtDNA fragmentation

In order to demonstrate that Mhr1 is required to maintain mtDNA integrity, we introduced *mhr1::LEU2* DNA fragments into WT/WT diploid cells to disrupt one of the two *MHR1* alleles, thereby creating haploinsufficient WT/*Δmhr1* diploid cells (see: Table 3.1). We then conducted tetrad analysis to determine whether haploid spores with the nuclear genotype *mhr1::LEU* (*Δmhr1*) retain respiratory function. All leucine prototrophic spores were unable to grow on YPGly plates, confirming that the *Δmhr1* mutation causes complete loss of respiratory function (Fig. 3.3A). We further cultivated WT cells and *Δmhr1* spores (Figure 3.3B, a-g) in glucose medium, after selecting cells that still displayed mtDNA signals upon DAPI-staining. *Apa*I-digests of mtDNA from wild-type cells gave rise to many discrete bands, while *Apa*I-digests of mtDNA from *Δmhr1* cells gave only a few discrete bands (Fig. 3.3B), indicating mtDNA deletions also occur in *Δmhr1* cells with some observable amounts of mtDNA remaining.

3.3.4 MtDNA deletion mutagenesis in *Δabf2 mhr1-1* cells

To determine whether mtDNA deletion mutagenesis or the complete loss of mtDNA occurred in *Δabf2* single- or *Δabf2 mhr1-1* double-mutant cells, we analyzed suppressiveness according to previously established methods (*59*). The degree of suppresiveness is determined by: (1) The length of the remnant mtDNA molecule

after undergoing a deletion and (2) the preservation of an active *ori* sequence (Fig. 3.4A). Small mtDNA deletions result in relatively large remnant molecules. Therefore, when crossed with ρ^+ haploid cells, small mtDNA deletion-bearing cells give rise to diploid populations that are in a range of 10% to 90% ρ^+. In contrast, when mitochondrial genomes undergo a large deletion event but retain at least one active replication origin, crosses of these haploid cells with ρ^+ haploid cells of the opposite mating type will give rise to <5% ρ^+ diploid progeny, a phenotype termed "hypersuppressive" (*130*). Finally, crossing haploid cells without mtDNA (ρ^0) with ρ^+ haploid cells will result in 100% ρ^+ diploid progeny, a phenotype termed "non-suppressive".

We crossed a ρ^+ strain with haploid WT ρ^+, ρ^-, HS ρ^- or ρ^0 cells as controls (Fig. 3.4B, top four panels) and *Δabf2* or *Δabf2 mhr1-1* cells, and analyzed the respiratory phenotypes of the resulting diploid progeny. In crosses with the *Δabf2* background, 20% ~ 80% of diploid colonies were ρ^+, with a single distribution centered at around 55% ρ^+ (Fig 3.4B, second panel from bottom). In contrast to this moderately suppressive phenotype, crossing Δ*abf2 mhr1-1* cells yielded a bimodal distribution in which resulting diploid cells either displayed a hypersuppressive, or moderate to non-suppressive phenotype, ranging from 0% ~ 20% and 50% ~ 100% ρ^+, respectively (Fig. 3.4B, bottom panel). These results indicate that large-scale mtDNA deletions or the complete loss of mtDNA occurs in *Δabf2 mhr1-1* cells, suggesting that the increased production of ρ^- progeny (Fig. 3.1C and G) is due to a deficiency of Mhr1-driven mtDNA recombination.

Next, we analyzed mtDNA from ρ^- *Δabf2* and *Δabf2 mhr1-1* colonies by Southern blot analysis. Compared to ρ^+ WT and *Δabf2* controls (Figure 3.5A), we observed that ρ^- *Δabf2* mtDNA generally lacked several mtDNA-specific bands that were present in ρ^+ mtDNA (Figure 3.5B). Similarly, *Δabf2 mhr1-1* double-mutant cells generally lacked many mtDNA-specific bands and some samples lacked mtDNA signals altogether, compared to the signals derived from ρ^+ WT and *mhr1-1* cells (Figure 3.5A and B). Also, to our surprise we observed several more small, mtDNA-specific bands in the *mhr1-1* control compared to the ρ^+ WT and *Δabf2* controls. One explanation is that mtDNA deletions caused by the *mhr1-1* mutation result in

heteroplasmy, which would be stable since the *mhr1-1* mutation delays mitochondrial allele segregation (*59*). Collectively, these results indicate that mtDNA deletions occur in ρ^- *Δabf2* cells and that large-scale mtDNA deletion or the complete loss of mtDNA occurs in ρ^- or ρ^0 *Δabf2 mhr1-1* cells.

3.3.5 Mhr1 overproduction prevents mtDNA deletion mutagenesis

To verify that Abf2 and Mhr1 are required for mtDNA maintenance, we analyzed mtDNA levels relative to nuclear DNA using quantitative PCR (*131*). We observed that the mtDNA level in *Δabf2* cells was less than half (46.3 ± 8.6%) that of WT cells grown in YPGly medium (Fig. 3.6A). Consistent with our previous results (*57*), a large proportion (83.9 ± 15.3%) of mtDNA content was retained in *mhr1-1* cells grown in glycerol medium, while we observed no additive effect on the depletion of mtDNA in *Δabf2 mhr1-1* double-mutant cells (51.4 ± 8.8%), suggesting Abf2 is dispensable for Mhr1-driven mtDNA replication (Fig. 3.6A).

To investigate the effects of increasing the amount of Mhr1 on mtDNA content and cellular respiratory function, we constitutively overexpressed *MHR1* under the ADH promoter via plasmid in *Δabf2* single-mutant and *Δabf2 mhr1-1* double-mutant cells, and confirmed Mhr1 overproduction by immunoblot analysis (Fig. 3.6B). qPCR analysis revealed that *Δabf2 mhr1-1* double-mutant cells harboring an empty vector had 68.4 ± 11.9% of the mtDNA level of wild-type cells. In contrast, Mhr1 overexpression resulted in an mtDNA level of 97.5 ± 26.5% (Fig. 3.6C).

To examine whether exogenous *MHR1* expression rescues respiratory function, we compared *Δabf2* single-mutant and *Δabf2 mhr1-1* double-mutant cells harboring empty (pVT) or *MHR1*-overexpressing plasmids (pVT-*MHR1*) after 48 hours of growth (equivalent to less than eight generations) in fermentable glucose minus uracil (Glu-U) or raffinose-galactose minus uracil (RGal-U) media at 30°C or 34°C (Fig. 3.6D). We then spread equal amounts of dilute culture on YPD and YPGly plates, as described in Fig. 3.1. Glucose strongly reduced respiratory growth levels in *Δabf2*/pVT cells, a result closely matching that in *Δabf2* cells without plasmid DNA (Fig. 3.1C). *Δabf2*/pVT cells grown in Glu-U medium produced 67.0 ± 6.9% ρ^+ colonies at 30°C and only 16.1 ± 9.4% at 34°C. In contrast, *Δabf2*/pVT cells yielded 92.9 ± 13.3% and 94.6 ± 10.8% ρ^+ colonies when grown in RGal-U at 30°C or 34°C, respectively. In agreement with our result from *Δabf2* cells, cellular respiratory

function is significantly reduced following cultivation of *Δabf2*/pVT cells at 34°C in Glu-U medium, but not in RGal-U. There was a small decrease in respiratory growth upon *MHR1*-overexpression in the *Δabf2*/pVT-*MHR1* cells in Glu-U or RGal-U media at either 30°C or 34°C, indicating that additional Mhr1 is not sufficient to offset a lack of Abf2. Although nucleoid formation defects in the *Δabf2* background cause respiratory defects (*113*), it is very likely such defects are unable to be prevented by *MHR1*-overexpression. On the other hand, ρ^+ CFU formation rates were only 50.3 ± 14.8% and 3.3 ± 4.2% in *Δabf2 mhr1-1*/pVT cells in Glu-U medium at 30°C, and 34°C, respectively. Importantly, *Δabf2 mhr1-1*/pVT cells also displayed highly temperature-sensitive respiratory function after cultivation in RGal-U, giving ρ^+ CFU formation rates of 81.0 ± 6.6% and 12.4 ± 7.4% at 30°C and 34°C, respectively. Addition of *MHR1* in *Δabf2 mhr1-1*/pVT-*MHR1* cells significantly rescued the respiratory function of these cells in RGal-U at 34°C, to a ρ^+ CFU formation rate of 69.1 ± 27.5%. On the other hand, *Δabf2 mhr1-1*/pVT-*MHR1* cells cultivated in Glu-U showed no rescue effect, with ρ^+ CFU formation rates of 54.5 ± 3.2% and 6.3 ± 6.8% at 30°C and 34°C, respectively (Fig. 3.6E and F).

To further advance the notion that Mhr1 can protect mtDNA integrity, we examined the effect of an extended cultivation time in fermentable media of approximately 20 generations. Simultaneous spreading of *Δabf2 mhr1-1*/pVT and *Δabf2 mhr1-1*/pVT-*MHR1* cells onto YPD and YPGly plates (Fig. 3.6G) yielded 4.5 ± 4.1% and 54.0 ± 3.6% ρ^+ CFUs, respectively (Fig. 3.6H and I), reinforcing the notion of a rescue effect for additional Mhr1 in RGal-U media. Similarly, replica-plating *Δabf2 mhr1-1*/pVT and *Δabf2 mhr1-1*/pVT-*MHR1* colonies from RGal-U to YPGly plates showed a clear increase in the proportion of ρ^+ CFUs upon *MHR1* overexpression (Fig. 3.6J and K), while only a small proportion of CFUs remained ρ^+ after cultivation in Glu-U medium (Fig. 3.6L and M). These results indicate that glucose impairs Mhr1-mediated action, which protects against mtDNA deletions. In summary, Mhr1 functions to prevent loss of respiratory function due to mtDNA deletion mutagenesis, although deletions are not completely prevented by overproduced Mhr1 (Fig. 3.7).

3.4 Discussion

In this chapter, we found that increasing Mhr1 protein level partially prevents loss of respiratory function in cells lacking Abf2 and functional Mhr1*,* which display an mtDNA-instability phenotype similar to several other nuclear mutations in yeast. Our results provide further support for the notion that Mhr1 has a pivotal role in the maintenance of mitochondrial genomic integrity (*132*), and that DSB-induced mtDNA replication by Mhr1 is the predominant replication form of mtDNA replication in ρ^+ yeast cells (*62*). We previously reported that Mhr1-dependent mtDNA replication and homologous recombination are crucial for repair of mtDNA DSBs (*61*). Collectively, our results here suggest that mitochondrial homologous DNA recombination may have utility in preventing spontaneous generation of mtDNA deletions in a variety of circumstances (Fig. 3.7).

The requirement for Abf2 and Mhr1 in mtDNA stability raises the question of how increasing the amount of Mhr1 alone prevents generation of deleted mtDNA and helps to sustain cellular respiratory function. The answer likely comes from one of the mechanisms of mtDNA deletion formation proposed by Krishnan *et al.*, in which mtDNA deletions occur during repair of damaged mtDNA with DSBs, rather than during replication (*133*). We inferred that a lack of Abf2 might weaken DSB repair by homologous recombination and increase the accumulation of deleted mtDNA molecules*.* Since DSB repair can be accomplished by homologous DNA recombination (*134-136*), an increased amount of Mhr1 may enhance the number of homologous DNA recombination events to repair DSBs (*61*). This interpretation implies that mtDNA deletions are prevented, mtDNA integrity is maintained, and a large proportion of cells with the *Δabf2* mutation sustain respiratory function upon overexpression of *MHR1* (Fig. 3.6). On the other hand, since mtDNA deletion mutagenesis still occurs upon Mhr1 overproduction in *Δabf2* cells, the stabilization of mtDNA recombination intermediates by Abf2 (*120*) is important. In addition, we found that a fraction of the population of *Δabf2 mhr1-1* cells contains HS ρ^- mtDNA molecules (less than 20%; Fig. 3.4B), however this proportion is likely large enough to reduce the beneficial effect of Mhr1 overproduction on preventing deleterious mtDNA mutations. Due to the presence of HS ρ^- mtDNA mutant molecules, Mhr1

overexpression likely increases the amounts of both wild-type and HS ρ^- mtDNA. Thus, it is very unlikely that the observed rescue of respiratory function in *Δabf2 mhr1-1* cells upon *MHR1* overexpression (Fig. 3.6) is due only to increase replication and selection for wild-type mtDNA over deleterious mtDNA mutations. These results therefore indicate that increased amounts of Mhr1 can prevent mitochondrial genomic instability.

Mhr1 promotes homologous DNA pairing (*58*, *126*), while Abf2 packages mtDNA and is the main component of the nucleoid (*113*). Both of these molecular functions resemble that of RecA in *Escherichia coli*. RecA forms a nucleoprotein complex that both ensures the formation of heteroduplex DNA and protects DNA from nuclease degradation (*137*). Since these roles are performed by discrete proteins in *S. cerevisiae* mitochondria, whether mtDNA-Mhr1 nucleoprotein formation occurs prior to packaging of concatemeric mtDNA molecules by Abf2 or by a contrary process remains for further investigation.

TFAM, the mammalian ortholog of Abf2, contains an additional C-terminal domain predicted to be essential for transcription (*119*). TFAM can complement Abf2 in yeast by rescuing the loss-of-mtDNA phenotype of yeast *Δabf2* cells (*138*). In contrast to Abf2/TFAM, the existence of a metazoan ortholog of Mhr1 and therefore the occurrence of mtDNA recombination in animals remains an open issue (*139*). To date, there have been several lines of evidence to indicate that human mtDNA recombination may occur (*140-142*). For example, we demonstrated that ROS stimulate mitochondrial allele segregation from heteroplasmy towards homoplasmy in human fibroblasts (*11*), a result consistent with the stimulatory effect of ROS and mechanism of recombination-driven mtDNA replication in yeast mitochondria (*10*). Consistent with the results reported here, a method to stimulate recombination function in human mitochondria may similarly prevent human mtDNA instability and present numerous other health benefits.

3.5 Figures and Table

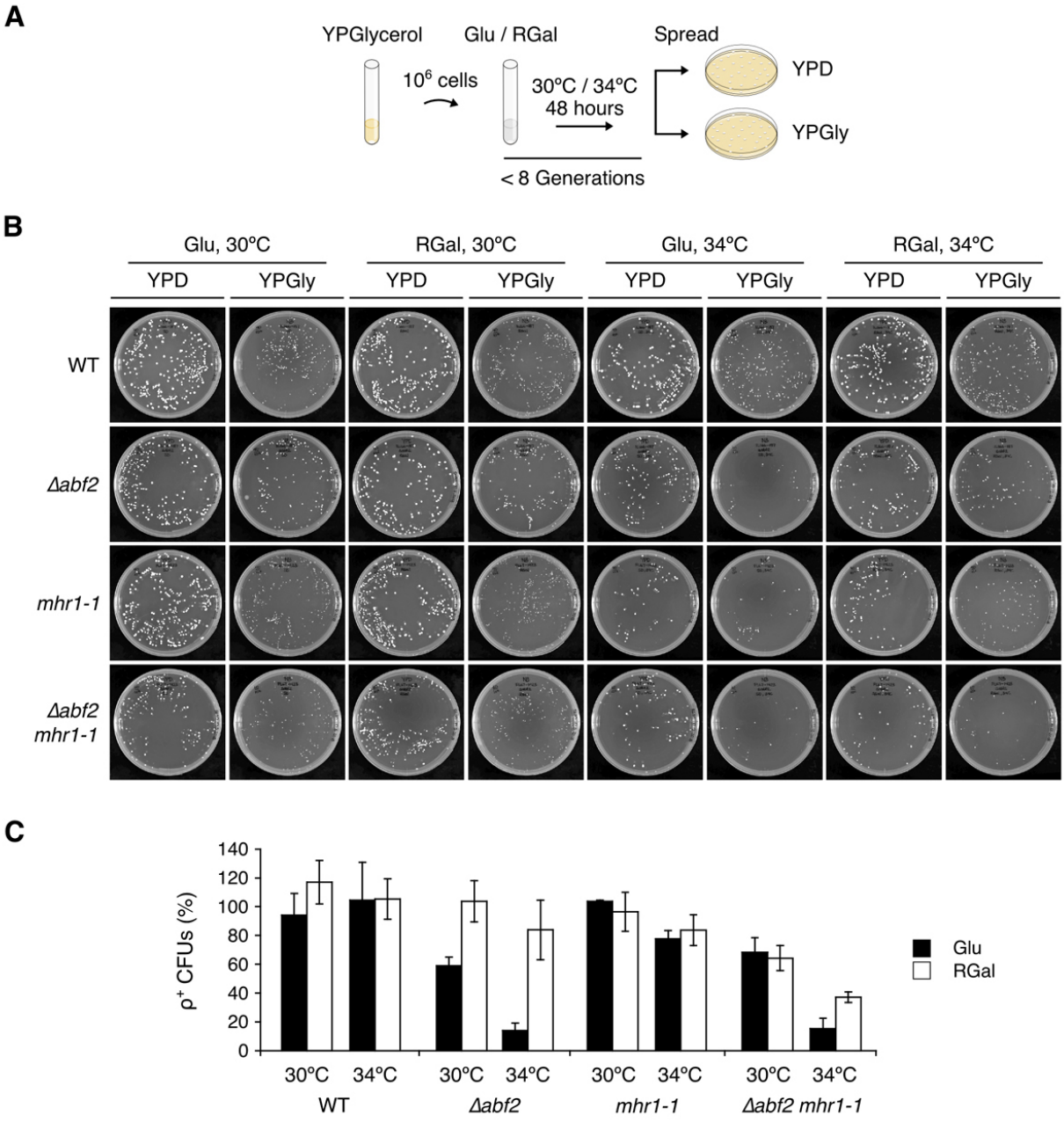

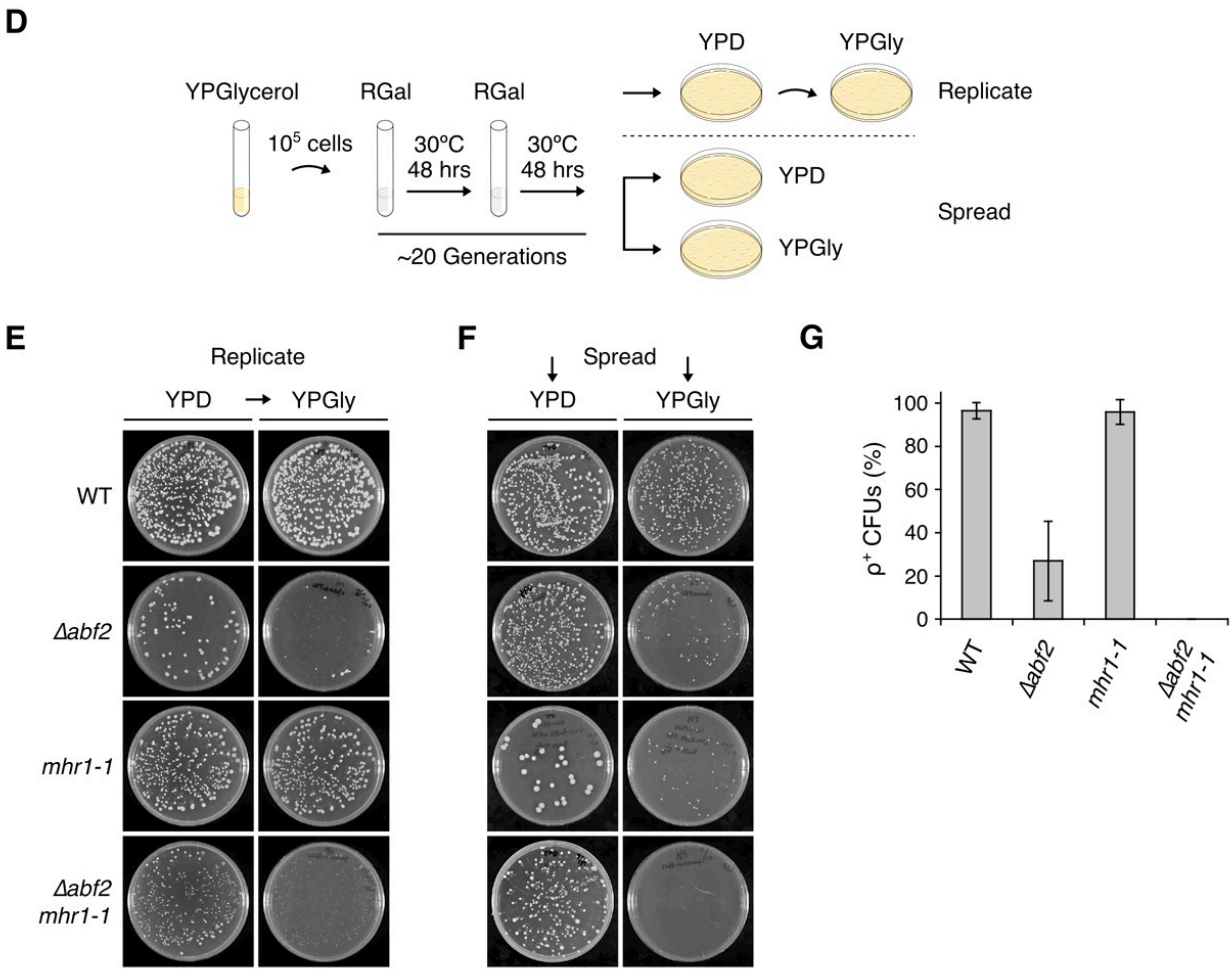

Figure 3.1 | Loss of respiratory function in *Δabf2*, *mhr1-1* and *Δabf2 mhr1-1* cells. (A) Scheme of respiratory function assay. Cells were selectively pre-cultured in YPGly medium, then 10^6 cells were transferred to Glu or RGal media and cultivated for <8 generations at 30°C or 34°C. Equal volumes of dilute culture were then spread onto YPD and YPGly plates to measure the proportion of CFUs retaining respiratory function. (B) Representative plate images of wild-type, *Δabf2*, *mhr1-1*, and *Δabf2 mhr1-1* CFU formation on YPD and YPGly plates following cultivation in Glu or RGal media at 30°C or 34°C. (C) ρ^+ CFU formation rate based on n = 3 independent experiments described in (A). (D) Scheme of extended respiratory function assay. Cells were selectively grown in YPGly media, then 10^5 cells were transferred to RGal media and cultivated for two consecutive 48-hour rounds (approximately 20 generations) at 30°C. Equal volumes of dilute culture were then: (E) Spread onto YPD and YPGly plates, or (F) spread onto YPD plates, grown for four days, and then replica-plated onto YPGly plates. (G) ρ^+ CFU formation rate from cells simultaneously

spread onto YPD and YPGly, based on *n* = 3 independent experiments. All error bars represent ±SD.

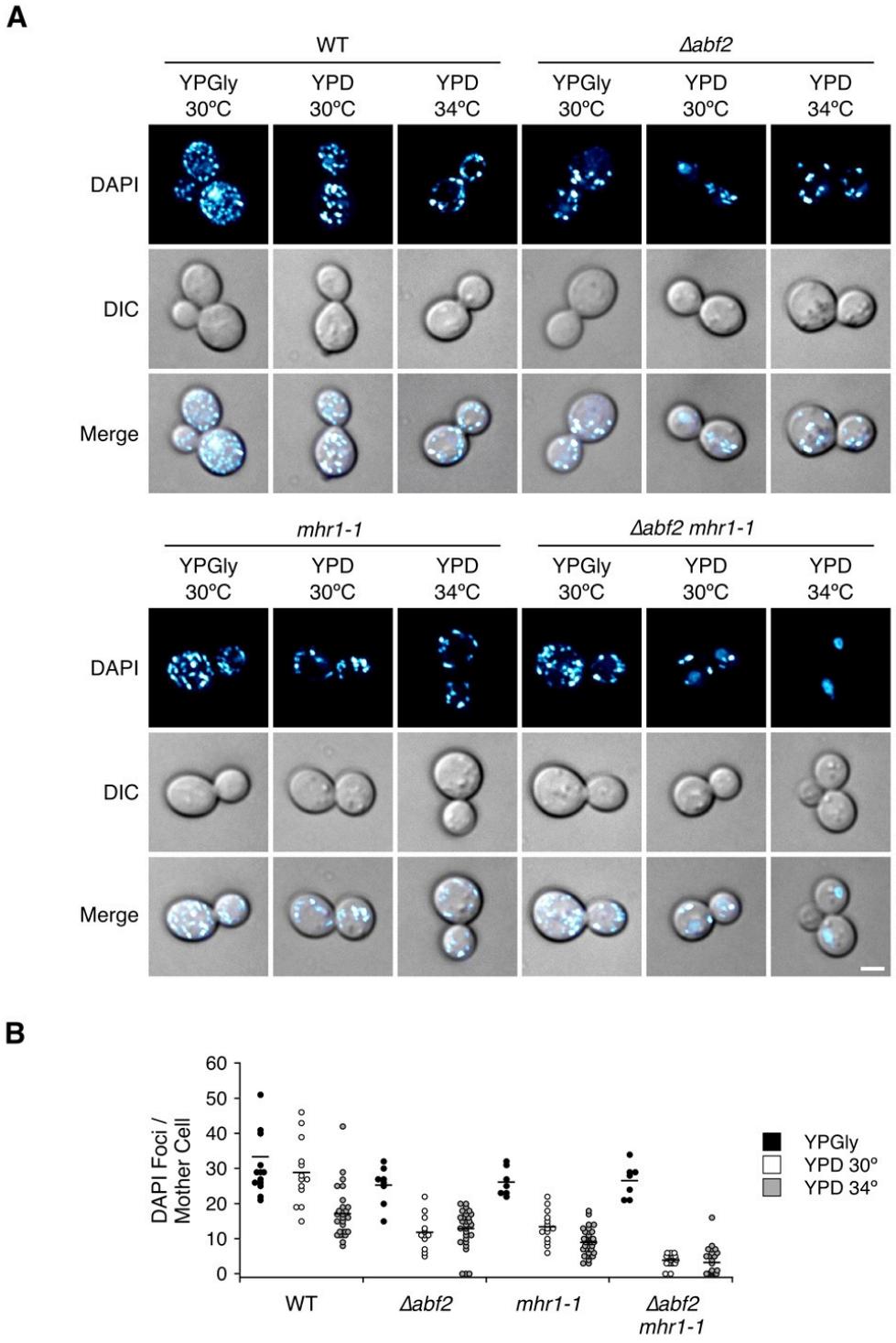

Figure 3.2 | Reduction in mtDNA-derived DAPI signals in *Δabf2*, *mhr1-1* and *Δabf2 mhr1-1* mutant cells. (A) Mitochondrial nucleoid signals in wild-type, *Δabf2*, *mhr1-1*

and *Δabf2 mhr1-1* cells cultivated in YPGly media, or in YPD media to log-phase at 30°C or 34°C. Scale bar = 2µm. (B) Numbers of mtDNA-DAPI foci in individual mother cells. The number of individual cells measured for WT, *Δabf2, mhr1-1* and *Δabf2 mhr1-1* mother cells cultivated in YPGly at 30°C was *n* = 14, 8, 7 and 7, respectively. For cells grown in YPD at 30°C, *n* = 13, 12, 14 and 17, respectively. For cells grown in YPD at 34°C, *n* = 28, 30, 38 and 27, respectively. Horizontal lines represent the mean number of DAPI foci.

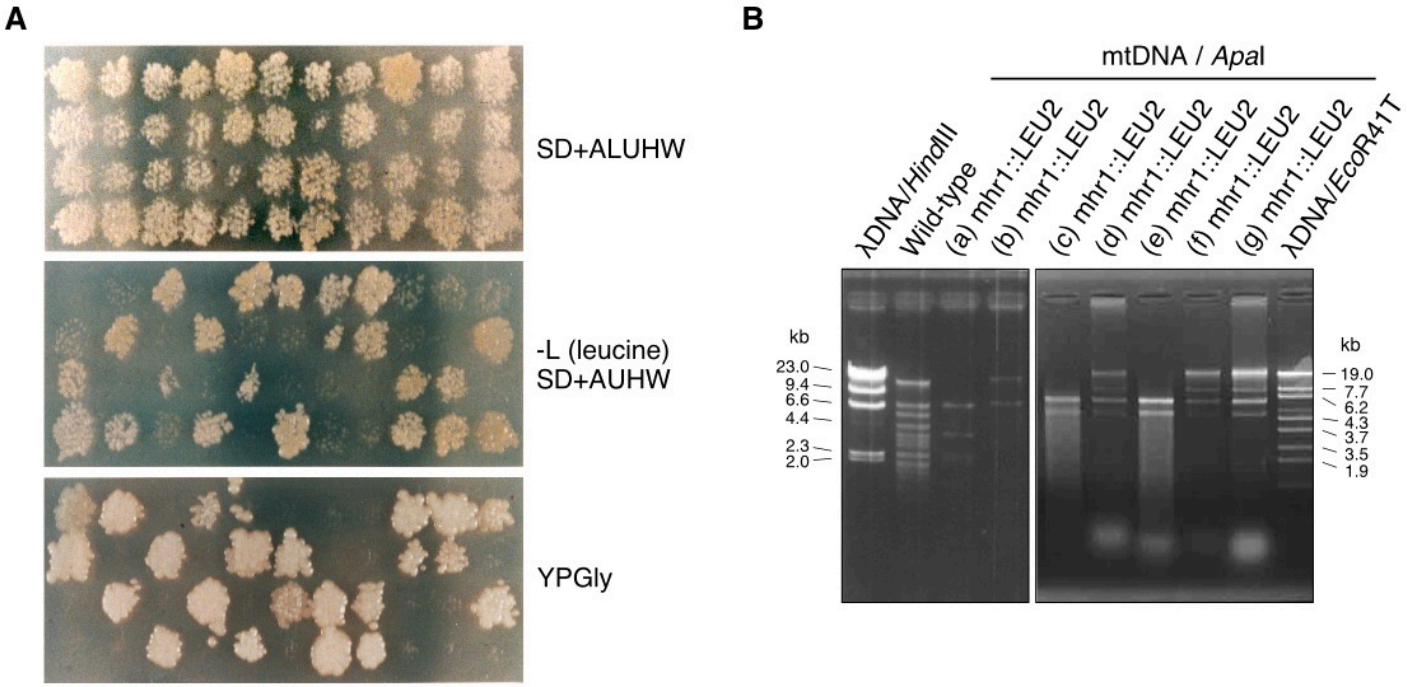

Figure 3.3 | Tetrad analysis of respiratory function and mtDNA deletions in *Δmhr1* cells. (A) Respiratory function of *Δmhr1* spores was analyzed by replica plating colonies derived from spores (top) onto synthetic media lacking leucine (middle) and YPGly media (bottom). (B) *Apa*I-digests of purified mtDNA molecules derived from wild-type and *Δmhr1* spores.

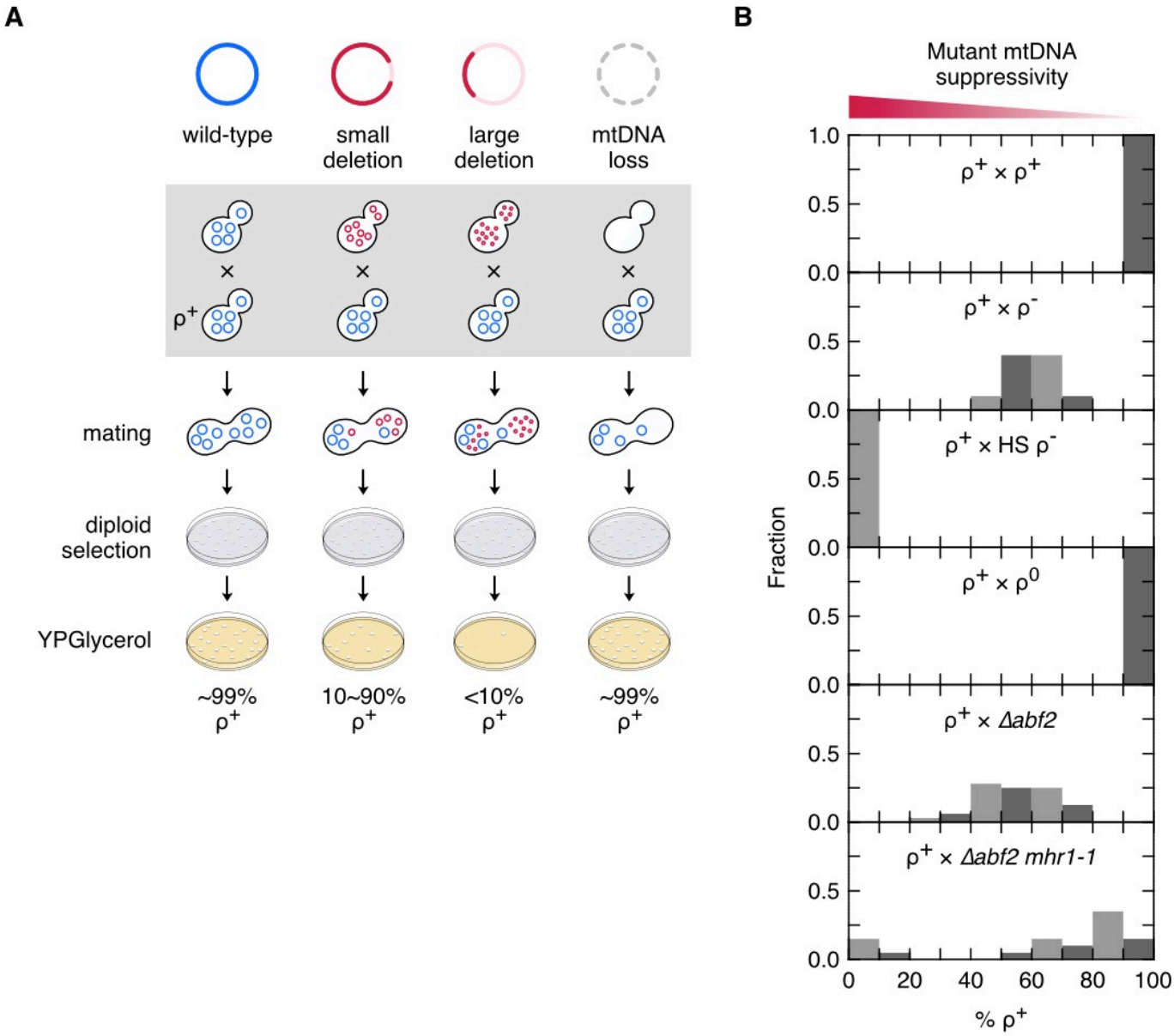

Figure 3.4 | Degree of mtDNA suppressivity in *Δabf2* or *mhr1-1 Δabf2* mutant cells. (A) Illustration of the effect of mtDNA deletion size on the suppressive phenotype. (B) Frequency distribution of the ρ^+ phenotype in crosses of ρ^+, ρ^-, HS ρ^-, ρ^0, *Δabf2* or *Δabf2 mhr1-1* cells (top to bottom, respectively) with ρ^+ haploid cells (see Table 3.1). The numbers of independent crosses conducted for each result (shown top to bottom) was, *n* = 5, 10, 5, 5, 32 and 20, respectively.

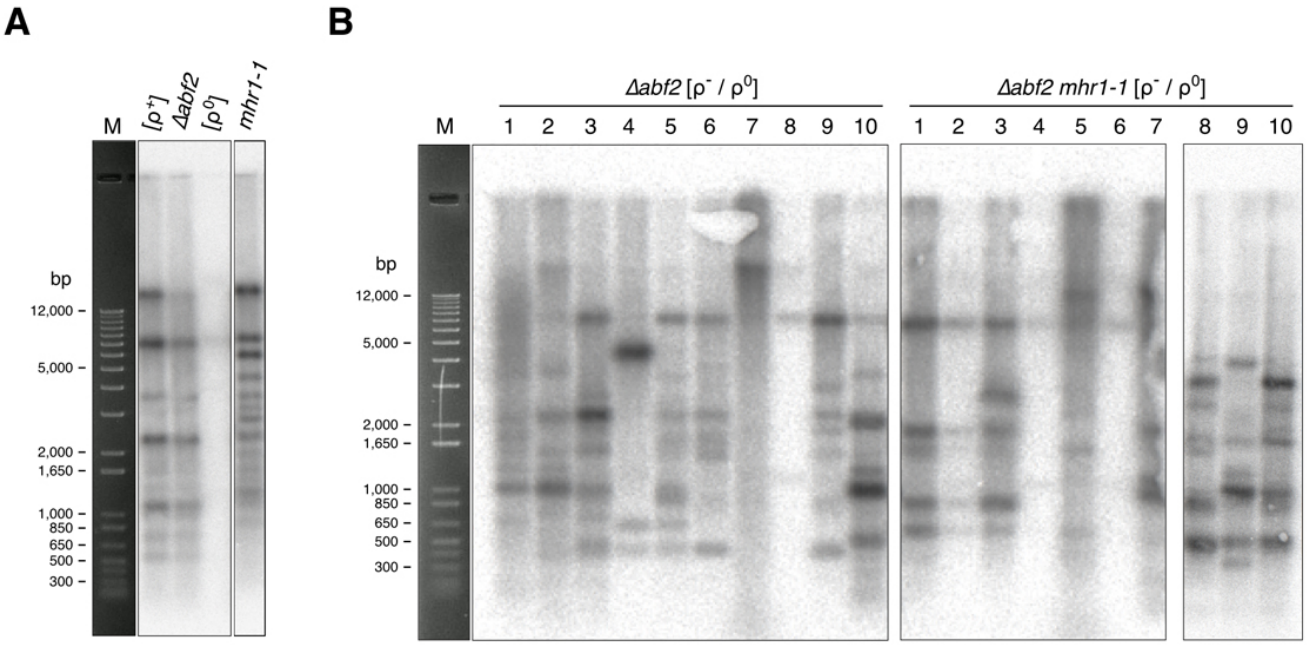

Figure 3.5 | Southern blot analysis of *Apa*I-digested mtDNA from *Δabf2* or *Δabf2 mhr1-1* cells. (A) MtDNA signals from ρ^+ WT, *Δabf2*, ρ^0 and *mhr1-1* cells. (B) MtDNA signals from ten ρ^- / ρ^0 *Δabf2* colonies and ten ρ^- / ρ^0 *Δabf2 mhr1-1* colonies. M: 1-kb plus DNA ladder marker.

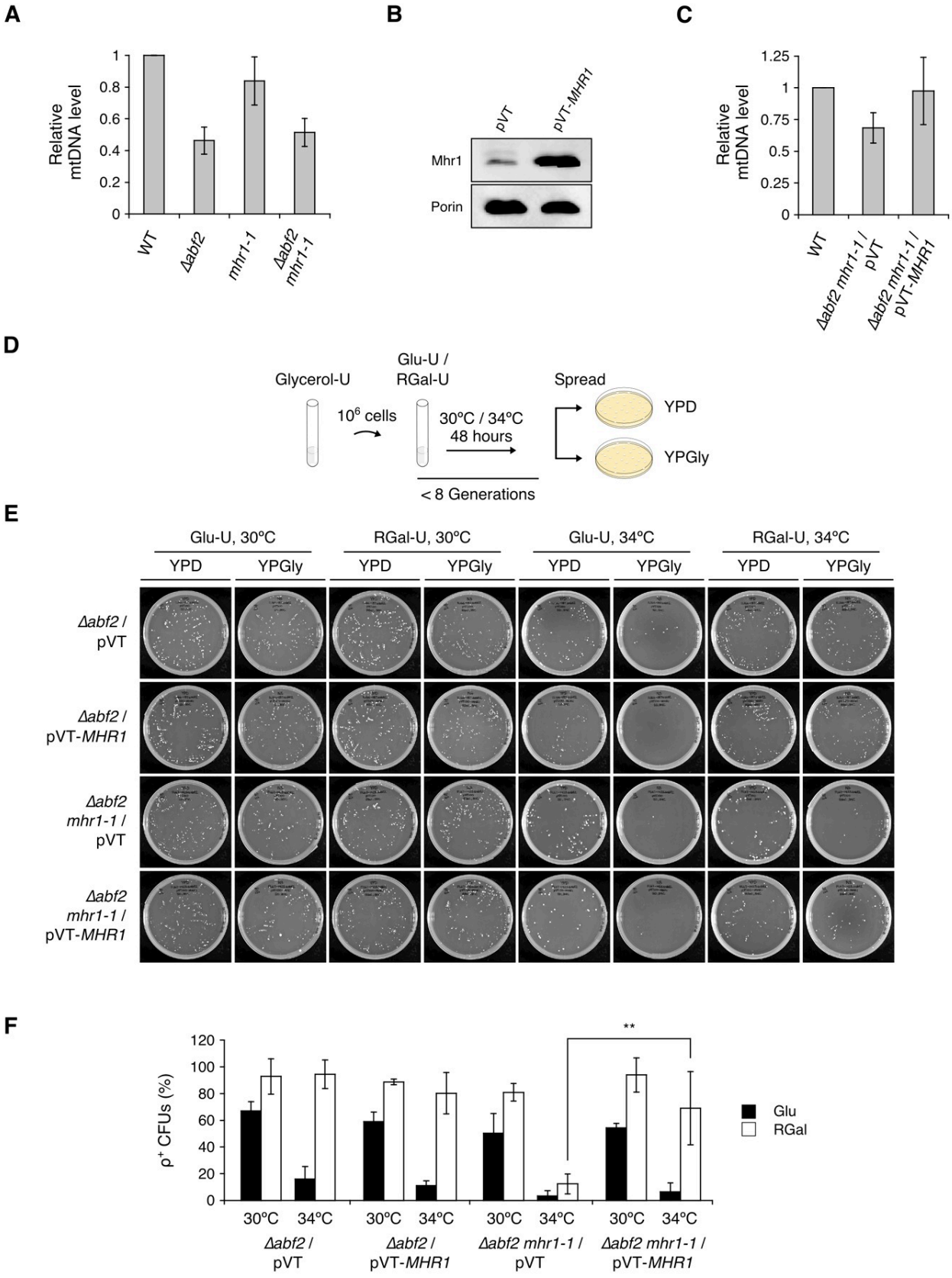
A
Relative mtDNA level
1
0.8
0.6
0.4
0.2
0
WT
Δabf2
mhr1-1
Δabf2 mhr1-1
B
pVT
pVT-MHR1
Mhr1
Porin
C
Relative mtDNA level
1.25
1
0.75
0.5
0.25
0
WT
Δabf2 mhr1-1 / pVT
Δabf2 mhr1-1 / pVT-MHR1
D
Glycerol-U
Glu-U / RGal-U
Spread
10^6 cells
30°C / 34°C 48 hours
YPD
YPGly
< 8 Generations
E
Glu-U, 30°C
RGal-U, 30°C
Glu-U, 34°C
RGal-U, 34°C
YPD
YPGly
Δabf2 / pVT
Δabf2 / pVT-MHR1
Δabf2 mhr1-1 / pVT
Δabf2 mhr1-1 / pVT-MHR1
F
ρ+ CFUs (%)
120
100
80
60
40
20
0
**
Glu
RGal
30°C
34°C
Δabf2 / pVT
Δabf2 / pVT-MHR1
Δabf2 mhr1-1 / pVT
Δabf2 mhr1-1 / pVT-MHR1

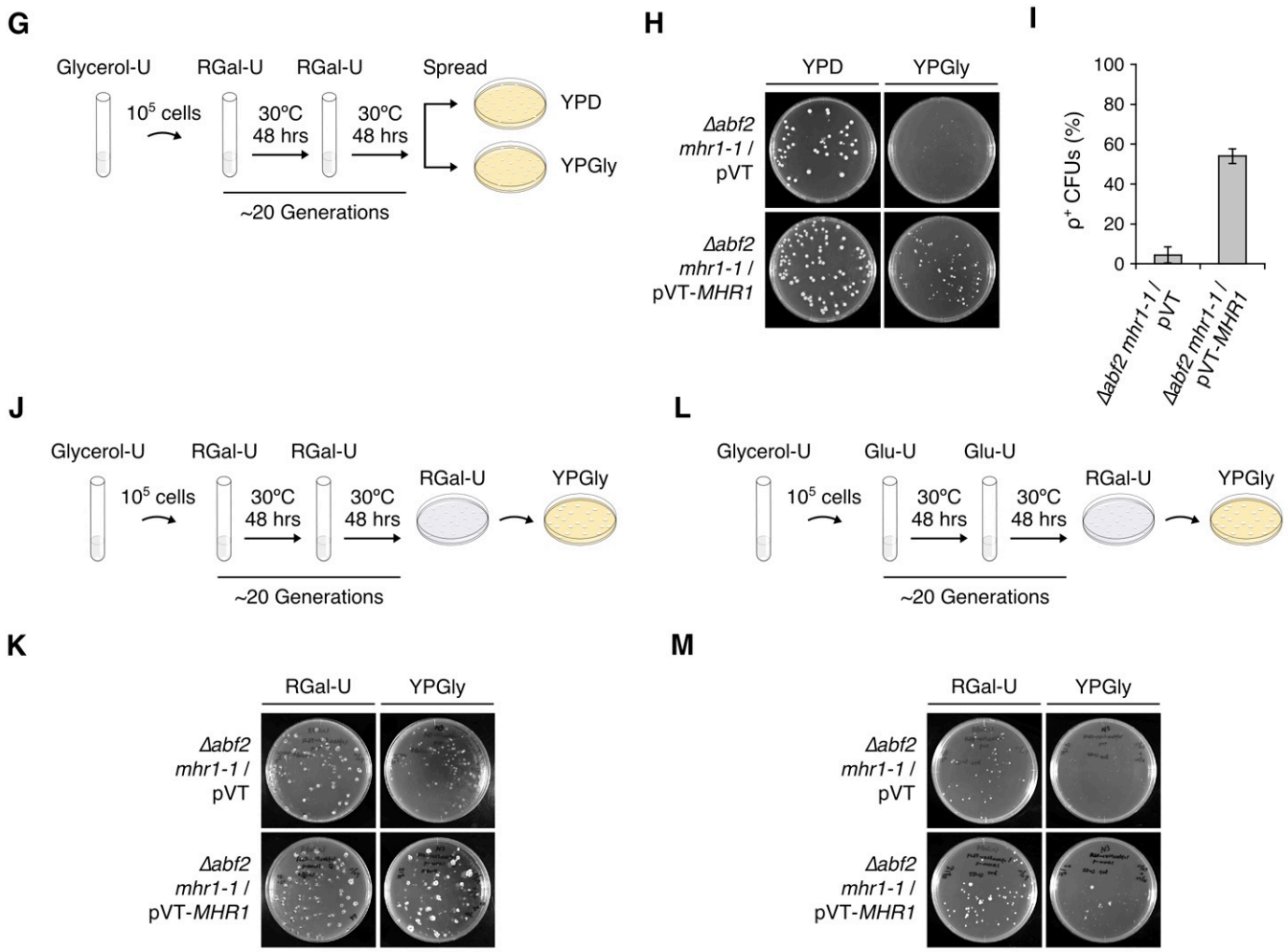

Figure 3.6 | Effects of Mhr1 overproduction on mtDNA content and respiratory function. (A) Relative mtDNA level in wild-type, *Δabf2*, *mhr1-1* or *Δabf2 mhr1-1* cells cultivated in YPGly media. (B) Immunoblot analysis of Mhr1 protein content in cells containing the pVT or pVT-*MHR1* plasmids. (C) Relative mtDNA levels in wild-type or *Δabf2 mhr1-1* cells containing empty or *MHR1*-overexpressing plasmids after cultivation in Gly-U media. (D) Scheme of respiratory function assay. Cells were selectively pre-cultured in Gly-U media, then 10^6 cells were transferred to Glu-U or RGal-U media and cultivated for <8 generations at 30°C or 34°C. Cells were then spread onto YPD and YPGly plates. (E) Representative plate images of *Δabf2* and *Δabf2 mhr1-1* CFUs harboring empty or *MHR1*-overexpression plasmids, following growth in Glu-U or RGal-U media at 30°C or 34°C for <8 generations. (F) ρ^+ CFU formation rate based on *n* = 3 independent experiments described in (D). (G) Scheme of extended respiratory function assay. Cells were selectively grown in Gly-U media, then 10^5 cells were transferred to RGal-U media and cultivated for two

consecutive 48-hour rounds (approximately 20 generations) at 30°C. Cells were then spread onto YPD and YPGly plates. (H) Representative plate images and (I) ρ^+ CFU formation rate based on *n* = 3 independent experiments described in (G). (J) Scheme of extended respiratory function assay. Cells were selectively grown in Gly-U media, then 10^5 cells were transferred to RGal-U media and cultivated for two consecutive 48-hour rounds (approximately 20 generations) at 30°C. Cells were then spread onto RGal-U plates, grown for four to seven days, and then replica-plated onto YPGly plates. (K) Representative plate images for *n* = 3 independent experiments described in (J). (L) Scheme of extended respiratory function assay. Cells were selectively grown in Gly-U media, then 10^5 cells were transferred to Glu-U media and cultivated for two consecutive 48-hour rounds (approximately 20 generations) at 30°C. Cells were then spread onto RGal-U plates, grown for four to seven days, and then replica-plated onto YPGly plates. (M) Representative plate images for *n* = 2 independent experiments described in (L). All error bars indicate ±SD.

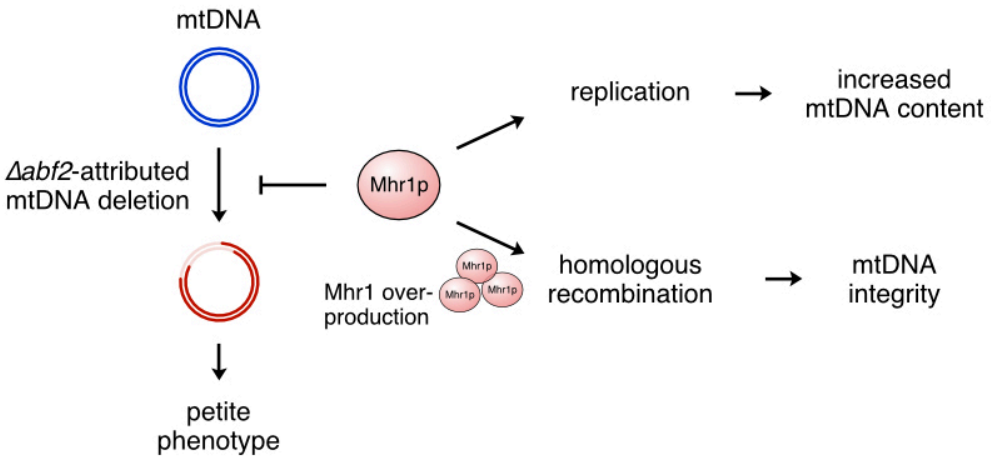

Figure 3.7 | Model for the prevention of mtDNA deletion mutagenesis by Mhr1-driven mtDNA recombination and replication. MtDNA deletions threatening cellular respiratory function arising from nuclear mutations such as *Δabf2 mhr1-1* can be prevented by increased homologous recombination via overproduction of Mhr1 recombinase.

Table 3.1 | Yeast strains used in this chapter

Abbreviation	Strain	Nuclear genotype	Mitochondrial genotype	Source
WT/WT	CG380	*MATa/MATα ade5/ade5 +/his7 leu2/leu2 ura3/ura3 trp1/trp1*	[ρ^+]	Stock culture
WT/*Δmhr1*	CG380 *Δmhr1*	*MATa/MATα ade5/ade5 +/his7 leu2/leu2 ura3/ura3 trp1/trp1 mhr1::LEU2*	[ρ^+]	Stock culture
mhr1-1	FL67-1423	*MATα his1 trp1 ura3 can1 mhr1-1*	[$\rho^+ \omega^+$ *Δens2* $Oli2^R$]	(*57*)
Δabf2 mhr1-1	FL67-1423 *Δabf2*	*MATα his1 trp1 ura3 can1 mhr1-1 abf2::KAN*	[$\rho^+ \omega^+$ *Δens2* $Oli2^R$]	This study
Δabf2 mhr1-1/pVT	FL67-1423 *Δabf2*/pVT100U	*MATα his1 trp1 ura3 can1 mhr1-1 abf2::KAN* pVT100U (*URA3*)	[$\rho^+ \omega^+$ *Δens2* $Oli2^R$]	This study
Δabf2 mhr1-1/pVT-*MHR1*	FL67-1423 *Δabf2*/pVT100U-*MHR1*	*MATα his1 trp1 ura3 can1 mhr1-1 abf2::KAN* pVT100U (*MHR1*, *URA3*)	[$\rho^+ \omega^+$ *Δens2* $Oli2^R$]	This study
	IL166-187	*MATα his1 trp1 can1*	[$\rho^+ \omega^+$ *ens2* Chl_{321}^R]	Stock culture
	IL166-187 *Δabf2*	*MATα his1 trp1 can1 abf2::KAN*	[$\rho^+ \omega^+$ *ens2* Chl_{321}^R]	This study
WT	IL166-187 *Δura3*	*MATα his1 trp1 ura3 can1*	[$\rho^+ \omega^+$ *ens2* Chl_{321}^R]	This study
Δabf2	IL166-187 *Δura3 Δabf2*	*MATα his1 trp1 ura3 can1 abf2::KAN*	[$\rho^+ \omega^+$ *ens2* Chl_{321}^R]	This study
Δabf2/pVT	IL166-187 *Δura3 Δabf2*/pVT100U	*MATα his1 trp1 ura3 can1 abf2::KAN* pVT100U (URA3)	[$\rho^+ \omega^+$ *ens2* Chl_{321}^R]	This study
Δabf2/pVT-*MHR1*	IL166-187 *Δura3 Δabf2*/pVT100U-*MHR1*	*MATα his1 trp1 ura3 can1 abf2::KAN* pVT100U (*MHR1*, *URA3*)	[$\rho^+ \omega^+$ *ens2* Chl_{321}^R]	This study
	OP11c-55R5	*MATa leu2 ura3 trp1*	[$\rho^+ \omega^-$ *ens2* $Oli1^R$]	(*57*)
	YKN1423	*MATα leu2 ura3 met3*	[$\rho^+ \omega^+$ *Δens2* $Oli2^R$]	(*59*)
	YKN1423A-2	*MATα leu2 ura3 met3*	Normal suppressive [ρ^-]	(*59*)
	YKN1423C-1	*MATα leu2 ura3 met3*	[HS ρ^-]	(*59*)
	YKN1423 ρ^0	*MATα leu2 ura3 met3*	[ρ^0]	EtBr treatment of YKN1423

Chapter 4: Influence of cytosolic pH on small mitochondrial DNA heteroplasmy in *Saccharomyces cerevisiae*

4.1 Introduction

Glucose is the preferred carbon source for yeast and its depletion or substitution with nonfermentable carbon sources results in vast changes to the transcriptional landscape (*122, 143, 144*). Glucose depletion is accompanied by an immediate drop in cytosolic pH that is due in part to the rapid disassembly of the vacuolar H^+-ATPase and the influx of protons from the media to the cytosol (*143*), effectively making cytosolic pH a second messenger for glucose. Separately, mtDNA copy number is dependent on growth conditions and is generally higher when cells utilize nonfermentable carbon sources. We therefore investigated whether change in cytosolic pH acts as a signal to mitochondria that affects the heteroplasmy of wild-type and small mtDNA.

4.2 Materials and methods

4.2.1 Yeast crossing experiments

Crossing experiments were conducted as indicated in Chapter 2, for six hours in YPD media containing 2% glucose. Following crossing, 20 µl of mated cells were transferred to tubes containing 2 ml of synthetic defined plus leucine (SD+L) or plus leucine and uracil (SD+LU) media for diploid selection. For vegetative growth of diploid cells, we used SD media containing the indicated amounts of glucose, or 0.5% glucose buffered with 12 mM Tris-HCl or 12mM PIPES at the indicated pH values. Diploid cells were cultivated upright at 30°C on a shaker at 75 rpm for 48 hrs before transferring 20 µl cells to subsequent tubes containing the same media. In order to monitor ρ^+ CFU formation, cells were diluted in ddH_2O and spread on SD+L or SD+LU plates containing 2% glucose and incubated at 30°C for two days. SD plates were photographed in a LAS-4000 imager (GE Healthcare) before replica-plating onto YPGlycerol plates. YPGlycerol plates were then incubated at 30°C for two days before photography. Images of the diploid selection plate and YPGlycerol plate were

overlaid with Photoshop Elements software (Adobe) and colonies were counted manually to determine the percentage of ρ^+ CFUs.

4.2.2 Detection of cytosolic pH with superecliptic pHluorin

Superecliptic pHluorin (SEP) was cloned into the *Sac*I and *Xba*I cutting sites of the plasmid pVT100U (*95*) and transformed into yeast as pVT100U-pHluorin. All strains expressing SEP were subjected to three independent *in situ* calibration experiments using a protocol modified from Orij *et al*., 2009 (*145*). Specifically, cells expressing pVT100U-Empty and pVT100U-pHluorin were cultivated separately overnight in 5 ml synthetic defined minus uracil (SD-U) media in 30 ml flasks at 30°C on a shaker at 150 rpm. The following day, 2 ml of fresh SD-U was added and cultivation was continued for 40 min. 5 ml of cultures were transferred to 50 ml falcon tubes, centrifuged at 2,380 × g for 4 min and resuspended in ddH_20 at an OD_{600} of 0.8. Cells were then permeabilized by adding 100 µg/ml digitonin and incubated at 30°C on a shaker at 75 rpm. 200 µl aliquots of cells were then transferred to 1.5 ml microcentrifuge tubes, centrifuged at 5,000 rpm for 2 min, and resuspended in McIlvaine buffers (citric acid / NaH_2PO_4) at pH values ranging from 5.0 to 8.2. Fluorescence was then measured with a SpectraMax M2 plate reader (Molecular Devices) at excitation wavelengths of 390 and 470 nm and emission at 512 nm. Background values from pVT100U-Empty containing cells were subtracted and the ratio of emission intensity was calculated as $R_{470/390}$ and plotted against the corresponding McIlvaine buffer pH. Three independent calibration experiments were performed for each cell background measured. Cytosolic pH measurements of diploid cells from crossing experiments was performed by transferring 75 µl aliquots of pVT100U-Empty and pVT100U-pHluorin expressing cells to a 96-well black-bottomed plate (Grenier) and measuring the $R_{470/390}$ signals.

4.2.3 Quantification of mtDNA levels in heteroplasmic cells

MtDNA in heteroplasmic cells was measured relative to nDNA as described in Chapter 2, except that cells were obtained from 2 ml SD+L 0.5% glucose cultures after 144 hrs of vegetative growth. Total DNA including mtDNA was prepared and DNA concentrations were measured with a NanoVue spectrophotometer (GE Healthcare). 95 ng of total DNA was used as the standard template concentration for PCR analyses. Primers used to specifically detect nuclear DNA, ρ^+ mtDNA and HS ρ^-

mtDNA were: *NUC1*-Fwd, 5'- GATACTCTTGTCCGGTTTAGTCG-3'; *NUC1*-Rev, 5'-ATCTTTCGACTGTTTGATCGCC-3'; *COX3*-Fwd, 5'-ATGCCTTCACCATGACCTATTG-3'; *COX3*-Rev, 5'-CCAACATGATGTCCAGCTGTTA-3'; HSC1-Fwd, 5'-GAAGATATCCGGGTCCCAATAATAA-3'; HSC1-Rev, 5'-AATATAATAGTCCCCACTCCGCG-3'. PCR amplification was done in steps of 5 cycles up to 25 cycles for each sample. At each indicated cycle, 3 µl of PCR products from each of the NUC1, COX3 and HSC1 reactions were mixed and run in a 1.9% agarose gel. Gels were photographed using a FAS-IV imaging system (Nippon Genetics) and band intensities were measured with ImageJ software (*96*). MtDNA level was calculated relative to nuclear DNA using the $2^{-\Delta CT}$ method (*97*).

4.3 Results

4.3.1 Vegetative growth in low glucose media promotes ρ^+ colony formation from heteroplasmic cells with hypersuppressive mtDNA

To investigate the effects of glucose metabolism on mtDNA heteroplasmy, we crossed parental cells containing 85.7-kbp ρ^+ mtDNA with cells containing small 1.1-kbp HS [*ori5*] ρ^- mtDNA. Following crossing, we transferred the mated cells into diploid selection media (SD+LU) containing 0.5%, 2.0% or 4.0% glucose and monitored formation of ρ^+ colonies over several generations of vegetative growth (Figure 4.1A). We found that diploid cells cultivated in 0.5% glucose media for approximately 24 generations produced 68.8 ± 5.4% ρ^+ CFUs, while diploids cultivated in 2.0% or 4.0% media produced 26.5 ± 5.0% or 4.5 ± 1.0% ρ^+ CFUs, respectively (Figure 4.1B and C). Thus, ρ^+ CFU formation is inversely proportional to glucose concentration in growth media.

4.3.2 An early drop in cytosolic pH stimulates ρ^+ colony formation

Upon depletion of glucose, cytosolic pH undergoes a rapid but reversible drop, which occurs in part due to V-ATPase disassembly (*143*). We hypothesized that cells cultivated in low glucose media experience an early drop in cytosolic pH and that a lower pH in these cells is likely sustained for a longer period compared with cells cultivated in higher concentrations of glucose. Sustained periods of lower cytosolic pH may therefore be a signal to mitochondria affecting mtDNA heteroplasmy level. To examine this possibility, we employed superecliptic pHluorin

(SEP), a pH-sensitive green fluorescent protein that undergoes ratiometric fluorescence changes over a pH range of 6.0 ~ 8.5 (*145*). We crossed and cultivated mated cells expressing pVT100U-Empty or pVT100U-pHluorin in 0.5, 2.0 or 4.0% glucose (Figure 4.2A) and monitored pHluorin signals in these cells. Indeed, we found that cells cultivated in 0.5% glucose underwent a drop in cytosolic pH much earlier than cells grown in 2.0% glucose, and cells cultivated in 4.0% glucose never displayed a cytosolic pH level below 7.2 (Figure 4.2B). Surprisingly, cells cultivated in 0.5% glucose did not repeat this pH drop after the first 48-hour cultivation period. Cells cultivated in 2.0% glucose did experience repeated drops in cytosolic pH, but those occurred relatively late in each 48-hour cultivation period. In addition, ρ^+ CFU formation rates in empty plasmid or pHluorin-expressing cells were similar to cells without the plasmid, indicating that the presence of the plasmid did not alter mtDNA segregation (Figure 4.2C; Figure 4.1B). Together, these cytosolic pH measurements reveal a correlation between low cytosolic pH and formation of ρ^+ CFUs.

4.3.3 Increased cytosolic pH suppresses ρ^+ colony formation and ρ^+ mtDNA level

To directly investigate the effect of cytosolic pH on the formation of ρ^+ CFUs in cells cultivated in low glucose, we used buffered media to partially suppress cytosolic acidification upon glucose depletion. We crossed parental cells (Figure 4.3A) and used SEP to monitor pH in live cells during vegetative cultivation in unbuffered media, or media buffered with 12 mM Tris-HCl to pH 5.6 or pH 7.3. We found that during the first 48-hour cultivation period, cells in 0.5% glucose-pH 7.3 media experienced a much more gradual cytosolic pH decline, compared with unbuffered or pH 5.6 cells (Figure 4.3B). In subsequent rounds of cultivation, all cultures showed similar pH profiles, which began at pH 7.5 in fresh media and slowly declined to around pH 7.0 over 48 hours. However, the ρ^+ CFU formation rate of pH 7.3-cultivated cells was very low compared to unbuffered or pH 5.6 cells (Figure 4.3C and D). These results indicate that the first 48-hour cultivation period is the most crucial determinant of subsequent ρ^+ CFU formation. Moreover, we used PIPES-buffered media and observed that diploid cells cultivated in 0.5% glucose media at pH 6.1 produced a high proportion of ρ^+ CFUs after approximately 25 generations, similarly to cells cultivated in unbuffered media. On the other hand, cells cultivated in PIPES-pH 7.1 media gave mostly ρ^- CFUs, similarly to Tris-HCl-pH 7.3-cultivated

cells (Figure 4.3E and F). We next analyzed the mtDNA content of diploid cells from Tris-HCl pH 5.7 and 7.3 media after 144 hours of vegetative growth. Quantitative PCR analysis revealed that the ρ^+ mtDNA content in pH 5.7-cultivated cells was 3.0-fold higher than in pH 7.3 cells (Figure 4.3G and H). On the other hand, levels of HS ρ^- mtDNA were 1.87-fold higher on average in pH 7.3-buffered cells compared to pH 5.7-buffered cells. Together, these results show that segregation toward increased ρ^+ CFU formation from heteroplasmic ρ^+ / HS ρ^- cells is a result of increased ρ^+ mtDNA content that is dependent on a drop in cytosolic pH.

4.3.4 The general stress response transcription factors Msn2 and Msn4 are not required for ρ^+ colony formation in low pH media

Msn2 and Msn4 are zinc-finger transcription factors of the PKA/Rim15 pathway that coordinate the cellular response to numerous stresses including the diauxic shift by binding to the STRE element in the promoters of several genes (*144, 146*). Heteroplasmic diploid cells grown for 48 hours in 0.5% glucose media likely undergo a diauxic shift during the first 24 to 30 hours of vegetative cultivation, as indicated by the measured drop in cytosolic pH (Figure 4.2A). We therefore sought to examine the requirement for *MSN2* and *MSN4* in ρ^+ CFU formation in low glucose. *MSN2* and *MSN4* are partially functionally redundant (*144*); we therefore constructed double-mutants of the ρ^+ and HS ρ^- parental strains. We performed crossing followed by vegetative growth in 0.5% or 4.0% glucose media (Figure 4.4A) and monitored the ρ^+ CFU formation rate as in previous experiments. Unfortunately, the rates of ρ^+ CFU formation were similar to WT cells, indicating that transcription by Msn2 and Msn4 are not required for this phenotype (Figure 4.4B and C).

4.4 Discussion

Crossing two parental yeast strains containing different mitochondrial alleles produces a transient state of heteroplasmy that is segregated to homoplasmy at a rapid rate, typically within 10 generations of vegetative growth (*43, 59*). Rapid mtDNA allele segregation occurs due to mtDNA concatemer formation, allowing multiple copies of mtDNA to be transmitted as a single unit (Figure 1.2B; *43*). In this chapter, we followed the hypersuppressive phenotype after continuous cultivation for up to ~25 generations while monitoring the ρ^+ CFU formation rate.

Heteroplasmic colonies formed on the first round of diploid selection plates were all of similarly small size, however those that grew on diploid selection plates after 48 hours or more of vegetative growth were generally either large or petite (see: Fig. 4.1C, Fig 4.2D and Fig. 4.3D and F). This marked size difference is likely due to the formation of homoplasmy for ρ^+ or HS ρ^- mtDNA in the large or small colonies, respectively. It is therefore possible that cytosolic acidification upon glucose depletion induces mtDNA allele segregation toward ρ^+ mtDNA homoplasmy, while the hypersuppressive phenotype persists during glucose abundance and stable cytosolic pH (Figure 4.5).

Cells with functional mitochondrial metabolism are able to switch to ethanol as a carbon source during the diauxic shift (*144*), therefore ρ^+ cells in 0.5% glucose media may be able to sustain growth longer than ρ^- cells. However, our data reveal that a drop in cytosolic pH is still required for the increase in the population of ρ^+ cells, and could therefore be an important signal for the switch to ethanol catabolism. In addition, the uptake of various nutrients by *S. cerevisiae* relies on active transport across the plasma membrane by symporters that require a proton gradient (*146*), hence alkaline media pH impacts nutrient uptake and induces many stress response genes. While our results using alkaline-buffered media showed reduced ρ^+ CFU formation that correlated with a delayed drop in cytosolic pH, this condition likely produces a wide range of effects. Therefore, lower ρ^+ CFU formation in alkaline-buffered pH may represent effects beyond a higher cytosolic pH alone. Further experiments will be necessary to address these possibilities.

4.5 Figures and Table

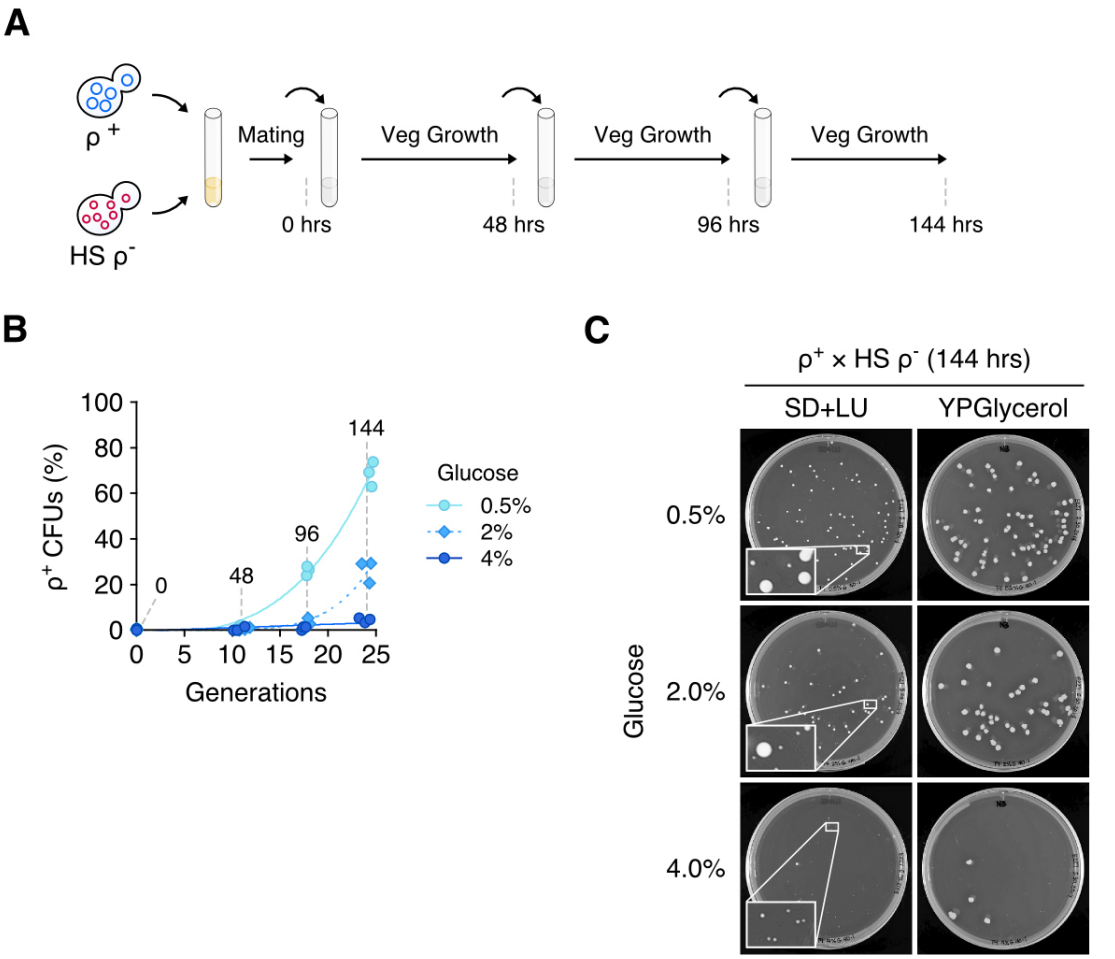

Figure 4.1 | Influence of glucose concentration on heteroplasmy of wild-type and small mtDNA over several generations of vegetative growth. (A) Scheme of yeast hypersuppressive crossing experiments followed by three, 48-hour rounds of vegetative growth in media containing 0.5%, 2% or 4% glucose. Hours of vegetative cultivation after crossing are indicated. (B) ρ^+ colony formation rate from n = 3 independent crossing experiments. Hours of vegetative cultivation after crossing are indicated. (C) Representative plate images from diploid cells after 144 hours of vegetative growth in media containing 0.5%, 2% or 4% glucose.

A

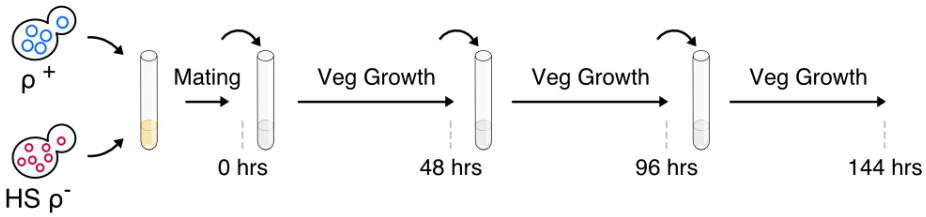
ρ +
HS ρ-
Mating
Veg Growth
Veg Growth
Veg Growth
0 hrs
48 hrs
96 hrs
144 hrs

B

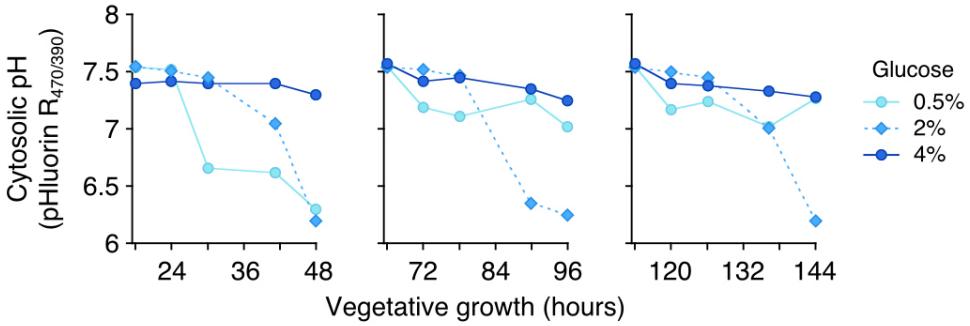
Cytosolic pH
(pHluorin R470/390)
8
7.5
7
6.5
6
24
36
48
72
84
96
120
132
144
Vegetative growth (hours)
Glucose
0.5%
2%
4%

C

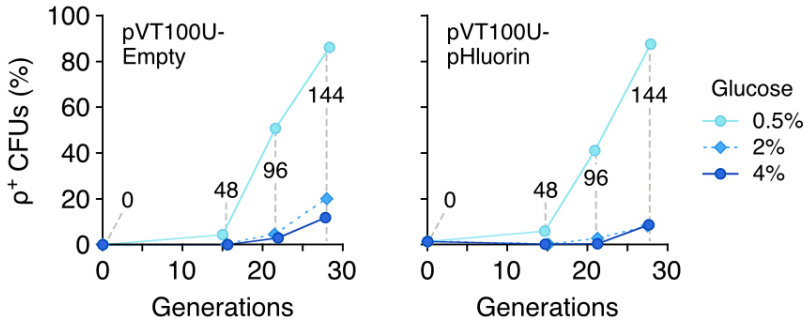
ρ+ CFUs (%)
pVT100U-
Empty
pVT100U-
pHluorin
0
48
96
144
0
10
20
30
Generations
Glucose
0.5%
2%
4%

D

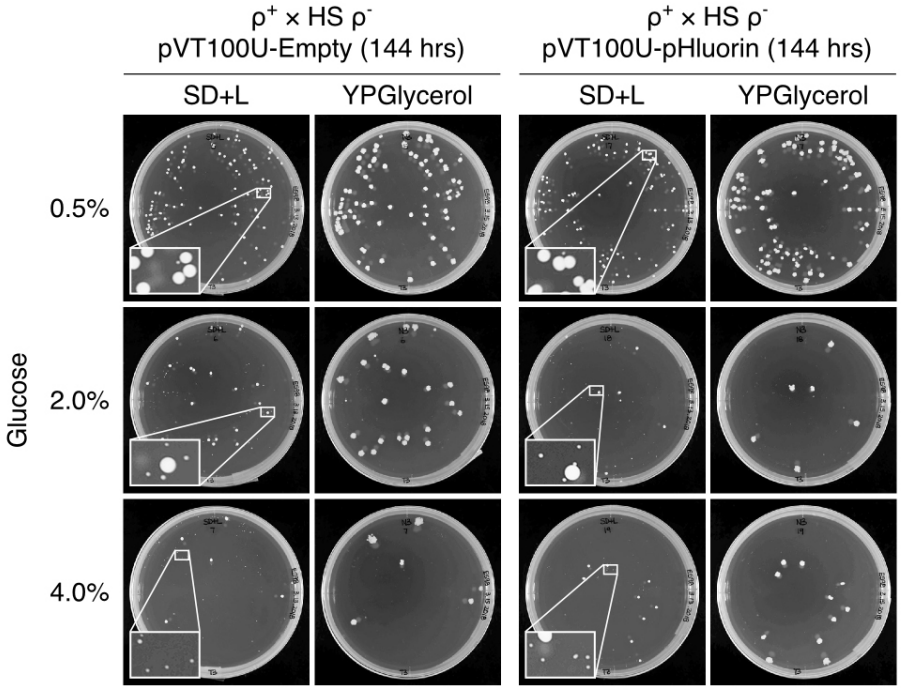
ρ+ × HS ρ-
pVT100U-Empty (144 hrs)
ρ+ × HS ρ-
pVT100U-pHluorin (144 hrs)
SD+L
YPGlycerol
SD+L
YPGlycerol
Glucose
0.5%
2.0%
4.0%

Figure 4.2 | Effect of media glucose concentration on cytosolic pH and ρ^+ colony formation during the vegetative growth of heteroplasmic cells. (A) Scheme of yeast hypersuppressive crossing experiments followed by three, 48-hour rounds of vegetative growth in media containing 0.5%, 2% or 4% glucose. Hours of vegetative cultivation after crossing are indicated. (B) Cytosolic pH in live cells during vegetative growth in media containing 0.5%, 2% or 4% glucose. (C) ρ^+ colony formation rates during vegetative growth in cells containing an empty plasmid or plasmid expressing pHluorin in the indicated media. Hours of vegetative cultivation after crossing are indicated. (D) Representative plate images from plasmid-containing diploid cells after 144 hours of vegetative growth in media containing 0.5%, 2% or 4% glucose. Results shown are derived from *n* = 1 experiment run in biological duplicate for both pVT100U-Empty and pVT100U-pHluorin cells.

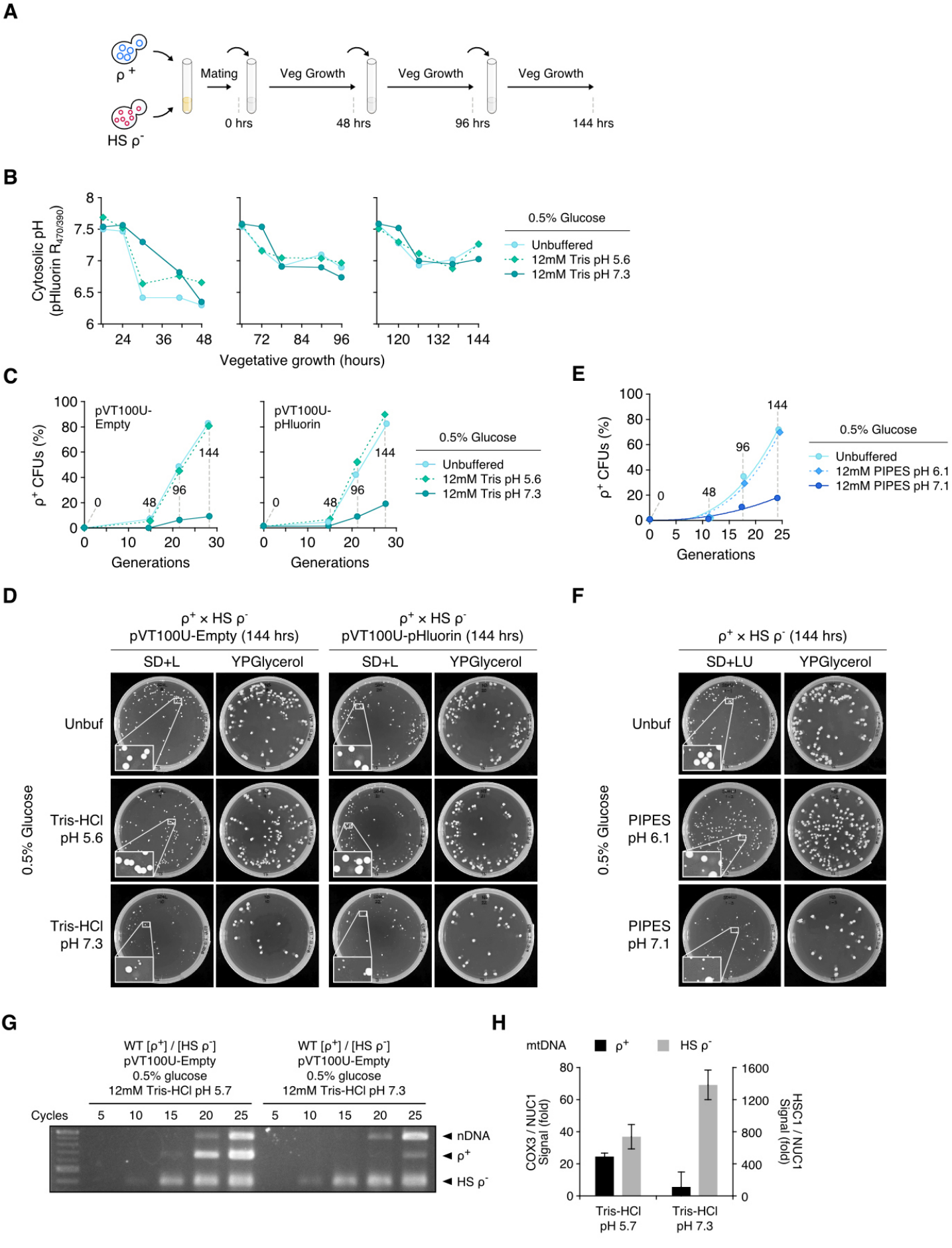
A
ρ +
HS ρ⁻
Mating
Veg Growth
Veg Growth
Veg Growth
0 hrs
48 hrs
96 hrs
144 hrs
B
Cytosolic pH (pHluorin R470/390)
Vegetative growth (hours)
0.5% Glucose
Unbuffered
12mM Tris pH 5.6
12mM Tris pH 7.3
C
ρ+ CFUs (%)
pVT100U-Empty
pVT100U-pHluorin
Generations
0.5% Glucose
Unbuffered
12mM Tris pH 5.6
12mM Tris pH 7.3
E
ρ+ CFUs (%)
Generations
0.5% Glucose
Unbuffered
12mM PIPES pH 6.1
12mM PIPES pH 7.1
D
ρ+ × HS ρ-
pVT100U-Empty (144 hrs)
ρ+ × HS ρ-
pVT100U-pHluorin (144 hrs)
SD+L
YPGlycerol
Unbuf
Tris-HCl pH 5.6
Tris-HCl pH 7.3
0.5% Glucose
F
ρ+ × HS ρ- (144 hrs)
SD+LU
YPGlycerol
Unbuf
PIPES pH 6.1
PIPES pH 7.1
0.5% Glucose
G
WT [ρ+] / [HS ρ-]
pVT100U-Empty
0.5% glucose
12mM Tris-HCl pH 5.7
WT [ρ+] / [HS ρ-]
pVT100U-Empty
0.5% glucose
12mM Tris-HCl pH 7.3
Cycles
nDNA
ρ+
HS ρ-
H
mtDNA
ρ+
HS ρ-
COX3 / NUC1 Signal (fold)
HSC1 / NUC1 Signal (fold)
Tris-HCl pH 5.7
Tris-HCl pH 7.3

Figure 4.3 | Effect of buffered media on cytosolic pH, cytosolic acidification-driven ρ^+ colony formation and relative amounts of ρ^+ and HS ρ^- mtDNA in cultures. (A) Scheme of yeast hypersuppressive crossing experiments followed by three, 48-hour rounds of vegetative growth in unbuffered, Tris-HCl- or PIPES-buffered media. Hours of vegetative cultivation after crossing are indicated. (B) Measurements of cytosolic pH in diploid cells during vegetative growth in media containing 0.5% glucose, unbuffered or buffered with Tris-HCl to pH 5.6 or 7.3. (C) ρ^+ colony formation rates during vegetative growth in cells containing an empty plasmid or plasmid expressing pHluorin in unbuffered or Tris-HCl-buffered 0.5% glucose media. Hours of vegetative cultivation are indicated. (D) Representative plate images from diploid cells containing plasmid DNA cultivated for 144 hours in unbuffered or Tris-HCl media buffered to pH 5.6 or 7.3. (E) ρ^+ colony formation rates during vegetative growth in unbuffered, PIPES-pH 6.1 or PIPES-pH 7.1 buffered 0.5% glucose media. (F) Representative plate images from diploid cells grown for 144 hours in unbuffered, PIPES-pH 6.1 or PIPES-pH 7.1 buffered media. (G) PCR amplification of nDNA and mtDNA from heteroplasmic cells expressing pVT100U-Empty cultivated in SD+L 0.5% glucose Tris-HCl media buffered to pH 5.7 or 7.3 and sampled at 144 hours. (H) Quantification of ρ^+ and HS ρ^- mtDNA levels relative to nDNA signals. Results shown in B and C are averages from *n* = 1 experiment run in biological duplicate for both pVT100U-Empty and pVT100U-pHluorin cells. Results shown in E are averages from *n* = 1 experiment run in biological duplicate. Results shown in G and H are representative of *n* = 3 independent experiments. Error bars represent ±SD.

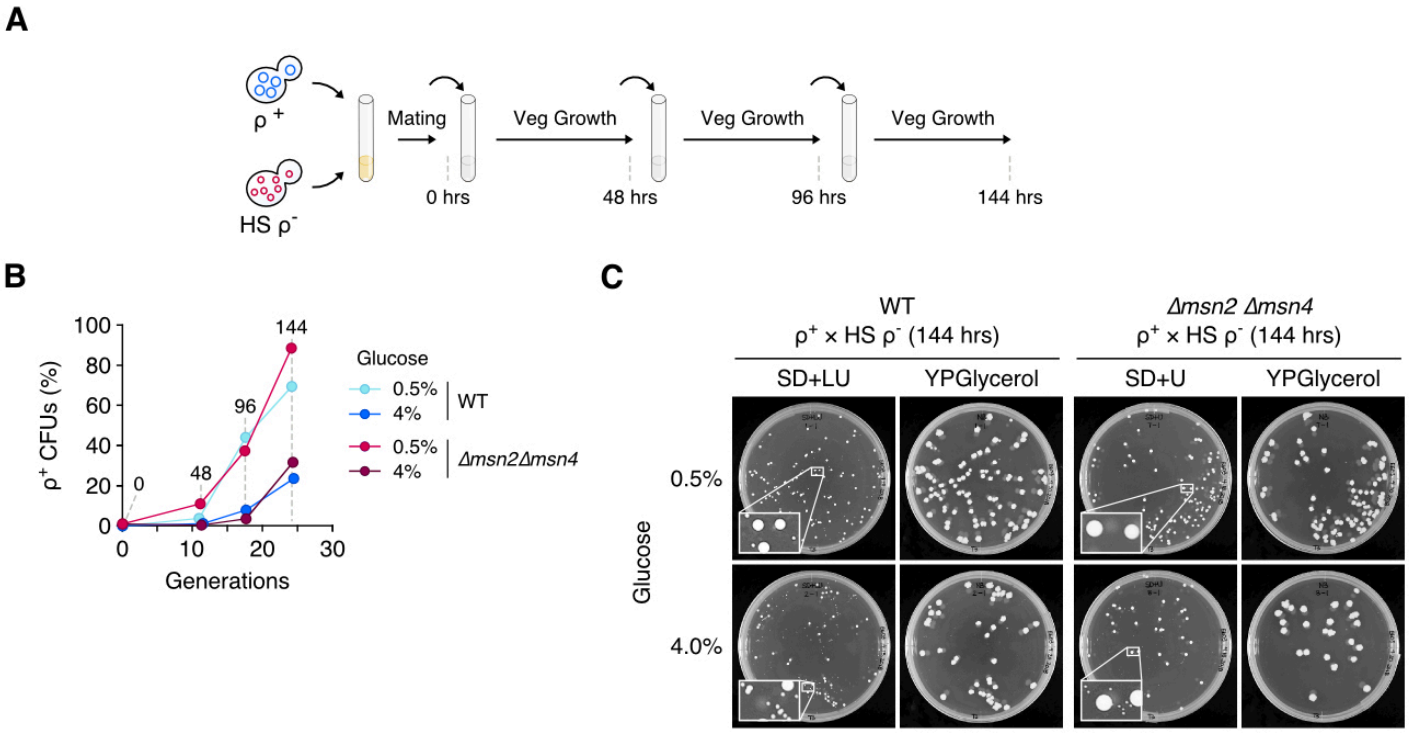

Figure 4.4 | Analysis of the involvement of the transcription factors Msn2 and Msn4 in formation of ρ^+ colonies during vegetative growth of heteroplasmic cells. (A) Scheme of yeast hypersuppressive crossing experiment followed by three, 48-hour rounds of vegetative growth in media containing 0.5% or 4% glucose. Hours of vegetative cultivation after crossing are indicated. (B) Quantified results from *n* = 1 crossing experiment of one WT ρ^+ × WT HS ρ^- crossing and the average of three biological replicates of *Δmsn2Δmsn4* ρ^+ × *Δmsn2Δmsn4* HS ρ^- crossings followed by 144 hours of vegetative growth in 0.5% or 4.0% glucose diploid selection media. Hours of vegetative cultivation after crossing are indicated. (C) Representative plate images from WT or *Δmsn2Δmsn4* diploid cells grown for 144 hours in diploid selection media containing 0.5% or 4% glucose.

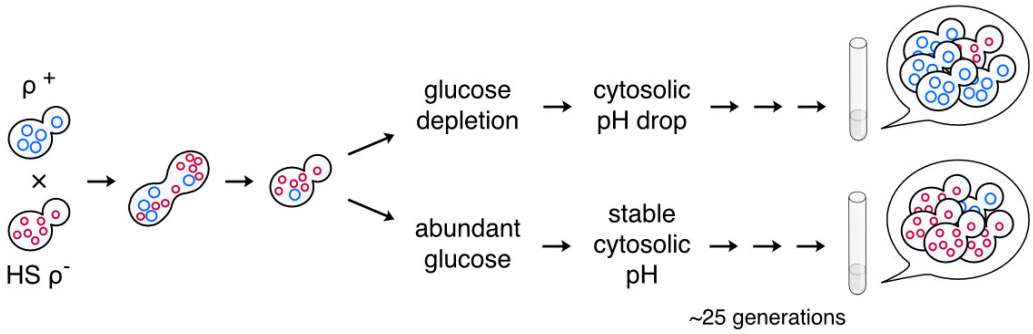

Figure 4.5 | Model for effect of cytosolic pH on the vegetative segregation of mtDNA alleles. Diploid cells containing a mixture of ρ^+ and HS ρ^- mtDNA can undergo segregation to a ρ^+ phenotype depending on glucose depletion from media and subsequent drop in cytosolic pH. On the other hand, if glucose is abundant or cytosolic pH remains sufficiently high, the hypersuppressive phenotype will persist.

Table 4.1 | Yeast strains used in this chapter

Strain	Nuclear genotype	Mitochondrial genotype	Source
W303a-187	*MAT*a *ade2 leu2 his3 ura3 trp1 can1*	[ρ^+ ω^- *ens*2 Chl_{321}^R]	(*58*)
W303a-187/pVT100U	*MAT*a *ade2 leu2 his3 ura3 trp1 can1* (*URA3*)	[ρ^+ ω^- *ens*2 Chl_{321}^R]	This study
W303a-187/pVT100U-pHluorin	*MAT*a *ade2 leu2 his3 ura3 trp1 can1* (pHluorin, *URA3*)	[ρ^+ ω^- *ens*2 Chl_{321}^R]	This study
W303a-187 *Δmsn2Δmsn4*	*MAT*a *ade2 leu2 his3 ura3 trp1 can1 msn2::LEU2 msn4::KAN*	[ρ^+ ω^- *ens*2 Chl_{321}^R]	This study
YKN1423C-1	*MATα leu2 ura3 met3*	[HS ρ^-]	(*59*)
YKN1423C-1/pVT100U	*MATα leu2 ura3 met3* pVT100U (*URA3*)	[HS ρ^-]	This study
YKN1423C-1/pVT100U-pHluorin	*MATα leu2 ura3 met3* pVT100U (pHluorin, *URA3*)	[HS ρ^-]	This study
YKN1423C-1 *Δmsn2Δmsn4*	*MATα leu2 ura3 met3 msn2::LEU2 msn4::KAN*	[HS ρ^-]	This study

Chapter 5: Conclusion

5.1 Concluding remarks

In this study we revealed two regulatory mechanisms that influence deleted mtDNA content in yeast cells and a role for cytosolic pH that influences mtDNA heteroplasmy. First, ribonucleotide reductase activity influences the replicative advantage of small mtDNA molecules through changes to cytosolic dNTP pool levels. Small dNTP pools are largely insufficient for replication of a large template in a heteroplasmic mixture containing a small template, as we demonstrated *in vivo* through *SML1* overexpression and *in vitro* by PCR amplification of small and large templates at various dNTP concentrations. RNR activity is therefore an important regulator of small mtDNA replicative advantage by determining dNTP availability to the larger mitochondrial allele.

Second, we showed a role for mtDNA recombination in preventing deletion mutagenesis. In yeast, mitochondrial recombination by Mhr1 functions in both mtDNA repair (*129*) and the rolling-circle mode of replication (*43*), and as shown in Chapter 3, Mhr1 is essential for mtDNA integrity in the absence of selective pressure. Reintroducing *MHR1* by plasmid significantly increased the respiratory function of *Δabf2 mhr1-1* cells, indicating that *MHR1* has an important role in preventing mtDNA deletion mutagenesis.

Finally, glucose depletion leads to a drop in cytosolic pH and a switch to ethanol catabolism (*144*). We found that diploid cells heteroplasmic for wild-type and small mtDNA cultivated in low glucose media experience a drop in cytosolic pH during early vegetative growth and form a high proportion of ρ^+ colonies in subsequent generations. In contrast, cells cultivated in high glucose media or alkaline-buffered low glucose media, experience neither an immediate drop in cytosolic pH nor formation of a substantial proportion of ρ^+ colonies. The transcription factors Msn2 and Msn4 are not required for this cytosolic acidification-mediated induction of ρ^+ colony formation, and further study will be needed to determine the precise mechanism(s) at work.

References

1. Stock, D., Leslie, A. G., Walker, J. E. (1999). Molecular architecture of the rotary motor ATP synthase. *Science* 286(5445): 1700-1705.
2. Salway, J. G. (2004). Metabolism at a glance. Third edition. *John Wiley & Sons.*
3. Eaton, S., Bartlett, K., Pourfarzam, M. (1996). Mammalian mitochondrial *β*-oxidation. *Biochem. J.* 320 (Pt 2): 345-357.
4. Lill, R., Mühlenhoff, U. (2008). Maturation of iron-sulfur proteins in eukaryotes: mechanisms, connected processes and diseases. *Annu. Rev. Biochem.* 77: 669-700.
5. Pijuan, J., María, C., Herrero, E., Bellí, G. (2015). Impaired mitochondrial Fe-S cluster biogenesis activates the DNA damage response through different signaling mediators. *J. Cell Sci*. 128(24): 4653-4665.
6. Suen, D. F., Norris, K. L., Youle, R. J. (2008). Mitochondrial dynamics and apoptosis. *Genes Dev.* 22(12): 1577-1590.
7. Nunnari, J., Suomalainen, A. (2012). Mitochondria: In sickness and in health. *Cell* 148(6): 1145-1159.
8. Hamanaka, R. B., Chandel, N. S. (2010). Mitochondrial reactive oxygen species regulate cellular signaling and dictate biological outcomes. *Trends Biochem. Sci.* 35(9): 505-513.
9. Love, N. R., Chen, Y., Ishibashi, S., Kritsiligkou, P., Lea, R., *et al.* (2013). Amputation-induced reactive oxygen species are required for successful Xenopus tadpole tail regeneration. *Nat. Cell Biol.* 15(2): 222-229.
10. Hori, A., Yoshida, M., Shibata, T., Ling, F. (2009). Reactive oxygen species regulate DNA copy number in isolated yeast mitochondria by triggering recombination-mediated replication. *Nucleic Acids Res*. 37: 749-761.
11. Ling, F., Niu, R., Hatakeyama, H., Goto, Y. I., Shibata, T., *et al*. (2016). Reactive oxygen species stimulate mitochondrial allele segregation toward homoplasmy in human cells. *Mol. Biol. Cell* 27(10): 1684-1693.

12. Twig, G., Elorza, A., Molina, A. J., Mohamed, H., Wikstrom, J. D., *et al*. (2008). Fission and selective fusion govern mitochondrial segregation and elimination by autophagy. *EMBO J.* 27(2): 433-446.
13. Okamoto, K., Kondo-Okamoto, N., Ohsumi, Y. (2009). Mitochondria-anchored receptor Atg32 mediates degradation of mitochondria via selective autophagy. *Dev. Cell* 17(1): 87-97.
14. Youle, R. J., Narendra, D. P. (2011). Mechanisms of mitophagy. *Nat. Rev. Mol. Cell Biol.* 12(1): 9.
15. Jin, S. M., Lazarou, M., Wang, C., Kane, L. A., Narendra, D. P., *et al*. (2010). Mitochondrial membrane potential regulates PINK1 import and proteolytic destabilization by PARL. *J. Cell Biol.* 191(5): 933-942.
16. Lazarou, M., Sliter, D. A., Kane, L. A., Sarraf, S. A., Wang, C., *et al*. (2015). The ubiquitin kinase PINK1 recruits autophagy receptors to induce mitophagy. *Nature* 524(7565): 309.
17. Lee, J. Y., Nagano, Y., Taylor, J. P., Lim, K. L., Yao, T. P. (2010). Disease-causing mutations in parkin impair mitochondrial ubiquitination, aggregation, and HDAC6-dependent mitophagy. *J. Cell Biol.* jcb-201001039.
18. Palikaras, K., Lionaki, E., Tavernarakis, N. (2015). Coordination of mitophagy and mitochondrial biogenesis during ageing in *C. elegans*. *Nature* 521(7553): 525.
19. Westermann, B. (2010). Mitochondrial fusion and fission in cell life and death. *Nat Rev Mol. Cell Biol*. 11: 872-884.
20. Chan, D. C. (2012). Fusion and fission: interlinked processes critical for mitochondrial health. *Annu. Rev. Genet.* 46.
21. Mendl, N., Occhipinti, A., Müller, M., Wild, P., Dikic, I., *et al*. (2011). Mitophagy in yeast is independent of mitochondrial fission and requires the stress response gene WHI2. *J. Cell Sci*. 124(8): 1339-1350.
22. Kanki, T., Wang, K., Baba, M., Bartholomew, C. R., Lynch-Day, M. A., *et al*. (2009) A genomic screen for mutants defective in selective mitochondria autophagy. *Mol. Biol. Cell* 20: 4730-4738.

23. Goyal, G., Fell, B., Sarin, A., Youle, R. J., Sriram, V. (2007). Role of mitochondrial remodeling in programmed cell death in Drosophila melanogaster. *Dev. Cell* 12(5): 807-816.

24. Lee, Y. J., Jeong, S. Y., Karbowski, M., Smith, C. L., Youle, R. J. (2004). Roles of the mammalian mitochondrial fission and fusion mediators Fis1, Drp1, and Opa1 in apoptosis. *Mol. Biol. Cell* 15(11): 5001-5011.

25. Hermann, G. J., Thatcher, J. W., Mills, J. P., Hales, K. G., Fuller, M. T., *et al*. (1998). Mitochondrial fusion in yeast requires the transmembrane GTPase Fzo1p. *J. Cell Biol.* 143(2): 359-373.

26. Merz, S., Westermann, B. (2009). Genome-wide deletion mutant analysis reveals genes required for respiratory growth, mitochondrial genome maintenance and mitochondrial protein synthesis in Saccharomyces cerevisiae. *Genome Biol.* 10(9): R95.

27. Hori, A., Yoshida, M., Ling, F. (2011). Mitochondrial fusion increases the mitochondrial DNA copy number in budding yeast. *Genes Cells* 16(5): 527-544.

28. Gomes, L. C., Di Benedetto, G., Scorrano, L. (2011). During autophagy mitochondria elongate, are spared from degradation and sustain cell viability. *Nat. Cell Biol.* 13(5): 589.

29. Rambold, A. S., Kostelecky, B., Elia, N., Lippincott-Schwartz, J. (2011). Tubular network formation protects mitochondria from autophagosomal degradation during nutrient starvation. *Proc. Natl. Acad. Sci. USA.* 108(25): 10190-10195.

30. Rugarli, E. I., Langer, T. (2012). Mitochondrial quality control: a matter of life and death for neurons. *EMBO J.* 31(6): 1336-1349.

31. Matsushima, Y., Goto, Y. I., Kaguni, L. S. (2010). Mitochondrial Lon protease regulates mitochondrial DNA copy number and transcription by selective degradation of mitochondrial transcription factor A (TFAM). *Proc. Natl. Acad. Sci. USA*. 107(43): 18410-18415.

32. Lu, B., Lee, J., Nie, X., Li, M., Morozov, Y. I., *et al*. (2013). Phosphorylation of human TFAM in mitochondria impairs DNA binding and promotes degradation by the AAA+ Lon protease. *Mol. Cell* 49(1): 121-132.

33. Quirós, P. M., Español, Y., Acín-Pérez, R., Rodríguez, F., Bárcena, C., *et al*. (2014). ATP-dependent Lon protease controls tumor bioenergetics by reprogramming mitochondrial activity. *Cell Rep.* 8(2): 542-556.

34. Boldogh, I. R., Pon, L. A. (2007). Mitochondria on the move. *Trends Cell Biol.* 17(10), 502-510.

35. McFaline-Figueroa, J. R., Vevea, J., Swayne, T. C., Zhou, C., Liu, C., *et al*. (2011). Mitochondrial quality control during inheritance is associated with lifespan and mother–daughter age asymmetry in budding yeast. *Aging Cell* 10(5): 885-895.

36. Vevea, J. D., Swayne, T. C., Boldogh, I. R., Pon, L. A. (2014). Inheritance of the fittest mitochondria in yeast. *Trends Cell Biol.* 24(1): 53-60.

37. Westermann, B. (2014) Mitochondrial inheritance in yeast. *Biochim. Biophys. Acta* 1837: 1039-1046.

38. Chernyakov, I., Santiago-Tirado, F., Bretscher, A. (2013). Active segregation of yeast mitochondria by Myo2 is essential and mediated by Mmr1 and Ypt11. *Curr. Biol.* 23(18): 1818-1824.

39. Higuchi-Sanabria, R., Charalel, J. K., Viana, M. P., Garcia, E. J., Sing, C. N., *et al*. (2016). Mitochondrial anchorage and fusion contribute to mitochondrial inheritance and quality control in the budding yeast Saccharomyces cerevisiae. *Mol. Biol. Cell* 27(5): 776-787.

40. Farkasovsky, M., & Küntzel, H. (1995). Yeast Num1p associates with the mother cell cortex during S/G2 phase and affects microtubular functions. *J. Cell Biol.* 131(4): 1003-1014.

41. Lackner, L. L., Ping, H., Graef, M., Murley, A., Nunnari, J. (2013). Endoplasmic reticulum-associated mitochondria–cortex tether functions in the distribution and inheritance of mitochondria. *Proc. Natl. Acad. Sci. USA*. 110(6): E458-E467.

42. Shadel, G. S., Clayton, D. A. (1997) Mitochondrial DNA maintenance in vertebrates. *Annu. Rev. Biochem*. 66(1): 409-435.

43. Ling, F. and Shibata, T. (2004). Mhr1p-dependent concatemeric mitochondrial DNA formation for generating yeast mitochondrial homoplasmic cells. *Mol. Biol. Cell* 15: 310-322.

44. Falkenberg, M., Larsson, N. G., Gustafsson, C. M. (2007). DNA replication and transcription in mammalian mitochondria. *Annu. Rev. Biochem.* 76: 679-699.

45. Karnkowska, A., Vacek, V., Zubáčová, Z., Treitli, S. C., Petrželková, R., *et al*. (2016). A eukaryote without a mitochondrial organelle. *Curr. Biol.* 26(10): 1274-1284.

46. Larsson, N. G. (2010). Somatic mitochondrial DNA mutations in mammalian aging. *Annu. Rev. Biochem.* 79: 683-706.

47. Clayton, D. (1982). Replication of animal mitochondrial DNA. *Cell* 28: 693-705.

48. Holt, I. J., Lorimer, H. E., Jacobs, H. T. (2000). Coupled leading-and lagging-strand synthesis of mammalian mitochondrial DNA. *Cell* 100(5): 515-524.

49. Yang, M. Y., Bowmaker, M., Reyes, A., Vergani, L., Angeli, P., *et al*. (2002). Biased incorporation of ribonucleotides on the mitochondrial L-strand accounts for apparent strand-asymmetric DNA replication. *Cell* 111(4): 495-505.

50. Yasukawa, T., Reyes, A., Cluett, T. J., Yang, M. Y., Bowmaker, M., *et al*. (2006). Replication of vertebrate mitochondrial DNA entails transient ribonucleotide incorporation throughout the lagging strand. *EMBO J.* 25(22), 5358-5371.

51. Holt, I. J., Reyes, A. (2012). Human mitochondrial DNA replication. *Cold Spring Harb. Perspect. Biol*. 4(12): a012971.

52. MacAlpine, D. M., Kolesar, J., Okamoto, K., Butow, R. A., Perlman, P. S. (2001). Replication and preferential inheritance of hypersuppressive petite mitochondrial DNA. *EMBO J.* 20: 1807-1817.

53. Greenleaf, A. L., Kelly, J. L., Lehman, I. R. (1986). Yeast RPO41 gene product is required for transcription and maintenance of the mitochondrial genome. *Proc. Natl. Acad. Sci. USA.* 83: 3391-3394.

54. Graves, T., Dante, M., Eisenhour, L., & Christianson, T. W. (1998). Precise mapping and characterization of the RNA primers of DNA replication for a yeast hypersuppressive petite by in vitro capping with guanylyltransferase. *Nucleic Acids Res.* 26(5): 1309-1316.

55. Fangman, W. L., Henly, J. W., Brewer B. J. (1990). RPO41-independent maintenance of [rho-] mitochondrial DNA in Saccharomyces cerevisiae. *Mol. Cell Biol*. 10: 10-15.

56. Lorimer, H. E., Brewer, B. J., Fangman, W. L. (1995). A test of the transcription model for biased inheritance of yeast mitochondrial DNA. *Mol. Cell Biol*. 15:

4803-4809.

57. Ling, F., Makishima, F., Morishima, N., Shibata, T. (1995). A nuclear mutation defective in mitochondrial recombination in yeast. *EMBO J*. 14(16): 4090-4101.
58. Ling, F. and Shibata, T. (2002). Recombination-dependent mtDNA partitioning: in vivo role of Mhr1p to promote pairing of homologous DNA. *EMBO J*. 21(17): 4730-4740.
59. Ling, F., Hori, A., Shibata, T. (2007). DNA recombination-initiation plays a role in the extremely biased inheritance of yeast [rho$^-$] mitochondrial DNA that contains the replication origin *ori5*. *Mol. Cell Biol.* 27: 1133-1145.
60. Murphy, M. P. (2009). How mitochondria produce reactive oxygen species. *Biochem. J.* 417(1): 1-13.
61. Ling, F., Hori, A., Yoshitani, A., Niu, R., Yoshida, M., *et al.* (2013). Din7 and Mhr1 expression levels regulate double-strand-break-induced replication and recombination of mtDNA at *ori5* in yeast. *Nucleic Acids Res.* 41(11): 5799-5816.
62. Prasai, K., Robinson, L. C., Scott, R .S., Tatchell, K., Harrison, L. (2017). Evidence for double-strand break mediated mitochondrial DNA replication in *Saccharomyces cerevisiae. Nucleic Acids Res.* 45(13): 7760-7773.
63. Lewis, S. C., Joers, P., Willcox, S., Griffith, J. D., Jacobs, H. T., *et al*. (2015). A rolling circle replication mechanism produces multimeric lariats of mitochondrial DNA in *Caenorhabditis elegans*. *PLOS Genet*. 11(2): e1004985.
64. Backert, S., Dörfel, P., Lurz, R., Börner, T. (1996). Rolling-circle replication of mitochondrial DNA in the higher plant Chenopodium album (L.). *Mol. Cell Biol*. 16(11): 6285-6294.
65. Kraytsberg, Y., Kudryavtseva, E., McKee, A. C., Geula, C., Kowall, N. W., *et al.* (2006). Mitochondrial DNA deletions are abundant and cause functional impairment in aged human substantia nigra neurons. *Nat. Genet.* 38: 518-520.
66. Dahal, S., Dubey, S., Raghavan, S. C. (2018) Homologous recombination-mediated repair of double-strand breaks operates in mammalian mitochondria. *Cell Mol. Life Sci.* 75: 1641-1655.
67. Moretton, A., Morel, F., Macao, B., Lachaume, P., Ishak, L., *et al*. (2017). Selective mitochondrial DNA degradation following double-strand breaks. *PLOS One* 12(4): e0176795.

68. Peeva, V., Blei, D., Trombly, G., Corsi, S., Szukszto, M. J., *et al*. (2018). Linear mitochondrial DNA is rapidly degraded by components of the replication machinery. *Nat. Comms.* 9.

69. Stewart, J.B., Chinnery, P. F. (2015). The dynamics of mitochondrial DNA heteroplasmy: implications for human health and disease. *Nat. Rev. Genetics* 16: 530-542.

70. Diaz, F., Bayona-Bafaluy, M. P., Rana, M., Mora, M., Hao, H., *et al.* (2002). Human mitochondrial DNA with large deletions repopulates organelles faster than full-length genomes under relaxed copy number control. *Nucleic Acids Res.* 30: 4626-4633.

71. Blanc, H. and Dujon, B. (1980). Replicator regions of the yeast mitochondrial DNA responsible for suppressiveness. *Proc. Natl. Acad. Sci. USA.* 77: 3942-3946.

72. Cortopassi, G. A., Shibata, D., Soong, N. W., Arnheim, N. (1992). A pattern of accumulation of a somatic deletion of mitochondrial DNA in aging human tissues. *Proc. Natl. Acad. Sci. USA.* 89: 7370-7374.

73. Melov, S., Lithgow, G. J., Fischer, D. R., Tedesco, P. M. and Johnson, T. E. (1995). Increased frequency of deletions in the mitochondrial genome with age of *Caenorhabditis elegans*. *Nucleic Acids Res.* 23: 1419–1425.

74. Fukui, H., Moraes, C. T. (2009). Mechanisms of formation and accumulation of mitochondrial DNA deletions in aging neurons. *Hum. Mol. Genet.* 18: 1028-1036.

75. Samuels, D. C., Schon, E. A., Chinnery, P. F. (2004). Two direct repeats cause most human mtDNA deletions. *Trends Genet.* 20(9): 393-398.

76. Trifunovic, A., Wredenberg, A., Falkenberg, M., Spelbrink, J. N., Rovio, A. T., *et al*. (2004). Premature ageing in mice expressing defective mitoshondrial DNA polymerase. *Nature* 429(6990): 417-423.

77. Vermulst, M., Wanagat, J., Kujoth, G. C., Bielas, J. H., Rabinovitch, P. S., *et al*. (2008). DNA deletions and clonal mutations drive premature aging in mitochondrial mutator mice. *Nat. Genet.* 40(4): 392-394.

78. Khrapko, K., Bodyak, N., Thilly, W. G., Van Orsouw, N. J., Zhang, X., *et al*. (1999). Cell-by-cell scanning of whole mitochondrial genomes in aged human

heart reveals a significant fraction of myocytes with clonally expanded deletions. *Nucleic Acids Res.* 27(11): 2434-2441.

79. Bender, A., Krishnan, K. J., Morris, C. M., Taylor, G. A., Reeve, A. K., *et al*. (2006). High levels of mitochondrial DNA deletions in substantia nigra neurons in aging and Parkinson disease. *Nat. Genet.* 38(5): 515-517.
80. Russell, O. M., Fruh, I., Rai, P. K., Marcellin, D., Doll, T., *et al.* (2018). Preferential amplification of a human mitochondrial DNA deletion in vitro and in vivo. *Sci. Rep.* 8: 1799.
81. Elledge, S. J., Zhou, Z., Allen, J. B. (1992). Ribonucleotide reductase: regulation, regulation, regulation. *Trends Biochem. Sci.* 17(3): 119-123.
82. Zhang, Z., An, X., Yang, K., Perlstein, D. L., Hicks, L., *et al.* (2006). Nuclear localization of the Saccharomyces cerevisiae ribonucleotide reductase small subunit requires a karyopherin and a WD40 repeat protein. *Proc. Natl. Acad. Sci. USA.* 103: 1422-1427.
83. Huang, M., Zhou, Z., Elledge, S.J. (1998). The DNA replication and damage checkpoint pathways induce transcription by inhibition of the Crt1 repressor. *Cell* 94: 595-605.
84. Chabes, A., Domkin, V., Thelander, L. (1999). Yeast Sml1, a protein inhibitor of ribonucleotide reductase. *J. Biol. Chem*. 274: 36679-36683.
85. Chabes, A., Georgieva, B., Domkin, V., Zhao, X., Rothstein, R., *et al.* (2003). Survival of DNA damage in yeast directly depends on increased dNTP levels allowed by relaxed feedback inhibition of ribonucleotide reductase. *Cell* 112: 391-401.
86. Taylor, S. D., Zhang, H., Eaton, J. S., Rodeheffer, M. S., Lebedeva, M. A., *et al.* (2005). The conserved Mec1/Rad53 nuclear checkpoint pathway regulates mitochondrial DNA copy number in Saccharomyces cerevisiae. *Mol. Biol. Cell* 16: 3010-3018.
87. Paulovich, A. G. and Hartwell, L. H. (1995). A checkpoint regulates the rate of progression through S phase in *S. cerevisiae* in response to DNA damage. *Cell* 82: 841-847.

88. Ivessa, A.S., Lenzmeier, B.A., Bessler, J.B., Goudsouzian, L.K., Schnakenberg, S.L., *et al.* (2003). The Saccharomyces cerevisiae helicase rrm3p facilitates replication past nonhistone protein-DNA complexes. *Mol. Cell* 12: 1525-1536.

89. Zhao, X., Muller, E. G., Rothstein, R. (1998). A suppressor of two essential checkpoint genes identifies a novel protein that negatively affects dNTP pools. *Mol. Cell* 2: 329-340.

90. Zhao, X., Chabes, A., Domkin, V., Thelander, L., Rothstein, R. (2001). The ribonucleotide reductase inhibitor Sml1 is a new target of the Mec1/Rad53 kinase cascade during growth and in response to DNA damage. *EMBO J*. 20: 3544-3553.

91. Zhao, X., Rothstein, R. (2002). The Dun1 checkpoint kinase phosphorylates and regulates the ribonucleotide reductase inhibitor Sml1. *Proc. Natl. Acad. Sci. USA.* 99: 3746-51.

92. Ephrussi, B., Margerie-Hottinguer, H., Roman, H. (1955). Suppressiveness: A new factor in the genetic determinism of the synthesis of respiratory enzymes in yeast. *Proc. Natl. Acad. Sci. USA.* 41: 1065-1070.

93. Solieri, L. (2010). Mitochondrial inheritance in budding yeasts: towards an integrated understanding. *Trends Microbiol.* 18: 521-530.

94. Ito, H., Fukuda, Y., Murata, K., Kimura, A. (1983). Transformation of intact yeast cells treated with alkali cations. *J. Bacteriol.* 153: 163-168.

95. Westermann, B. and Neupert, W. (2000). Mitochondria-targeted green fluorescent proteins: convenient tools for the study of organelle biogenesis in Saccharomyces cerevisiae. *Yeast* 16: 1421-1427.

96. Rasband, W. S. (1997-2018). ImageJ, U. S. National Institutes of Health, Bethesda, Maryland, USA. https://imagej.nih.gov/ij/

97. Livak, K. J. and Schmittgen, T. D. (2001). Analysis of relative gene expression data using real-time quantative PCR and the 2(-Delta Delta C(T)) method. *Methods* 25: 402-408.

98. Zhang, T., Lei, J., Yang, H., Xu, K., Wang, R. *et al.* (2011). An improved method for whole protein extraction from yeast *Saccharomyces cerevisiae*. *Yeast* 28: 795-798.

99. Lockshon, D., Zweifel, S. G., Freeman-Cook, L. L., Lorimer, H. E., Brewer, B. J., *et al*. (1995). A role for recombination junctions in the segregation of mitochondrial DNA in yeast. *Cell* 81: 947-955.

100. Lecrenier, N., Foury, F. (1995). Overexpression of the RNR1 gene rescues Saccharomyces cerevisiae mutants in the mitochondrial DNA polymerase-encoding MIP1 gene. *Mol. Gen. Genet*. 249: 1-7.

101. Chabes, A., Stillman, B. (2007). Constitutively high dNTP concentration inhibits cell cycle progression and the DNA damage checkpoint in yeast *Saccharomyces cerevisiae*. *Proc. Natl. Acad. Sci. USA.* 104(4): 1183-1188.

102. Lebedeva, M. A., Shadel, G. S. (2007). Cell cycle- and ribonucleotide reductase-driven changes in mtDNA copy number influence mtDNA inheritance without compromising mitochondrial gene expression. *Cell Cycle* 6(16): 2048-2057.

103. Jordan, A., Reichard, P. Ribonucleotide reductases. (1998). *Annu. Rev. Biochem.* 67: 71-98.

104. Sinha, A., Maitra, P. K. (1992). Induction of specific enzymes of the oxidative pentose phosphate pathway by glucono-δ-lactone in Saccharomyces cerevisiae. *Microbiol.* 138(9): 1865-1873.

105. Song, S., Pursell, Z. F., Copeland, W. C., Longley, M. J., Kunkel, T. A., *et al*. (2005). DNA precursor assymetries in mammalian tissue mitochondria and possible contribution to mutagenesis through reduced replication fidelity. *Proc. Natl. Acad. Sci. USA.* 102: 4990-4995.

106. Burdon, A., Minai, L., Serre, V., Jais, J., Sarzi, E., *et al*. (2007). Mutation of RRM2B, encoding p53-controlled ribonucleotide reductase (p53R2), causes severe mitochondrial DNA depletion. *Nat. Genet.* 39(6): 776-780.

107. Gonzalez-Vioque, E., Torres-Torronteras, J., Andreu, A. L., Marti, R. (2011). Limited dCTP availability accounts for mitochondrial DNA depletion in mitochondrial neurogastrointestinal encephalomyopathy (MNGIE) *PLoS Genet*. 7(3): e1002035.

108. Dalla Rosa, I., Cámara, Y., Durigon, R., Moss, C. F., Vidoni, S., *et al*. (2016). MPV17 loss causes deoxynucleotide insufficiency and slow DNA replication in mitochondria. *PLoS Genet*. 12(1): e1005779.

109. Steitz, T. A. (1999). DNA polymerases: structural diversity and common mechanisms. *J. Biol. Chem.* 274: 17395-17398.
110. Elshawadfy, A. M., Keith, B. J., Ee Ooi, H., Kinsman, T., Heslop, P., *et al*. (2014). DNA polymerase hybrids derived from the family-B enzymes of Pyrococcus furiosus and Thermococcus kodakarensis: improving performace in the polymerase chain reaction. *Front. Microbiol*. 5: 224.
111. O'Rourke, T. W., Doudican, N. A., Zhang, H., Eaton, J. S., Doetsch, P. W. *et al.* (2005). Differential involvement of the related DNA helicases Pif1p and Rrm3p in mtDNA point mutagenesis and stability. *Gene* 354: 86-92.
112. Kauppila, T. E., Kauppila, J. H., Larsson, N. G. (2017). Mammalian mitochondria and aging: an update. *Cell Metab*. 25: 57-71.
113. Chen, X. J., Butow, R.A. (2005). The organization and inheritance of the mitochondrial genome. *Nat. Rev. Genet.* 6, 815.
114. Diffley, J. F., Stillman, B. (1992). DNA binding properties of an HMG1-related protein from yeast mitochondria. *J. Biol. Chem.* 267(5): 3368-3374.
115. Newman, S. M., Zelenaya-Troitskaya, O., Perlman, P. S., Butow, R. A. (1996). Analysis of mitochondrial DNA nucleoids in wild-type and a mutant strain of Saccharomyces cerevisiae that lacks the mitochondrial HMG box protein Abf2p. *Nucleic Acids Res.* 24(2): 386-389.
116. Brewer, L. R., Friddle, R., Noy, A., Baldwin, E., Martin, S. S., *et al*. (2003). Packaging of single DNA molecules by the yeast mitochondrial protein Abf2p. *Biophys. J.* 85(4): 2519-2524.
117. Fisher, R. P., Lisowsky, T., Parisi, M. A., Clayton, D. A. (1992). DNA wrapping and bending by a mitochondrial high mobility group-like transcriptional activator protein. *J. Biol. Chem*. 267(5): 3358-3367.
118. Van Dyck, E., Clayton, D. A. (1998). Transcription-dependent DNA transactions in the mitochondrial genome of a yeast hypersuppressive petite mutant. *Mol. Cell Biol.* 18(5): 2976-2985.
119. Kukat, C., Larsson, N. G. (2013). mtDNA makes a U-turn for the mitochondrial nucleoid. *Trends Cell Biol*. 23(9): 457-463.
120. MacAlpine, D. M., Perlman, P. S., Butow, R. A. (1998). The high mobility group protein Abf2p influences the level of yeast mitochondrial DNA recombination

intermediates in vivo. *Proc. Natl. Acad. Sci. USA*. 95: 6739-6743.

121. Cho, J. H., Lee, Y. K., Chae, C. B. (2001). The modulation of the biological activities of mitochondrial histone Abf2p by yeast PKA and its possible role in the regulation of mitochondrial DNA content during glucose repression. *Biochim. Biophys. Acta* 1522(3): 175-186.
122. DeRisi, J. L., Iyer, V. R., Brown, P. O. (1997). Exploring the metabolic and genetic control of gene expression on a genomic scale. *Science* 278(5338): 680-686.
123. Zelenaya-Troitskaya, O., Newman, S. M., Okamoto, K., Perlman, P. S., Butow, R. A. (1998). Functions of the high mobility group protein, Abf2p, in mitochondrial DNA segregation, recombination and copy number in *Saccharomyces cerevisiae*. *Genetics* 148: 1763-1776.
124. Contamine, V., Picard, M. (2000). Maintenance and integrity of the mitochondrial genome: a plethora of nuclear genes in the budding yeast. *Microbiol. Mol. Bio. Rev*. 64(2): 281-315.
125. Chen, X. J., Clark-Walker, G. D. (1999). The petite mutation in yeasts: 50 years on. *Int. Rev. Cytol.* 194: 197-238.
126. Ling, F., Yoshida, M, Shibata, T. (2009). Heteroduplex joint formation free of net topological charge by Mhr1, a mitochondrial recombinase. *J. Biol. Chem*. 284(14): 9341-9353.
127. Kaiser, C., Michaelis, S., Mitchell, A. (1994). Methods in yeast genetics: A Cold Spring Harbor laboratory course manual. *Cold Spring Harbor Laboratory Press, Plainview, New York, NY.*
128. Hudspeth, M. E., Shumard, D. S., Tatti, K. M., Grossman, L. I. (1980). Rapid purification of yeast mitochondrial DNA in high yield. *Biochim. Biophys. Acta* 610(2): 221-228.
129. Ling, F., Morioka, H., Ohtsuka, E., Shibata, T. (2000). A role for MHR1, a gene required for mitochondrial genetic recombination, in the repair of damage spontaneously introduced in yeast mtDNA. *Nucleic Acids Res*. 28(24): 4956-4963.

130. Ephrussi, B., Jakob, H., Grandchamp, S. (1966). Etudes sur la suppressivité des mutants a deficience respiratoire de la levure. II. Etapes de la mutation grande en petite provoquee par le facteur suppressif. *Genetics* 54(1): 1-29.
131. Bustin, S. A., Benes, V., Garson, J. A., Hellemans, J., Huggett, J., *et al*. (2009). The MIQE guidelines: minimum information for publication of quantitative real-time PCR experiments. *Clin. Chem*. 55(4): 611-622.
132. Fritsch, E. S., Chabbert, C. D., Klaus, B., Steinmetz, L. M. (2014). A genome-wide map of mitochondrial DNA recombination in yeast. *Genetics* 198(2): 755-771.
133. Krishnan, K. J., Reeve, A. K., Samuels, D. C., Chinnery, P. F., Blackwood, J. K., *et al*. (2008). What causes mitochondrial DNA deletions in human cells? *Nat. Genet.* 40(3): 275.
134. Mehta, A., & Haber, J. E. (2014). Sources of DNA double-strand breaks and models of recombinational DNA repair. *Cold Spring Harb. Perspect. Biol.* 6(9): a016428.
135. Osman, F. and Subramani, S. (1998). Double-strand break-induced recombination in eukaryotes. *Prog. Nucleic Acid Res. Mol. Biol.* 58: 263-299.
136. Jasin, M., Rothstein, R. (2013). Repair of strand breaks by homologous recombination. *Cold Spring Harb. Perspect. Biol.* 5(11): a012740.
137. Cox, M. M., Morrical, S. W., Neuendorf, S. K. (1984). Unidirectional branch migration promoted by nucleoprotein filaments of RecA protein and DNA. *Cold Spring Harb. Symp. Quant. Biol.* 49: 525-533.
138. Parisi, M. A., Xu, B., Clayton, D. A. (1993). A human mitochondrial transcriptional activator can functionally replace a yeast mitochondrial HMG-box protein both in vivo and in vitro. *Mol. Cell Biol.* 13(3): 1951-1961.
139. Wiuf, C. (2001). Recombination in human mitochondrial DNA? *Genetics* 159(2): 749-756.
140. Hagelberg, E., Goldman, N., Lio, P., Whelan, S., Schiefenhöel, *et al*. (1999). Evidence for mitochondrial DNA recombination in a human population of island Melanesia. *Proc. Bio. Sci*. 266(1418): 485-492.
141. Kraytsberg, Y., Schwartz, M., Brown, T. A., Ebralidse, K., *et al*. (2004). Recombination of human mitochondrial DNA. *Science* 304(5673): 981-981.

142. Zsurka, G., Kraytsberg, Y., Kudina, T., Kornblum, C., Elger, C. E., *et al*. (2005). Recombination of mitochondrial DNA in skeletal muscle of individuals with multiple mitochondrial DNA heteroplasmy. *Nat. Genet.* 37(8): 873.
143. Dechant, R., Binda, M., Lee, S. S., Pelet, S., Winderickx, J., *et al*. (2010). Cytosolic pH is a second messenger for glucose and regulates the PKA pathway through V-ATPase. *EMBO J.* 29(15): 2515-2526.
144. Galdieri, L., Mehrotra, S., Yu, S., Vancura, A. (2010). Transcriptional regulation in yeast during diauxic shift and stationary phase. *OMICS* 14(6): 629-638.
145. Orij, R., Postmus, J., Ter Beek, A., Brul, S., Smits, G. J. (2009). *In vivo* measurement of cytosolic and mitochondrial pH using a pH-sensitive GFP derivative in Saccharomyces cerevisiae reveals a relation between intracellular pH and growth. *Microbiol*. 155(1): 268-278.
146. Serra-Cardona, A., Canadell, D., Ariño, J. (2015). Coordinate responses to alkaline pH stress in budding yeast. *Microb. Cell*. 2(6): 182.